Virginia Commonwealth University
VCU Scholars Compass

Theses and Dissertations Graduate School

2010

B cell ADAM10 Activity is Increased by Kainate Receptor Activation: Potential Role of this Pathway in Th2 Immunity and Cancer

Jamie Sturgill
Virginia Commonwealth University

Follow this and additional works at: https://scholarscompass.vcu.edu/etd

Part of the Medicine and Health Sciences Commons

© The Author

Downloaded from
https://scholarscompass.vcu.edu/etd/142

This Dissertation is brought to you for free and open access by the Graduate School at VCU Scholars Compass. It has been accepted for inclusion in Theses and Dissertations by an authorized administrator of VCU Scholars Compass. For more information, please contact libcompass@vcu.edu.

المنارة للاستشارات

B cell ADAM10 Activity is Increased by Kainate Receptor Activation: Potential Role of this Pathway in Th2 Immunity and Cancer

A dissertation submitted in partial fulfillment of the requirements for the degree of Doctor of Philosophy at Virginia Commonwealth University

By

Jamie Lynn Sturgill
B.S., University of Kentucky, 2002

Director: Daniel H. Conrad, Professor, Department of Microbiology and Immunology

Virginia Commonwealth University
Richmond, Virginia
September 2010

ACKNOWLEDGEMENTS

First off, I would like to thank my graduate advisor, Dr. Daniel H. Conrad. Not only has Dr. Conrad been such a wonderful mentor and friend, I thank him for his guidance and career advice in choosing the path of graduate study. I will always be grateful for his patience, support, and direction.

Secondly, I would like to thank my graduate advisory committee members, Dr. Barbour, Dr. Schwartz, Dr. Smeltz, and Dr. Tew for their guidance and encouragement throughout my dissertation research.

I would also like to thank Dr. Jill Ford for her friendship, guidance and mentoring when I first entered the lab. Without her previous work in the discovery of the CD23 sheddase, much of the studies presented here would not have been possible. Furthermore, I thank Jill for her helpful guidance in learning to work with mouse models. I inherited a wonderful project from her and for that I will always be grateful.

I am especially thankful to the numerous collaborators. Dr. Carl P. Blobel, Dr. Gisela Weskamp, and Dr. Steve Swendeman at the Hospital for Special Surgery on the Weill Medical Campus of Cornell University in New York, NY for their collaboration in the CD23 Sheddase project. Without their partnership, we would never have been able to investigate nor identify the CD23 sheddase. Dr. Charles Chu at North Shore Long Island Jewish Health System has been a wonderful, patient collaborator and has provided numerous B cell chronic lymphocytic leukemia samples. I would like to thank all the kind staff at the VCU Tissue Data Analysis and Acquisition Core (TDAAC). The staff of TDAAC has always been willing to provide samples when needed and have always been a valuable resource. As many of the studies presented deal with primary human cells, these studies would not have been feasible without access to these reagents. Lastly, I would like to thank Dr. Anis Contractor at Northwestern University. He has been a valuable asset to the kainate receptor work, not only because he provided the GluK2 deficient mice, but for his eagerness to answer questions.

I would also like to thank all the members of the Conrad lab, both past and present, for their support and friendship. I would like to thank Dr. Timothy Caven for his friendship and for his work on the IL-21 studies. I would especially like to thank Rebecca Martin and Cate Kurkjian, two HHMI scholars who were wonderful to work with and assisted with the kainate receptor studies. In addition, I would like to acknowledge our past and present work study students Witemba Kabange, Yvette Orihuela, and Hannah Zellner for all their hard work.

I would especially like to thank my parents, Johnny and Barbara Sturgill, and my best friend, Dr. Tyler Stevens, for their love and support. I am also grateful to my siblings, extended family, and friends who have supported me along this path.

Lastly, I would like to thank Dr. John Yannelli and the University of Kentucky. It was during the time that I worked with him, that I first discovered my love for research, and if it had not been without his urging for me to look at VCU, I may not have been here today.

TABLE OF CONTENTS

Page

List of Figures……………………………………………………………………….v

List of Abbreviations………………………………………………………………viii

Abstract…………………………………………………………………………...xiii

Introduction…………………………………………………………………………1

I. Allergic Disease and Immunoglobulin E………………………………………1

II. Biological Properties of IgE……………………………………………………4

III. Control of IgE Synthesis and Allergic Disease…………………………...……6

IV. CD23……………………………………………………………………………10

V. Dissertation Objective…………………………………………………………...13

Materials and Methods…………………………………………………….........14

I. Animals, antibodies, cytokines, cell lines, and media reagents………...….........14

II. Preparation and purification of monoclonal antibodies………………….…..........15

III. B cell purification……………………………………………………………..….16

IV. Proliferation Analysis………………………………………………….........18

V. ADAM10 Inhibition Studies……………………………………………………19

VI. Kainate Receptor Studies…….………………………………………….....20

VII. RNA Isolation, RT-PCR, and qPCR reactions………………………….......21

VIII. Cloning and Sequence Analysis…………………...……………………………23

IX. Cell Surface Phenotyping……………………………………………..........24

X. Western Blot Analysis……………………………………………………........25

XI. Mouse Genotyping……………………..………………………………….…25

XII. *Nippostrongylus brasiliensis* isolation and culture …………………………..........26

XIII. Immunizations and bleeds……………………………………………….........31

XIV. ELISAs…………………..…………………………………………………31

XV. Statistics…………………………….……………………………........33

Results……………………………………………………………………........34

I. Identification of the CD23 Sheddase………………….………………………34

II. Identification of Mutations in Murine CD23 …………..…………….................47

III. Identification of Kainate receptors in the Immune System…………….….............60

IV. Identification of ADAM10 as a Novel Therapeutic Target in BCLL ………..117

Discussion…………………………………………………………….................151

References……………………………………………………………………...162

Vita……………………………………………………………………………..174

LIST OF FIGURES

FIGURE PAGE

1. Genotyping of GluK2 Deficient Mice……………………………………………...............29
2. CD23 shedding in wild-type and ADAM-deficient MEFs ……………….……………........37
3. ADAM10-dependent shedding of CD23 in MEFs …………………………………............39
4. Chemical structure of the ADAM10-specific inhibitor GI254023X……………….............41
5. GI254023X blocks ADAM10 mediated cleavage of CD23 and EGF……….…………...….43
6. siRNA against ADAM10 also inhibits sCD23 release………………………………...…….45
7. CD23 message levels are normal in 129/SvJ B cells………………………...……………....49
8. CD23 surface expression is reduced on 129/SvJ B cells………………………...…………...52
9. 129/SvJ CD23 surface levels can be up-regulated by stimulation……………...……………53
10. Lack of recognition of 129/SvJ CD23 by the mAb 2H10……………………..…..……......55
11. 129/SvJ CD23 is mutated……………………………………………………...……............58
12. Kainate receptor mRNA is expressed in the human immune system…………...………….63
13. Kainate receptor protein is expressed in the human immune system…………………...….65
14. Kainate Receptors are cell surface expressed in the human immune system…...………..…67
15. Kainate receptor activation increases ADAM10 mRNA levels…………………...……..69
16. Kainate receptor activation increases CD23 shedding…………………………...………72
17. Soluble CD23 release is increased in the presence of glutamate in primary B cells.............74
18. The increase in soluble CD23 release is specifically mediated through KAR activity………………..………………………………………….…………………………...76
19. The KAR mediated increase in sCD23 release is ADAM10 specific…………………...….78
20. Kainate receptor activation increases IgE synthesis……………………………………...……82

21. The increase in IgE synthesis is not through the NMDA receptor…………………...……..84

22. Kainate receptor activation increases cellular proliferation……………………….……..87

23. Kainate receptor activation increases cellular proliferation…………………..………...…..89

24. Kainate receptor activation increases total IgG synthesis…………………………......…91

25. Kainate receptor activation does not affect IgM synthesis…………………………...……..93

26. Kainate receptor activation in human PBMC model……………………………...……...96

27. Kainate Receptors are cell surface expressed in the mouse immune system………...…..…98

28. IgE Production is enhanced in murine B cells via KAR stimulation………………...……100

29. Immunophenotyping the GluK2 KO mouse……………………………….………...…104

30. Glutamate mediated enhancement of soluble CD23is not observed in GluK2 KO mice………………………………………………………………………………..…106

31. Glutamate mediated enhancement of IgE is not observed in GluK2 KO mice………...….108

32. Glutamate mediated enhancement of proliferation is not observed in GluK2 KO mice…………………………………………………………………………………..110

33. GluK2 mice have reduced IgE post immunization…………………………………..……113

34. GluK2 mice have reduced IgE post *Nippostrongylus brasillensis* challenge………..……115

35. Experimental Outline for B cell chronic lymphocytic cancer studies…………………......…120

36. Hematological Parameters of the VCU Subjects…………………………………...…..122

37. Peripheral blood mononuclear cells from BCLL patients have higher levels of membrane bound CD23…………………………………………………………...124

38. BCLL patients have significantly higher levels of sCD23 than controls…………...……..126

39. BCLL Samples have elevated ADAM10 mRNA………………………………...……..128

40. BCLL Samples express high levels of ADAM10 Protein…………………………......…130

41. ADAM10 over-expression is unique to BCLL B cells……………………………...….132

42. Marimastat prevents the release of sCD23 in a concentration dependent manner………...135

43. ADAM10 is clearly involved in CD23 ectodomain shedding…………………………....137

44. ADAM10 is involved in CD23 ectodomain shedding in Jiyoye…………...………...…139

45. Fludarabine has no inhibitory effect on ADAM10 in BCLL…………………………...…142

46. Marimastat inhibits proliferation of both 8866 and BCLL PBMC in a concentration dependent manner…………………………………………………………..144

47. ADAM10 Inhibition reduced cellular proliferation in BCLL cells……………..………147

48. ADAM10 Inhibition leads to apoptosis induction…………..…………...…………..149

49. Structure of human and mouse CD23…………………………………………………152

LIST OF ABBREVIATIONS

129/SvJ	Inbred mouse strain; commonly used for gene targeting
2.4G2	mAb recognizing the murine FcγRII and FcγRIII
2H10	mAb recognizing the lectin domain of murine CD23
a.a.	Amino Acid
Ab	Antibody
ACL4	Media used for growth of primary human leukemic cells
Ag	Antigen
Alum	Aluminum hydroxide
APC	Allophycocyanin
ADAM	A disintegrin and metalloprotease
AMPA	α-amino-3-hydroxy-5-methyl-4-isoxazole propionic acid
AMPAR	receptor that binds AMPA
B220	mAb recognizing the murine CD45R; mouse B cell marker
B3B4	mAb recognizing the lectin domain of murine CD23
BALB/c	Inbred mouse strain; high IgE responder
BAFF	B cell activation factor of the TNF family
BB94	Batimastat, inhibitor of ADAMs
BCLL	B cell Chronic Lymphocytic Leukemia
BSA	Bovine serum albumin
BU38	mab used to detect human CD23
C57BL/6	Inbred mouse strain; intermediate IgE responder

CD	Clusters of differentiation
CD23Tg	CD23 transgenic
CFSE	Carboxyfluroescein diacetate succinimidyl ester
CNS	Central Nervous System
CPM	Counts per minute
DMEM	Dulbecco’s Modified Eagle Media
DMSO	Dimethyl sulfoxide
DNA	Deoxyribonucleic acid
dNTP	Deoxynucleotide-triphosphate
EBV	Epstein Barr Virus
ECCD23	Extracellular CD23 generated in *E.coli*
ELISA	Enzyme-linked immunosorbent assay
FACS	Fluorescence activated cell sorter
FBS	Fetal bovine serum
Fc	Fragment crystallizable
FcεRI	The high affinity IgE receptor
FcεRII	The low affinity IgE receptor (CD23)
FDC	Follicular dendritic cells
FITC	Fluorescein isothiocyanate
GI254023X	ADAM10 selective inhibitor
Glu	Glutamate
GluK	Protein designation of KAR subunit
GRIK	Glutamate receptor, inotropic, kainate. Gene names for KAR subunits

hCD23	human CD23
HBS	HEPES buffered saline
HEPES	Buffering agent
HIES	Hyper IgE Syndrome
HRP	Horseradish peroxidase
IFN	Interferon
IL	Interleukin
Ig	Immunoglobulin
i.p.	Intraperitoneal
ITAM	Immunoreceptor tyrosine-based activation motif
ITIM	Immunoreceptor tyrosine-based inhibitory motif
i.v.	Intravenous
J	Jackson laboratory (as in BALB/cJ)
Ka	Affinity constant
KA	Kainic Acid
KAR	Kainic acid receptor
kDa	Kilodalton
LPS	Lipopolysaccharide
LM	Littermate control
LZ-CD23	Chimeric CD23 composed of a leucine zipper attached to the extracellular domain of CD23 (also called LZ-ECCD23)
mCD23	mouse CD23
Mar	Marimastat, matrix metalloproteinase inhibitor

MEFs	Mouse embryonic fibroblasts
MEP	4-mercaptoethylpyridine
MMP	Matrix metalloproteinase
mRNA	Messenger ribonucleic acid
NBQX	1,2,3,4-Tetrahydro-6-nitro-2,3-dioxo-benzo[f]quinoxaline-7-sulfonamide disodium salt hydrate. Antagonist to AMPAR.
NF-κB	Nuclear factor kappa B
Nippo or Nb	*Nippostrongylus brasiliensis*
NMDA	N-methyl-D-aspartic acid
NMDAR	Receptor that binds NMDA
NP40	Nonidet-P40
NS102	6,7,8,9-Tetrahydro-5-nitro-1H-benz[g]indole-2,3-dione 3-oxime. Antagonist to KAR
NZB	New Zealand Black; inbred mouse strain
OVA	Ovalbumin
PBMC	Peripheral blood mononuclear cells
PBS	Phosphate buffered saline
PCR	Polymerase chain reaction
PE	Phycoerythrin
Rabbit anti-LZ-CD23	polyclonal Ab recognizing murine LZ-CD23
RPM	Revolutions per minute
RPMI	Roswell Park Memorial Institute
RPMI 8866	Human lymphoblastoid cell line
RT-PCR	Reverse transcriptase polymerase chain reaction

s.c.	Subcutaneous
sCD23	Soluble CD23
STAT	Signal transducer and activator of transcription
T_H2	T helper cell type 2
TNF	Tumor necrosis factor
TPM	Topiramate, 2,3:4,5-Bis-O-(1-methylethylidene)-36-D-fructo-pyranose sulfamate. Antagonist to NMDAR
WHO	World Health Organization
WT	wild-type

ABSTRACT

B CELL ADAM10 ACTIVITY IS INCREASED BY KAINATE RECEPTOR ACTIVATION: POTENTIAL ROLE OF THIS PATHWAY IN TH2 IMMUNITY AND CANCER

By Jamie Lynn Sturgill, Ph.D.

A dissertation submitted in partial fulfillment of the requirements for the degree of Doctor of Philosophy at Virginia Commonwealth University.

Virginia Commonwealth University, 2010

Director: Daniel H. Conrad, Professor, Department of Microbiology and Immunology

CD23 has long been appreciated to be a natural, negative regulator of IgE synthesis. This understanding is due in part to animal models in which CD23 deficient or CD23 transgenic animals display exacerbated or reduced IgE levels respectively. Interestingly, CD23 is susceptible to proteolytic cleavage from the cell surface. When this occurs, CD23 loses its regulatory capability and the solubilized form can lead to pro-inflammatory events through its cytokinergic activity on macrophages. Thus, targeting this specific cleavage would be beneficial to the control of allergic disease by stabilizing CD23 at the cell surface. Inhibitor studies performed by our group as well as others indicate that the enzyme responsible for CD23 ectodomain shedding is a hydroxamate-sensitive metalloproteinase. Through collaboration with the Blobel group, we analyzed various ADAM KO mouse embryonic fibroblasts (MEFs) and found no involvement of ADAMs 8,9,12,15,17,19, and 33 in CD23 shedding, however we did find a role for ADAM10. Using ADAM10 KO MEFs and ADAM10 specific inhibitors, we discovered that ADAM10 is indeed the CD23 cleaving enzyme or “sheddase”. Thus, developing strategies that would target ADAM10 could have an effect on sCD23 release and IgE production.

In the CNS, signaling through the kainate receptor (KAR) by glutamate causes an increase in ADAM10 expression. Human B cells were found to express a GluK2 containing kainate receptor and its activation increased ADAM10 expression which is in agreement with KAR activation in the CNS. Although glutamate is considered a neurotransmitter, it signals in the periphery and elevated levels are associated with certain immune disorders. A significant corresponding increase in sCD23 release is observed as well. Remarkably, this activation induced a strong increase in B cell proliferation, IgG, and IgE production and these events can be reversed through the use of NS102, a specific KAR antagonist. Thus, we report for the first time the unique presence on B cells of a neurotransmitter receptor and that activation of this receptor could serve as a novel mechanism for enhancing B cell activation and Ig production. This enhancement and control thereof has implications for allergic and autoimmune diseases. Lastly, the CD23-ADAM10 axis was examined in a non-allergic disease state, B cell chronic lymphocytic leukemia (BCLL). BCLL is characterized by a large accumulation of CD23+ cells and high levels of soluble CD23 in the sera. After further analysis, we show that ADAM10 is indeed over-expressed in BCLL and could account for the high levels seen in this patient population. Furthermore, specifically targeting ADAM10 resulted in reduced soluble CD23 release, reduced proliferation, and enhanced apoptosis induction. Taken together the novel finding that ADAM10 is involved in CD23 shedding allows for targeted therapeutic intervention of both atopic and non-atopic disease states.

INTRODUCTION

I. Allergic disease and Immunoglobulin E

Allergies are defined as the body’s response to a normally innocuous substance, such as pollen. Allergic diseases occur in many forms, such as rhinitis, sinusitis, conjunctivitis, eczema, asthma, gastroenteral complications, or in severe cases anaphylaxis or even death. The World Health Organization (WHO) estimates that over 20% of the world’s population suffers from some type of allergic disease with about 150 million people having allergic asthma alone. In the United States, the National Institute of Allergy and Infectious Diseases (NIAID) approximates that between 40 and 50 million Americans suffer from these types of illnesses. With such widespread prevalence in the global population, allergic disease ranks as one of the highest causes of chronic illness and costs billions of dollars annually.

While the general public is all too familiar with the outward signs and symptoms, the underlying biological cause of allergic disease is due to a hypersensitivity reaction of the immune system to inherently harmless matter. Hypersensitivity reactions were classified into four distinct groups, or types, by Gell and Coombs in 1963 (1). Allergic reactions are classified as type 1 because they are mediated by IgE. However at the time, Gell and Coombs referred to Type 1 simply as an “immediate hypersensitivity” because a reaction occurred in minutes. Furthermore, this temporal classification stood because IgE was not officially recognized as the fifth immunoglobulin subtype until 1968.

Although the immediate hypersensitivity phenomenon was officially classified in the 1960s, its existence had been reported since the early 1800s. In 1819, Dr. John Bostock reported the first case of pollen-induced hay fever to the Royal Medical and Chirurgical

Society in London and the patient he presented was himself (2). It would take almost another 100 years, however, to link the symptoms of hay fever to a soluble serum factor. In the early 1900s, a French physiologist by the name Richet observed that "*while a foreign substance might induce a mild reaction upon first exposure, it could produce severe hypersensitive symptoms and even death when re-introduced late.*" (3). Richet observed that a repeated dose offered no protection, or phylaxis, thus he coined the term, "anaphylaxis", meaning without protection. In 1919, Ramirez reported the first case of an asthma attack subsequent to a blood transfusion. In this case, a man by the name of "H.T", who had no prior personal or family medical history of allergic disease, received a blood transfusion for anemia. Subsequently, after an encounter with a horse at Central Park, the man suffered a violet asthma attack (4). While this was an observational report, the first experimental evidence was provided by Prausnitz and Küstner. Küstner, who was a German gynecologist, had previously noted that he developed allergic symptoms after consuming fish. Prausnitz, who was also a fellow German physician, decided to inject some of Küstner's serum into the skin of his abdomen. After eating some fish himself, Prausnitz's, who had no prior adverse reactions to fish, suffered from hot, red, swollen skin at the site of the serum injection, confirming their hypothesis that Küstner was indeed allergic to fish. The work of these two men led to the development of the passive transfer of a positive skin test, later coined the PK test (5).

Although these types of hypersensitivities had been described as allergies, a term coined by Clemens Peter Freiherr von Pirquet, two American physicians felt that the "allergy" label was too limiting. Thus, in 1923, Coca and Cooke introduced the word "atopy" into medical vernacular. They felt atopy, which was derived from the Greek word "*ἀτοπία"* meaning placelessness was a more suitable term to cover all forms of immediate hypersensitivities (6). They went on to add that atopy was a result of "bodies" they referred to as "reagins". However, ironically enough they recommended that the term "antibody" should be avoided as they determined that "no evidence of these bodies appear as the result of immunologic stimulation" (7).

It took the next 40 years and the work of two pioneering groups to determine that "reagin" was indeed an antibody. Two Swedish scientists by the name of Bennich and Johansson studied structure and function of immunoglobulins (Ig). Their primary source of human Ig was multiple myeloma serum. In the summer of 1965, they came across a serum of a patient, ND, whose serum contained an atypical Ig subtype. When compared to IgA, IgM, IgG, or even the newly identified IgD, they saw no similarities. They called this new protein IgX, for the unknown Ig. After further investigation, they discovered that IgX had unique biochemical properties which were distinct from the other four types. They went on to develop very sensitive assays for the detection of IgX and noted that the normal serum concentration of IgX as compared to IgG was about 200,000 fold less. After collaborating with D.R. Stanworth, it was shown that IgX could block the PK test. Thus, all evidence was pointing to a new class of Ig. Eventually IgX was renamed IgND after the initial patient from which it was isolated. Because of the finding that IgND could inhibit the PK test, Bennich and Johansson began to look at IgND in the context of atopic disease and ultimately went on to develop the radioallergosorbent test (RAST) (8).

Meanwhile in Denver CO, a husband and wife team were approaching a similar problem but from a different angle. Kimishige and Teruka Ishizaka were interested in identifying the biological cause of the reagin-mediated histamine release reaction. In 1964, they first reported that the antibody responsible for this was a type of IgA, which they initially called γA (9). While this was not widely accepted in the field, they persevered and ultimately identified an antiserum capable of precipitating a serum fraction that could block the PK reaction (10). This activity did not appear to be similar to any of the other known four Ig types, thus they called it γE-globulin because it had the ability to cause an erythema reaction. However, despite all their hard work, the Ishizakas were never able to make a purified preparation of γE-globulin from normal human serum, which given its extremely low concentration in normal serum is not too surprising.

In early 1967, a fruitful collaboration between the Ishizakas and the Swedish took place. They decided to swap reagents and it was indeed found that IgND and γE-globulin were one in the same. In February of 1968 at a workshop at the WHO, it was agreed upon that IgE would be the new nomenclature for the newly identified fifth Ig subclass (11).

II. Biological properties of IgE

Like all immunoglobulins, IgE is comprised of two identical light chains, either κ or λ, and two identical heavy chains, the ε chains, which are held together by disulfide bonds. Both light and heavy chains each contain a variable and constant domain. This basic chemical structure of Igs was solved by the work of Edelman and Porter for which they received the Nobel Prize in 1972 (12). The variable regions of IgE are responsible for antigen binding specificity, whereas the heavy chain determines effector function. The characteristics that make IgE unique from the other subclasses reside in the ε heavy chain component. IgE has a molecular weight of about 190kDa, which when resolved under reducing conditions yields two light chains and two heavy chains of about 23kDa and 72kDa respectively (13). IgE is slightly larger than the monomeric forms of IgG, IgA, and IgD because it has an additional domain in the heavy ε chain called Cε4 and it is more heavily glycosylated. Studies with tunicamycin have shown that the glycosylation of IgE is N-linked, however these additional sugar moieties are not critical for IgE binding to its receptors on mast cells (Reviewed in 14).

In addition to its unique structure, IgE has biological activities that are much different that it's other Ig counterparts. IgE fails to neutralize, opsonize, participate in antibody directed cellular cytotoxity (ADCC), or fix complement. IgE also fails to transport across epithelial surfaces or the placenta and only under instances of widespread inflammation, can IgE diffuse into extravascular sites. IgE has a half life of approximately 2 days whereas IgG is stable for up to three weeks. The reported mean serum levels of IgE are approximately 0.5 -3 x 10^{-5} mg/mL which is much less than 1.5mg/mL, 9mg/mL, or 2.1mg/mL as seen with IgM, IgG1, or IgA respectively (Reviewed in15).

Although most equated with unwanted reactions of the immune system, IgE serves a very important evolutionary role in the defense against parasitic disease. Elevated levels of IgE are observed in both man and mouse during parasite infections. Capron *et al.* have shown a critical role for IgE in the clearance of *Schistosoma mansoni* (16) and it has been reported that IgE deficient mice have increased worm burden following infection with *S. mansoni* (17), *Brugia malayi* (18), and *Trichinella spiralis* (19). This protective effect of IgE in the context of microbial pathogens is the basis for the Hygiene Hypothesis. This theory, originally proposed by the epidemiologist Strachan in the 1980s, states that the declining microbial exposure in industrialized countries is a major causative factor in the increased rise in atopic disease (20).

Whether the IgE is directed against a pathogenic helminth or against normally innocuous pollen, IgE's effector functions are mediated through its ability to bind and cross-link IgE receptors through its Fc portion. There are two major classes of IgE Fc receptors which are named due to their relative binding of IgE, the high affinity, FcεR1, and the low affinity, FcεRII. In fact FcεR1 has the highest affinity for its ligand out of all the known Fc receptors with measurements in the range of 10^{10} to 10^{12} M^{-1}. Furthermore, in addition to its high affinity, FcεR1 has an extremely low dissociation rate which results in a lengthy retention rate. The presence of FcεR1 was first discovered by Ishizaka when radioalabeled human IgE was shown to bind monkey mast cells and human basophils (17). FcεR1 is comprised of four distinct subunits called the alpha (α), beta (β), and gamma (γ) chains resulting in an actual stoichiometry of $\alpha\beta\gamma_2$. The alpha chain is responsible for ligand binding, the beta chain serves as an amplifier, whereas the gamma chain contains an immunoreceptor tyrosine based activation motif (ITAM) responsible for initiating the signaling cascade. FcεR1 is expressed in this form in both rodent and human mast cells and basophils, however a $\alpha\gamma_2$ trimer has been reported to be present on human antigen presenting cells, eosinophils, and platelets (21,22). Upon initial encounter with antigen, B cells produce IgE which then binds to FcεR1. Upon second antigen encounter, cross linking of the receptor-bound antigen specific IgE occurs, leading to cellular degranulation and the biosynthesis of bioactive lipid mediators (23). Although both FcεR1 and FcεRII bind IgE, molecular analysis has shown that their only similarity is a common ligand. FcεRII will be discussed in more detail below.

III. Control of IgE Synthesis and Allergic Disease

Since IgE is the instigator of allergic disease, it is important to understand the mechanisms of IgE synthesis and regulation. B cells must participate in a two step process in order to successfully produce IgE, or any other Ig subtype for that matter. The first step requires that the B cell produce a functional Ig gene. This process known as VDJ recombination begins in the pro B cell stage and is completed by the pre B cell stage of lymphocyte development. VDJ occurs through a series of DNA rearrangement and recombination events and was first described by Susumu Tonegawa, for which he received the Nobel Prize in 1987 (12). VDJ recombination does not occur in the absence of the recombination activating genes (RAG-1 and RAG-2). The importance of RAG in the immune system is exemplified by patients with Omenn Syndrome. These patients have a mutation in either RAG-1 or RAG-2 and suffer from a severe immunodeficiency (24).

IgE, like other Ig subtypes, is produced after a B cell receives the appropriate signals to undergo class switch recombination (CSR). CSR allows the B cell to alter the isotype of the antibody they produce but maintain antigen specificity. This is important because different isotypes have different effector functions. In order for CSR to occur, the enzyme activation induced cytidine deaminase (AID) is critical. AID is an RNA editing enzyme that is responsible for deaminating cytidines on ssDNA. Base excision repair (BER) then occurs. BER results in dsDNA breaks which are repaired by non homologous end joining (NHEJ). The discovery of AID by the Honjo lab was a pivotal discovery in the field of CSR (25). The importance of AID is highlighted by the disease Hyper IgM (HIGM) syndrome type 2. This is an autosomal recessive disorder in which the affected persons express a mutation in AID and fail to undergo CSR, thus resulting in only the high production on IgM (26).

The appropriate signals that a B cell needs in order to undergo CSR come from cytokines and cell surface receptor signaling. The classical pathway leading to production of IgE requires interleukin 4 (IL-4) and CD40 in both man and mouse, however in the human interleukin 13 (IL-13) can work in place of IL-4. In order for CSR to occur, first the Iε promoter is activated which results in production of germline Cε transcripts (GLTs). The T_H2 type cytokines (IL-4 and IL-13) are potent inducers of εGLTs in B cells (27). Both of these cytokines signal through the signal transducers and activators of transcription 6 protein (STAT6). STAT6 is critical for the production of εGLT as it has been reported that mice lacking STAT6 fail to produce IgE (28). The second signal necessary for IgE production comes from ligation of CD40 on the B cell membrane. CD40 is a member of the tumor necrosis factor (TNF) superfamily and signals via nuclear factor kappa-light-chain-enhancer of activated B cells (NFκB). CD40 transmits its signal after binding its ligand CD154 (CD40L). CD154 is expressed on T cells, thus class switching to IgE is historically considered a T dependent phenomenon. The significance of this CD40-CD154 interaction is also highlighted by the disease HIGM. Although a mutation in AID can result in type 2 HIGM, mutations in either CD40 or CD154 result in types one and three respectively (29). Furthermore, mice with mutations in either CD40 or CD40L fail to produce IgE both at baseline or post immunization (30, 31).

Although classically IgE is produced via T cell help, there have been reports of alternative, T independent pathways of IgE production. However it is important to note that the presence of IL-4 is required for each of the following to occur. The corticosteroid, hydrocortisone, has been shown to stimulate IgE production from both leukemic (32) and normal (33) human B cells. When this observation was first made in the early 1990s, the mechanism of action was unknown. Today it is hypothesized the hydrocortisone up- regulates CD154 expression on B cells themselves. Thus despite the fact that the actual T cell is not required, this hormonally enhanced IgE production is still dependent on the CD40-CD154 interaction (34). Two new members of the TNF superfamily, B cell activating factor belonging to the TNF family (BAFF) and a proliferation inducing ligand (APRIL) have also been shown to induce CSR to yield IgE (35). These ligands bind specific receptors on the B cell and result in activation of NFκB. This pathway has proven important for the response to T independent antigens as mice lacking one of the BAFF and APRIL receptors, transmembrane activator and calcium modulator and ctyophilin ligand interactor (TACI), fail to produce Ig to T independent antigens, such as TNP-Ficoll (36). Lastly, infection with the Epstein Barr virus has been described as a means to induce IgE production from human cells. The proposed mechanism for the increase in IgE production is attributed to molecular mimicry between the virally encoded LMP1 protein and CD40 (37).

Because the IgE synthesis pathway has been so eloquently mapped, it is a logical target for pharmacologic intervention as a means to control atopic disease. Currently no treatments exist to prevent atopic disease, only to alleviate the symptoms. However, a major drawback to this is that mechanisms required for isotype switching to IgE are shared with other Ig subclasses. The adverse events of CSR blockade, such as the development of a secondary immunodeficiency, far outweigh the benefits of reducing allergic disease symptoms. One unique target in the control of IgE synthesis is that IgE depends on either IL-4 or IL-13, whereas the requirement for these cytokines is not apparent in other isotypes. Furthermore, IL-4 is not only important for isotype switching to IgE; it is central to the development and maintenance of a T_H2 phenotype which results in the production of IL-4, IL-5, and IL-13. Clinical trials have been performed using a soluble form of the IL-4 receptor, however unexceptional results were obtained. This could be due in part to the short half-life of the molecule (38). Another cytokine targeted means to control IgE is through the use of interferon gamma (IFNγ). IFNγ has been shown to inhibit the development of T_H2 cells, thus inhibiting IgE production (39) Although preliminary studies have shown promise in animal studies (40,41), as is the case with any cytokine based therapy, the side effects are great and the improvements must be greater than the adverse events.

Aside from the cytokine approach, a second area of investigation is focused on IgE's interaction with its receptors. Because most of the immunopathology seen in atopic disease is a result from cross linking of FcεRI, blocking this binding has been an attractive target. The crystal structure of the FcεRI/IgE complex is actually known (42) and may ultimately lead to the development of small molecular compounds that can block this interaction. However at present such drugs are not available. An FDA approved current treatment for severe asthma which involves a monoclonal anti-IgE antibody is available. This mab (Xolair® Omalizumab) binds the identical or closely associated region of IgE that interacts with the FcεRI (43, 44). While preliminary data indicates that Omalizumab is efficacious, the disadvantages of the drug regimen are cost and dosage form. Additionally, since IgE synthesis is not inhibited, the patient will need to have repeated, monthly injections.

IV. CD23

As stated before, IgE has two receptors, FcεRI, and FcεRII. FcεRII is sometimes referred to the low affinity IgE receptor, however this is a somewhat misleading name as the affinity of the binding has been reported to be in the 10^8 to 10^9 M^{-1} range (45, 46). FcεRII, also known as CD23, is very unique in terms of Fc receptors. Instead of the Ig-like domains usually seen in this class of receptors, CD23 is a member of the calcium dependent (C type) lectin family and is a type II integral membrane protein. The human form of CD23 is comprised of a 23 amino acid cytoplasmic domain, a 21 amino acid transmembrane domain, and a 277 amino acid extracellular domain which produces a final 321 amino acid (45kDa) protein with one N-linked glycosylation site at amino acid 81. The extracellular membrane bound forms of CD23 contains three lectin “heads” which extend outward from the plasma membrane by a triple α helical coiled-coil “stalk” (47). The gene for human CD23 lies on the 19th chromosome and is a single copy gene made up from 11 distinct exons. Human CD23 (hCD23) has two splice variants, CD23a and CD23b, which differ by six amino acids on the N-terminal side. CD23a is present only on B cells and follicular dendritic cells (FDCs), whereas CD23b is expressed on a wider variety of hematopoietic cells including monocytes and eosinophils and is induced by IL-4 (rev in 17). Murine CD23 (mCD23) on the other hand has no splice variants, limited cellular distribution, lies on the 8th chromosome, and is a 49 kDa protein with two N-linked glycosylation sites. The size discrepancy between the two species can be accounted for the mCD23 having an additional 21 amino acid repetitive sequence in the stalk. Another interesting difference between mCD23 and hCD23 is that hCD23 contains an inverted RGD sequence, which is thought to play a role in adhesion (rev in 48).

The first evidence that IgE could bind a hematopoietic cell other than the mast cell was provided by Lawrence *et al.* in 1975 (49) by using radiolabeled IgE and showing it had the capability to bind human peripheral blood mononuclear cells (PBMC). Years later, Sugden *et al.* would describe the presence of a cell surface specific protein that is expressed post Epstein Barr Virus (EBV) infection which was later referred to as the EBV cell surface antigen (EBVCS) (50,51). Two years later, another group would describe a B cell activation marker (BLAST-2) that is expressed on activated B cells and chronic lymphocytic leukemia cells (CLL) (52). At the Second International Workshop on Human Leukocyte Differentiation Antigens, a 45kDa B cell activation antigen was given the CD23 moniker (rev in (17). With the discovery of specific monoclonal antibodies, Kishimoto’s group (53) and

Bancherau's group (54) would show that FcεRII was identical to CD23. Thus it was determined that FcεRII, CD23, EBVCS, and BLAST-2 were all the same protein.

Because CD23 was identified as an IgE receptor, many studies have focused on the role of it in the context of allergic disease. A pivotal study by the Saxon group showed that the addition of antibodies targeted against the lectin domain of CD23, as well as anti-IgE/IgE complexes, inhibited human IgE synthesis *in vitro* using either an IgE producing plasmacytoma line or B cells from atopic patients (55). Animal models have proven valuable in better understanding CD23 biology. CD23 deficient mice exhibit elevated serum IgE post antigen challenge (56), whereas transgenic mice engineered to over-express CD23 (CD23Tg) showed a reduction in IgE after antigen challenge (57, 58). In recent studies, CD23-/- mice have been shown to exhibit increased antigen-specific IgE, airway hyperresponsiveness, and eosinophilia after sensitization and challenge in a murine asthma model (59, 60). Lastly mutations in CD23 in the NZB mouse strain have been reported and these mice have reduced cell surface expression of CD23 and higher levels of circulating IgE (61). Thus, CD23 has been appreciated to be a natural negative regulator of IgE synthesis although the exact signaling mechanism is unknown.

CD23 is prone to proteolytic cleavage which results in a soluble form of the receptor known as sCD23 being shed from the cell surface. Once CD23 is removed from the cell surface, its negative regulatory function is diminished and it can even boost IgE production. This is illustrated by the fact that enhanced CD23 cleavage results in increased IgE production in mice (62) and that the addition of sCD23 can enhance human *in vitro* IgE production (63). Through the use of inhibitor studies, cell-surface metalloproteases have previously been implicated as the "sheddase" involved in CD23 cleavage (64). Christie *et al.*

demonstrated that the metalloprotease inhibitor batimastat inhibited CD23 degradation which subsequently resulted in a decrease in the amount of IgE produced. Interestingly, IgE levels in immunized mice treated with batimastat were also suppressed (65). In addition to its effects on IgE, sCD23 has been linked to the activation of macrophages, via interaction with CD11b/CD18 or CD11c/CD18, resulting in the release of pro-inflammatory mediators and the onset of inflammatory disease in the human system (66). Thus targeting CD23 and its potential “sheddase” could serve as a potential therapeutic avenue to explore in the control of atopic disease.

V. Dissertation Objective

Based on CD23’s role as natural negative regulator of IgE synthesis, the major goal of this dissertation research was to further examine the role of CD23 in human B cell biology with the idea that we would elucidate the identity of the CD23 sheddase. In collaboration with the Blobel laboratory, ADAM10 was identified as the enzyme responsible for the ectodomain shedding of CD23 in both man and mouse. It was during the course of these studies that three important discoveries were serendipitously made. The first is that a specific inbred mouse strain, 129/SvJ, posses 5 mutations in CD23, resulting in reduced CD23 surface expression and higher levels of IgE. The second was that human and mouse B cells possess a unique neurotransmitter receptor, called the kainate receptor. This receptor when activated by glutamate led to an up-regulation of ADAM10, increased production of sCD23 and Ig, and increased cellular proliferation. The third is that a specific type of leukemia known as B cell chronic lymphocytic leukemia has extremely elevated levels of CD23, sCD23, and ADAM10. Thus this work highlights the importance of the CD23-ADAM10 interaction in human disease.

MATERIALS AND METHODS

I. Animals, antibodies, cytokines, cell lines, and media reagents.

BALB/cJ, C57BL/6J, 129/SvJ, and Wsh mice were all purchased from the Jackson Laboratory (Bar Harbor, ME). GluK2 deficient mice were generated as described (67) and kindly provided by Anis Contractor at Northwestern University. All mice were housed in the VCU Division of Animal Research accredited animal facilities. At the onset of experiments, mice were between the ages of 6 and 12 weeks. All studies involving the use of animals were approved by the VCU Institutional Animal Care and Use Committee (IACUC).

EC-CD23 (68), the mouse anti-CD23 monoclonal antibody 2H10 (69), and the anti-CD23 polyclonal antibody anti-LZ-CD23 (68) were manufactured in the Conrad laboratory as previously described. The anti-mouse IgE hybridomas B1E3 (70) and R1E4 (kindly provided by M. Kehry) and the mouse IgE anti-DNP hybridoma (kindly provided by D.H. Katz) were all maintained in our laboratory. For human studies, the anti-IgE hybridoma 4.15 and IgE hybridoma JW8 were both obtained from the American Type Culture Collection (ATCC, Manassas, VA) and maintained in our laboratory. For anti-CD40 stimulation, the anti-mouse monoclonal antibody FGK-45 hybridoma (kindly provided by F. Finkelmann) and the anti-human monoclonal antibody G28.5 hybridoma (ATCC) were both maintained in our laboratory. All the aforementioned antibodies were purified as described below. When called for, antibodies were biotinylated using a 100-fold molar excess of EZ-link Sulfo-NHS-biotin (Pierce, Rockford IL) per manufacturer’s protocol and dialyzed against 1X PBS.

Baculovirus supernatant containing recombinant murine IL-4 was a gift from Dr. William Paul (National Institutes of Health, Bethesda, MD). Human IL-4 was purchased from R&D Systems (Minneapolis, MN). Human IL-21 was produced as previously described (71). The human cell lines Daudi and Jiyoye were obtained from ATCC and 8866 was kindly provided by S. Ruddy.

RPM1-1640, Dulbecco's Modified Eagle Medium (DMEM), and DMEM:HAMS F-12 were all purchased from Invitrogen (Carlsbad, CA). Heat inactivated fetal bovine serum (FBS) was purchased from Gemini Bio-Products (West Sacramento, CA). L-glutamine, penicillin, streptomycin, sodium pyruvate, amphotericin B, non-essential amino acids (NEAA), gentamicin, and HEPES were all purchased from Invitrogen. 2-mercaptoethanol (2-ME), bovine serum albumin (BSA), insulin, transferrin, kainic acid (KA), dimethylsulfoxide (DMSO), L-glutamic acid (Glu), and antagonists (topiramate (TPM), NS102 and NBQX) were all purchased from Sigma-Aldrich (St. Louis, MO). Hank's balanced salt solution (HBSS) was purchased from Invitrogen.

II. Preparation and purification of monoclonal antibodies.

All antibodies were prepared from hybridoma cell culture supernatant using the CL-1000 Adhere CELLine flasks (Integra Biosciences, Switzerland). Cells were grown in complete RPMI-1640 containing 10% fetal bovine serum, 2 mM L-glutamine, 50 µg/mL penicillin, 50 µg/mL streptomycin, 1 mM sodium pyruvate, 50 µg/mL amphotericin B, 50µM 2-mercaptoethanol, 2 µg/mL gentamicin, 100 µM NEAA, and 20mM HEPES buffer. Flasks were seeded with 100 x 10^6 cells. Supernatants were harvested every three days and cells were kept in continuous culture for up to 6 months. When supernatants were harvested, they were centrifuged at 2000RPM for 5 minutes and stored at -20°C until purification. Just prior to purification, supernatants were pooled and further clarified by centrifugation at 5,000 RPM for 30 minutes. All antibodies were purified by hydrophobic charge induction chromatography using the MEP HypeCel sorbert (Pall Life Sciences, East Hills NY) which is immunoglobulin selective and binds a broad range of Ig subtypes as previously described (72). After chromatography was complete, fractions were separated on a 10% Bis-Tris gel (Invitrogen) by SDS-PAGE under reduced conditions. To visualize proteins, gels were stained with SDS-PAGE stain (2.5g Commassie Blue Brilliant Blue R-250, 100mL glacial acetic acid, 450mL methanol, and 450mL dH_2O) for 30 minutes during continual motion. Gels were then subsequently de-stained with SDS-PAGE Destain (30% methanol, 10% acetic acid, 60% dH_20). After the fractions which were determined to contain purified antibody were pooled together, protein was concentrated by ultrafiltration with an Amicon filtration unit (Millipore Corporation, Bedford, MA) and dialyzed against 1X PBS.

III. B cell purification and culture.

For murine studies, B cells were purified by negative selection from spleens as previously described (73). Briefly, splenectomies were performed and spleens were made into single cell suspensions by mechanical shearing between 2 sterile, frosted glass slides. Single cells suspension was washed one time in serum free media (SFM) and then red blood cells were lysed with ACK lysis buffer (Quality Biological, Inc. Gaithersburg, MD). T cells were depleted by complement mediated cell lysis. T cells were first labeled with rat anti-mouse Ly-1, rat anti- mouse Ly-2, and rat anti mouse Thy1.1 followed by labeling with Mar18.5 (anti-rat kappa). Guinea pig complement was added for 30 minutes at 37°C. After incubation, the cells were layered over a discontinuous Percoll (GE Healthcare, Piscataway, NJ) gradient and centrifuged at 3000 RPM for 13 minutes in the absence of a break. Percoll was used at a 70% solution and was diluted from stock using a Percoll mix solution (45mL 10X PBS, 3mL 0.6N HCl, and 132 mL dH_2O). If different percentages of percoll are needed, they are diluted from the 70% stock. Total B cells were taken which appear at the 70% and 50% Percoll interface. Alternatively, naïve B cells were isolated via negative selection through magnetic activated cell sorting (MACS) by using CD43 microbeads (Miltenyi, Auburn CA) according to manufacturer’s protocol.

Human tonsils were obtained from routine tonsillectomies at Henrico Doctors Hospital (Richmond, VA) or the VCU Tissue Data Acquisition and Analysis Core (TDAAC). Tonsils were placed in SFM supplemented with antibiotics and mechanically disrupted using a Seward Stomacher 80 Biomaster Lab Blender (Brinkmann, Westbury, NY) at normal speed for 60 seconds. To obtain a single cell suspension, the resulting product was underlayed with Ficoll–Hypaque (GE Healthcare Piscataway, NJ). Following centrifugation (20 min at 400 × g), the cells at the interface were removed under the laminar flow hood, transferred to new tubes and washed in sterile PBS. Assessment for total cell yield was done using Gentian Violet staining and viability using Trypan blue exclusion. Positive selection was used to isolate naïve B cells. The tonsilar cells were incubated with a FITC-anti-human IgD (BD Pharmingen San Diego, CA) for 30 min on ice and B cells were isolated by MACS using the Miltenyi anti-FITC microbeads, per manufacturer’s instructions (Miltenyi Biotec Auburn, CA). Final B cell preparations were >95% pure IgD+ by FACS analysis.

Once B cells were isolated, regardless of species, they were cultured in complete media containing 10% heat inactivated fetal bovine serum, 2 mM L-glutamine, 50 µg/mL penicillin, 50 µg/mL streptomycin, 1 mM sodium pyruvate, 50 µg/mL amphotericin B, 50µM 2-mercaptoethanol and 20mM HEPES buffer. The media base used was either RPMI or DMEM as indicated. Once the media is complete, it is referred to as either CRPMI-10 or CDMEM-10. Human B cells were cultured with 10ng/mL IL-4, 1µg/mL a-CD40, and 200ng/mL IL-21. Mouse B cells were cultured with 10,000U/mL IL-4 and µg/mL a-CD40. To examine immunoglobulin production, cells were cultured at cell densities ranging from 150,000 cells/well - 4,500 cells/well in 96 well tissue culture plates. The rationale for using various cell densities is so that all immunoglobulin isotypes can be analyzed simultaneously (74,75). For murine studies, cell free supernatants were harvested on day 8 whereas human studies required a longer culture period, thus cell free supernatants were harvested on day 14 post culture initiation.

As an alternative to purified naïve B cells, peripheral blood mononuclear cell (PBMC) cultures were sometimes employed. Buffy coats were provided by the Virginia Blood Center or EDTA Vaccutainer tubes were provided by TDAAC. Whole blood was transferred to 50mL tubes, diluted with PBS, and Ficoll-hypaque density gradient centrifugation was performed in a similar manner as with human tonsilar B cell preparations. For primary cell culture of PBMC from B cell chronic lymphocytic cultures (BCLL), ACL4 media was modified and used (76). Modified ACL4 media consists of a 50:50 (v/v) mixture of DMEM:HAMS F-12 supplemented with NEAA (100 µM), sodium pyruvate (1 mM), L-glutamine (2 mM), HEPES (20 mM), penicillin (50 000 U/L), streptomycin (50 mg/L), fungizone (1.25 mg/L), gentamicin (10 mg/L), bovine serum albumin (BSA, 2 g/L), insulin (5 mg/L), transferrin (5 mg/L), 2 -mercaptoethanol, and 10% heat inactivated FBS.

IV. Proliferation analysis.

Cells were grown in sterile 96-well culture plates at indicated concentrations in complete media. After 96 hours of growth, a 24 hr pulse $[H^3]$-thymidine (Perkin Elmer, Waltham, MA) was used. Plates were then harvested using a Packard Filtermate 196 cell harvester (Packard Instrument Co, Meriden CT) onto Unifilter GFC 96 well plates (Perkin Elmer). 24 hours later, a plastic backing was added to the plates, 40µL of Microscint-20 (Perkin Elmer) was added to each well, and plates were counted using a Topcount Scintillation MicroPlate Counter (Perkin Elmer).

Carboxyfluorescein diacetate succinimidyl ester (CFSE) (Molecular Probes Eugene, OR) was prepared according to the manufacturer's recommendations. Resting B cells were washed and re-suspended at $5x10^6$cells/mL in PBS. CFSE was then added at the manufacturer's recommended dilution and incubated in the dark at room temp for 5 minutes. Reaction was quenched by the addition of ice cold FBS and cells were then washed and plated at $1x10^4$ cells/200 µL in a 96 well plate containing 10 ng/mL IL-4, 1 µg/mL anti-CD40, and 200ng/mL IL-21 in the presence or absence of glutamate. After 5 days of culture, cells were harvested and analyzed by flow cytometry using a BD Canto. Analysis was performed using FCS Express software V3 (De Novo Software Los Angeles, CA).

V. ADAM10 inhibition studies.

The ADAM10 selective inhibitor GI254023X was kindly provided by Neil Broadway (GlaxoSmithKline, NC) (77). The ADAM10 selective inhibitor INCB008765, the ADAM10/ADAM17 selective inhibitors INCB003919 and INCB009588, and the ADAM17 selective inhibitor INCB012998 were kindly provided by Peggy Scherle (Incyte Corporation, Wilmington, DE) (78). Marimastat was kindly provided by Ouathek Ouerfelli (Memorial Sloan Kettering Cancer Center, New York, New York). All inhibitors were dissolved in DMSO and thus DMSO was used as a vehicle control for all studies. Optimal concentrations were used for each inhibitor based on suggestions of the manufacturer and dose response curves performed for each. The pSuper RNAi System vector containing an siRNA targeted against human ADAM10 was kindly provided by Carl Blobel. The pSuper siRNA was introduced into 8866 cells via AMAXA Nucleofector transfection technology (now owned by Lonza, Basel Switzerland). Readout for efficacy for all means of ADAM10 inhibition was soluble CD23 release.

VI. Kainate receptor studies.

To stimulate cells through the kainate receptor, the nonspecific agonist glutamate was used. All agonists were water soluble and thus dissolved in the complete culture medium used at the time. For agonistic studies, the stimulating agent was added simultaneously with cell culture reagents.

To antagonize the kainate receptor, the GluK2 specific antagonist 6,7,8,9-Tetrahydro-5-nitro-1H-benz[g]indole-2,3-dione 3-oxime (NS102) was used. As we saw no presence or involvement of GluK1 containing KAR, there was no need to antagonize this receptor subtype. Because there are three types of ionotropic glutamate receptors, we employed the use of specific antagonists against the AMPA receptor 1,2,3,4-Tetrahydro-6-nitro-2,3-dioxo-benzo[f]quinoxaline-7-sulfonamide disodium salt hydrate (NBQX) or 2,3:4,5-Bis-O-(1-methylethylidene)-36-D-fructo-pyranose sulfamate (TPM) against the NMDA receptor. All antagonists were purchased from Sigma-Aldrich, dissolved in DMSO, and used at recommended concentrations. Cells were pre-treated with either vehicle control or antagonist for 1hr at 37^{o}C prior to the addition of KAR stimulation. We saw no toxicity with at the concentrations of any antagonist used.

VII. RNA Isolation, RT-PCR reactions, and qPCR reactions.

Total RNA was isolated from cells using the Trizol (Invitrogen) reagent according to manufacturer's recommendation. Reverse transcriptase polymerase chain reaction (RT-PCR) was performed using the AccessQuick™ RT-PCR System (Promega Madison, WI). Briefly, 1000ng RNA was mixed with gene specific primers (10 pmoles/reaction), sterile nuclease free water, and 1X AccessQuick™ Master Mix which contains *Tfl* DNA polymerase, dNTPs, magnesium sulfate and a propriety reaction buffer. The reverse transcriptase reaction was performed using 5U of the avian myeloblastosis virus (AMV) reverse transcriptase. The following primers were used and synthesized by Integrated DNA technologies (Coralville, IA). All primers were designed using the VectorNTI software (Invitrogen).

mCD23 sense: CTG CCA TGG AAG AAA ATG
mCD23 antisense: TGA GCA GAA GTT TGT CAG G
ACTIN1: ACT CCT ATG TGG GTG ACG AG
ACTIN2: CAG GTC CAG ACG CAG GAT GGC
hADAM10 sense: CAT TAC ACC AAA AAC ACC AGC GTG
hADAM10 antisense: TCC ACA CCA ATA TTT GGG AAA CGG
GRIK1 sense: TTC CTC TGC TAT ATC CTC CCT CAG AC
GRIK1 antisense: CAA GTG TTT AGA CAC TTC GCC AGC AG
GRIK2 sense: ACC ACT CGA CGC ATC CTC ATT TCT AC
GRIK2 antisense: CAG ACA CCA CAT GCA CAG CAT CAT AC
GRIK3 sense: ATA CAA CAT CCG CCT GAA GAT CCG TCA G
GRIK3 antisense: TCG ATA CAG GAT GCT CAC ACC AAG TGT C
GRIK4 sense: CAG CTC CAT CAT CAG CAA CAT CTG TG

GRIK4 antisense: ATG TGG CCG GTA AGA CCT TCC AAT TC

GRIK5 sense: TCA AGG AGA TCC GTG ATG ACA AGG TGT C

GRIK5 antisense: TAG GCA AGA AGC ATG AAG AGC CAC ACA G

G3PDH sense: ACC ACA GTC CAT GCC ATC AC

G3PDH antisense: TCC ACC ACC CTG TTG CTG TA

PCR products were run on a 1% tris borate EDTA (TBE) or tris acetate EDTA (TAE) agarose gel, stained with either ethidium bromide (VWR, Chester, PA) or GelRed (Biotium, Hayward CA), and visualized using the Alpha Innotech Fluorchem imager (San Leandro, CA).

All quantitative polymerase chain reactions (qPCR) were performed in the Applied Biosystems Prism® 7900 Sequence Detection System (AB, Foster City, Ca) using the TaqMan® One Step PCR Master Mix Reagents Kit. All the samples were tested in triplicate under the conditions recommended by the fabricant. The cycling conditions were: 48ºC/30min; 95ºC/10min; and 40 cycles of 95ºC/15sec and 60ºC/1min. The cycle threshold was determined to provide the optimal standard curve values (0.98 to 1.0). The probes and primers for ADAM10 (#Hs00153853_m1) were synthesized and purchased from AB. The probes were labeled at the 5’ end with FAM (6-carboxyfluoresceine) and at the 3’ end with TAMRA (6-carboxytetramethylrhodamine). Human beta-actin or human glyceraldehyde 3-phosphate dehydrogenase (GAPDH) from the Pre-developed TaqMan®Assay Reagents was used as endogenous control. The reactions were performed in the VCU Nucleic Acid Research Facilities.

VIII. Cloning and sequence analysis.

Purified total B cells isolated from the spleens of BALB/cJ, 129/SvJ, and NZB mice were stimulated for 48 hours at $1x10^6$ cells/mL in CRPMI-10. RNA was isolated and RT-PCR was carried out as described above using mCD23 sense and antisense primers. The resultant 1.1 Kb PCR product was visualized and excised from a 1% TAE gel using the GeneClean III kit according to the manufacturer's protocol (QBiogene, Irvine, CA). The purified PCR product was ligated overnight at 14°C into the pCR2.1 vector (Invitrogen) following the manufacturer's protocol. From the ligation mixture, 2µL was used to transform INVαF' One Shot *E.coli* (Invitrogen) according to the manufacturer's heat-shock protocol. Prior to plating, 40 µL of a 40 mg/mL X-Gal solution (Fisher Bio-tech, Fair Lawn, NJ) was spread onto Luria Broth (LB) agarose plates containing 100 µg/mL ampicillin (Invitrogen) for blue/white screening. 50 and 150 µL of the bacteria culture from the heat shock step were spread onto the X-Gal soaked LB plates, which were incubated overnight at 37°C. Several white colonies were picked using the end of sterile flat toothpicks and grown overnight with shaking in 3 mL of liquid LB broth containing ampicillin. Plasmids were isolated by minipreps technique using the QIAprep Spin Miniprep Kit (Qiagen, Valencia, CA). 16 µL of miniprep DNA was digested overnight with 2 µL *Eco*RI (New England Biolabs, Ipswich, MA) plus 2 µL *Eco*RI Buffer in a 37°C water bath in a final volume of 20 µL. Positive clones were identified by running 10 µL of digested plasmid on a 1% TBE gel. Several positive clones were selected and grown up for MaxiPrep analysis. MaxiPrep DNA was isolated with the QIAfilter Plasmid Maxi Kit (Qiagen), digested exactly in the same manner as the miniprep DNA in order to verify positive clones, and sent to the Nucleic Acids Core Facility (VCU, Richmond, VA) for sequencing. DNA was sequenced using the ABI

3100 capillary sequencer and sequence analysis was performed using Vector NTI software (Invitrogen).

IX. Cell surface Phenotyping.

All cells were tested for cell surface antigen expression by direct immunofluorescence and flow cytometric analysis. The antibodies were anti-human IgD-FITC, anti-human CD14 FITC, anti-human CD3 FITC, anti-human CD19 FITC, or anti-human CD23 PE (BD Pharmingen San Diego, CA). For ADAM10 cell surface staining, we used a biotinylated anti-human ADAM10 (R&D Systems) followed by an anti-biotin FITC. For murine studies, anti-B220, anti-Thy1.1, anti NK1.1, and anti-Mac-1 FITC were used (BioLegend San Deigo, CA). For KAR staining, cells were stained with rat anti GluK4 (Santa Cruz Biotech, Santa Cruz, CA) followed by staining with a mouse and human adsorbed goat anti rabbit IgG PE (Southern Biotech Birmingham, AL). Prior to any staining Fc receptors were blocked either by the addition of 2.4G2 for mouse studies or human Fc blocking reagent (Miltenyi). Briefly, 1×10^6 cells were pelleted in 12mm×75mm tubes and washed once in cold FACS buffer (PBS with 0.5% FBS, 0.03% sodium azide). Cells were re-suspended in approximately 80 µL of FACS buffer and 10 µL of 1:1 antibody dilutions in PBS were added. Cells were incubated for 30 min at 4°C, washed once in cold FACS buffer, and then re-suspended in 1mL of FACS buffer. Prior to analysis, propidium iodide (PI) stain was added to determine cell viability. For determination of apoptosis, the Annexin V FITC kit (BD Pharmingen) was used per manufacture’s guidelines. Flow cytometric analyses were performed on a FACSCanto II (BD Biosciences) and data was analyzed using FCS software.

X. Western blot analysis.

Five million cells were lysed in Hepes Buffered Saline (HBS) with 1%NP-40 on ice for 10 minutes. Nuclei were removed by centrifugation and cytosolic proteins were treated with SDS buffer and heated at 70ºC for 10 minutes. Proteins were run on an MES NuPage gel (Invitrogen) and then transferred to nitrocellulose. Blots were stained with a rabbit polyclonal antibody against the human kainate receptor subunit GluK4 (known as *GRIK4* in Genbank) (Chemicon or Santa Cruz Biotech). Detection was performed with a goat anti-rabbit IgG HRP (Southern Biotech) and chemiluminescence was performed with SuperSignal West Pico Chemiluminescence Substrate (Pierce). To ensure equal loading, Ponceau S (Sigma) staining was performed.

XI. Mouse genotyping.

GluK2 mice were generated on a B6.129 mixed background. We received 2 male -/- mice, 1 male -/+ mouse, and 1 female -/+ mouse. All mice were mated to WT C57BL/6J mice and F1 progeny were genotyped. These mice served as foundations for the colony here at VCU. We chose to mate the mice to a pure C57BL/6J mouse so at to eventually move the mice on a pure background. At 21 days old and at the time of wean, mice were separated by gender, ear tagged (National Band and Tag, Newport, KY), and 1cm tail sections were clipped. DNA was isolated from tail samples using the DNeasy Blood & Tissue Kit (Qiagen). Genomic DNA was subjected to PCR using the MangoMix™ PCR reagent (Bioline Taunton, MA). Briefly, 1µL DNA was mixed with specific primers (20 µM), sterile nuclease free water, and 1X MangoMix™ which contains MangoTaq™ DNA polymerase (Bioline), dNTPs, magnesium sulfate and a propriety reaction buffer. Two sets of primers were used in separate PCR reactions. One set of primers was used to identify the presence of the GluK2 gene whereas the other set was used to identify the presence of the neomycin cassette used for disruption. The primers are as follows:

WT primer sense: CAA AGC TTA GTT AAC TGA TAT ACA G
WT primer antisense TTA TGG TTA CAT GCA CAG AGG C
Neomycin sense: TCT CAC CTT GCT CCT GCC GAG AAA G
Neomycin antisense: CAG AAG AAC TCG TCA AGA AGG CG

The resultant PCR reactions were run on a 1.5% TAE agarose gel. Because the MangoMix™ contains a visualization dye, no additional DNA labeling dye was added prior to gel electrophoresis. Representative gels are depicted in Figure 1. Resultant products were approximately 500bp each.

XII. *Nippostrongylus brasillensis* isolation and culture.

Nippostrongylus brasillensis (*Nb*) was kindly provided by Joseph Urban, Jr. (USDA, Beltsville, MD) and was maintained by passage through Wsh mice. *Nb* was isolated from fecal cultures using the Baermann Technique as previously described (79). Briefly, clusters of *Nb* were visualized under a dissecting microscope and isolated using sterile spatulas. The clumps of *Nb* were placed on a moist KimWipe which was resting in a funnel filled with pre-warmed 0.15M NaCl. The funnel was connected to rubber tubing which was clamped at the other end. The modified Baermann apparatus was incubated at 37°C for 45 minutes. After incubation, the clamps were loosened and the NaCl solution (containing the *Nb)* was collected in a 50 mL tube with the remaining fecal culture left on the KimWipe. The tube was centrifuged at 1000 RPM for 3 minutes in the absence of a brake. All but 2 mL of the supernatant was aspirated by sterile transfer pipette. The worms were mixed gently in the remaining NaCl and were counted under the dissecting scope (three counts of 5µL aliquots were performed). Mice were anesthetized in isoflurane (Baxter, Deerfield, IL) and injected (using a 26 gauge precision glide needle (Becton Dickinson, Franklin Lakes, NJ)) s.c. in the scruff of the neck with 500-550 stage three larvae (L3) in 100-200 μL NaCl. At day 5 after injection, mice were placed onto grates of chicken wire (Southern States, Richmond VA) that were fitted into mouse cages. This design allowed for fecal collection in that feces would fall through the grate onto a moist paper towel. The mouse food was replaced with autoclaved, irradiated food to avoid potential mold formation. The paper towel was moistened with water containing Nystatin using a squirt bottle on days 5, 6, and 7. On day 7, mice were sacrificed and feces were collected using an autoclaved spatula. Feces were placed in the bottom of a small Rubbermaid Tupperware container and prepared according to the protocol written by Urban. Briefly, feces were gently mashed so as not to crush the Nb eggs with the spatula and mixed with a roughly equal volume of crushed, autoclaved charcoal (The Scotts Company, Marysville, OH) to achieve a fecal paste. Water containing 240 U/mL Nystatin (Sigma) was added as needed. The fecal paste was mixed 1:2 with an equal mixture of vermiculite (A.H. Hoffman, Inc., Lancaster, NY) and peat moss (Scotts). Water was added as before to obtain a moist culture. The culture was covered with plastic wrap (Fisher) and small holes were punched in the wrap using a sterile pipette tip. The culture was stored in the dark in a drawer and watered every 3-4 days with ~8-10 mL water containing nystatin. *Nb* began hatching approximately 5 days after culture however they were not isolated for experiments until at least 8 days after hatching. New cultures were prepared every 4-6 weeks by isolation and injection into approximately 5 Wsh mice as described above. For experimental use, *Nb* was harvested in an identical manner however mice were not placed on grates and sacrificed at day various time points depending on experimental strain used at the time.

Figure 1. Genotyping of GluK2 KO Mice.

At 21 days old and at the time of wean, mice were separated by gender, ear tagged (National Band and Tag, Newport, KY), and 1cm tail sections were clipped. DNA was isolated from tail samples using the DNeasy Blood & Tissue Kit (Qiagen). Genomic DNA was subjected to PCR using the MangoMix™ PCR reagent (Bioline Taunton, MA). Briefly, 1µL DNA was mixed with specific primers (20 µM), sterile nuclease free water, and 1X MangoMix™ which contains MangoTaq™ DNA polymerase (Bioline), dNTPs, magnesium sulfate and a propriety reaction buffer. Two sets of primers were used in separate PCR reactions. One set of primers was used to identify the presence of the GluK2 gene whereas the other set was used to identify the presence of the neomycin cassette used for disruption. WT mice are indicated by the presence of the GluK2 band and absence of the neomycin band. KO mice are indicated by the absence of the GluK2 band and presence of the neomycin band. Heterozygous mice have the presence of both bands. Both bands are approximately 500bp each.

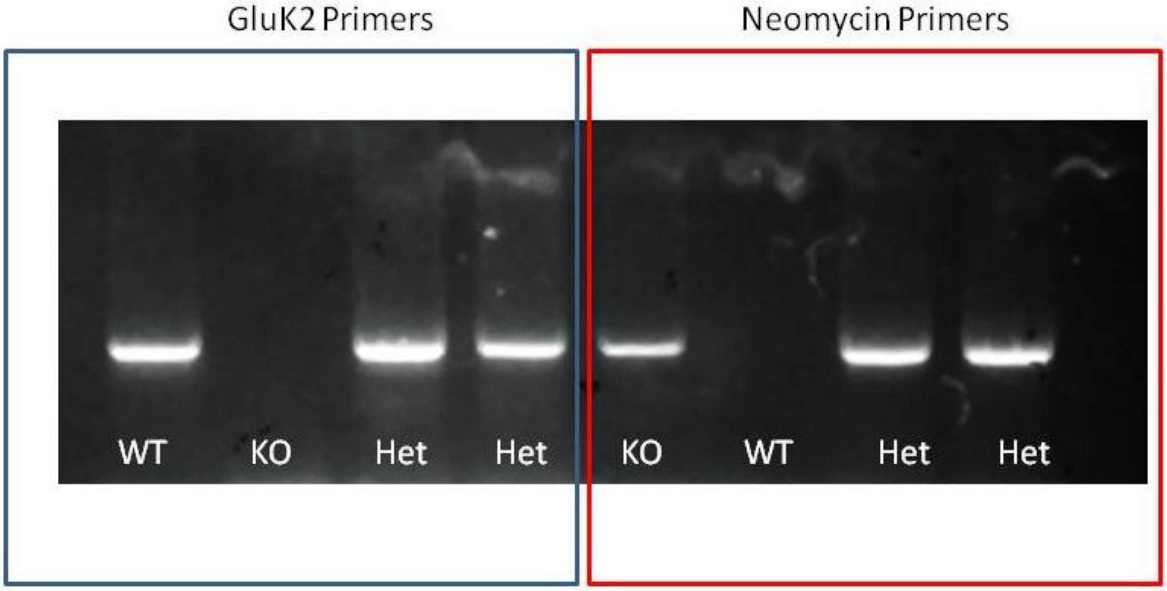
GluK2 Primers
Neomycin Primers
WT
KO
Het
Het
KO
WT
Het
Het

XIII. Immunizations and bleeds.

Prior to any immunization, mice were bled by tail nick with a surgical scalpel (Feather #11 Fisher Scientific). Blood was collected in heparin coated capillary tubes, transferred to 1.5mL eppendorf tubes, and spun at 10,000 RPM for 10 minutes to separate serum from cellular components. After centrifugation, serum was harvested and stored at -20°C until ELISA analysis performed (see section XIV). Mice were injected s.c. with 100µg ovalbumin (Sigma) in 4mg Imject Alum (Pierce) or alum in PBS as a control. On day 9 mice were bled once again. On day 15, mice were boosted with 100µg ova in alum or alum in PBS i.p. On day 22, mice were sacrificed by isoflurane inhalation, cardiac punctured for blood collection, and spleens were saved for analysis.

XIV. ELISAs.

All ELISA coating steps were done in borate buffered saline (BBS). Human soluble CD23 (sCD23) was measured using a standard sandwich ELISA approach, using a mouse anti-CD23 (Clone BU38) coating antibody and sheep anti-CD23 (both from The Binding Site Birmingham, UK). Detection is performed with a goat anti-sheep IgG tagged with horseradish peroxidase (HRP) (Southern Biotech Birmingham AL). Determination of human IgE levels utilized a monoclonal mouse anti-human IgE antibody (clone 4.15) as a capture. Samples and standards were detected using a rabbit anti-human IgE-HRP (Southern Biotech) diluted in PBS/10% FBS. Human IgG or IgM were detected using a goat anti-human IgG or IgM followed by detection with a goat anti-human IgG or IgM tagged with HRP (All from Southern Biotech). Standards for the IgG and IgM ELISAs were purchased from Sigma. IgE standards, JW8, were purified as described. All assays utilized TMB substrate (BD Pharmingen San Diego, CA) and the reactions stopped with 0.18M H_2SO_4. Plates are read at a wavelength of 450nm on a SpectraMax 250 and data analyzed using SOFTmax PRO 3.1.2 software (Molecular Devices, Los Angeles, CA). A four parameter analysis was performed on standard curves using Molecular Devices software. Only dilution values that fell in the linear portion of the curve were used for analysis.

IgE levels in mouse serum or from culture supernatants were determined by coating Immulon ELISA plates with 10 µg/mL of the rat anti-mouse IgE mab B1E3. Standard curves were generated with mouse IgE anti-DNP beginning at a concentration of 1000 ng/mL and diluted 1:2 across the plate. IgE levels were detected by incubation of the plates with the biotinylated rat anti-mouse IgE mab R1E4 followed by streptavidin-AP (Southern Biotech). Plates were developed using pNPP substrate tablets (1 tablet for every 5 mL of substrate buffer) diluted in substrate buffer and read at a dual wavelength of 405-650 nm.

To measure mouse sCD23 levels, plates were coated with 20 µg/mL of the anti-lectin CD23 mab 2H10. Plates were blocked with LZ Block (2mM $CaCl_2$, 10mM HEPES, 50mM NaCl, 1%FBS, and 0.04% Tween-20) and samples and standards were incubated in duplicate. Standard curves were generated using EC-CD23 starting at 100 ng/mL serially diluted across the plate. Samples were detected with rabbit polyclonal mouse anti-LZ-CD23 (1:4,000 dilution) followed by goat-anti-rabbit IgG-HRP (1:5000). Plates were developed using TMB substrate (BD) and read at a wavelength of 450 nm. To detect sCD23 levels in the ADAM deficient mice, 129/SvJ mice, and GluK2 deficient a polyclonal-sandwich assay was also performed. Plates were coated with 20 µg/mL of the rabbit polyclonal mouse anti-LZ-CD23. Samples and standards (EC-CD23) were detected using biotinylated rabbit polyclonal mouse anti-CD23 (1:1000) followed by streptavidin-HRP (1:1000). Plates were developed using TMB substrate (BD) and read at a wavelength of 450 nm.

XV. Statistics.

Data are summarized as mean ± Standard error (SE). The statistical analysis of the results was performed by the student's *t* test or ANOVA when appropriate. A p-value of <0.05 was considered significant. When human primary cells are used, data is one representative donor but all assays have been performed using a minimum of three donors with similar results.

RESULTS

I. Identification of the CD23 Sheddase

With such consequences resulting from cleavage of CD23, the CD23 releasing enzyme, or CD23 sheddase, is an attractive target for the design of drugs to treat allergic diseases. Early work with inhibitors of different enzyme classes implicated a hydroxamate sensitive metalloprotease of approximately 62 kDa in CD23 shedding in a variety of different cell types (80). This was the first evidence that the CD23 sheddase could possibly be a member of the "a disintegrin and metalloprotease" (ADAM) family. In 2003, Fourie *et al.* reported that catalytic activity of ADAMs8, 15, and 28 played a role in ectodomain cleavage of CD23 on synthetic peptide substrates (81). Although previous work indicated a member of the ADAM10 family in *in vitro* cleavage of CD23, the relevance of ADAM family members as a CD23 releasing enzyme *in vivo* remained unknown. Thus, we developed a fruitful collaboration with the Blobel laboratory to identify the exact ADAM involved in CD23 ectodomain shedding.

Once evidence pointed to a member of the ADAM family, we began to systematically rule out candidate proteases. Given the Blobel laboratory's long standing history in the ADAM field, they had access to numerous ADAM deficient mice which would prove a valuable resource. The first experiments performed to determine the role of ADAMs in CD23 shedding was to generate mouse embryonic fibroblasts (MEF) and transfect them with human CD23. These transfected MEFs were cultured in the presence or absence of 1uM BB94, a broad spectrum metalloprotease inhibitor. Cell free supernatants were then analyzed for soluble CD23 by Western Blot analysis. sCD23 was detected in the supernatants of CD23 transfected WT MEFs as well as ADAM8 KO, ADAM9, 12, 15 triple KO, ADAM17 KO, ADAM19 KO, and ADAM33 KO MEFs. Furthermore, the addition of BB94 blocked shedding in all MEFs tested, thus ruling out involvement of these particular ADAMs in the cleavage of CD23 (Figure 2) but still pointing to a hydroxamate sensitive protease. However, when ADAM10 KO MEFs were examined no detectable CD23 was released into the supernatants. Furthermore, when these ADAM10 deficient MEFs were complemented with ADAM10, cleavage was restored. Thus, this is the first evidence of ADAM10 playing a role in CD23 shedding (Figure 3).

We next wanted to further examine ADAM10's role as the CD23 sheddase. Because deletion of ADAM10 results in embryonic lethality (82), we were restricted to the use of the ADAM10 KO MEFs and the use of an ADAM10 selective inhibitor (77). This inhibitor, known as GI254023X, was kindly provided by Neil Broadway (GlaxoSmithKline) and has been shown to be highly specific for ADAM10. The chemical structure of the inhibitor is shown in Figure 4. Work by Jill Ford highlighted the efficacy of GI254023X in blocking both constitutive and antibody induced cleavage in mouse B cells (data not shown). When utilized in both human cell lines as well as human primary cells, we observed a concentration dependent inhibition of CD23 shedding in the presence of GI254023X. Furthermore this pattern of ADAM10 inhibition is identical to the GI254023X mediated inhibition of a known ADAM10 substrate, EGF (Figure 5). To confirm these inhibitor studies, we utilized an ADAM10 siRNA and also observe a decrease in the amount of sCD23 released from 8866, which is a human B cell line known to express high levels of CD23, further confirming ADAM10's role as the CD23 sheddase (Figure 6). Thus, ADAM10 should be considered as a potential target for the design of drugs that block CD23 shedding as a mechanism for controlling CD23 mediated disease.

Figure 2. CD23 shedding in wild-type and ADAM-deficient MEFs.

MEFs derived from wild-type (WT) or ADAM knock-out mice (ADAM8KO, ADAM9, 12, 15 triple KO, ADAM17KO, ADAM19KO, and ADAM33KO) were transfected with human CD23 cDNA (C-terminal V5 tag) and were either left untreated or were cultured with 1 µM BB94 (broad spectrum metalloprotease inhibitor) for 3 hours. sCD23 from culture supernatants was immunoprecipitated with anti-human CD23 and then blotted with anti-V5 tag. (Experiments performed by Gisela Weskamp (Hospital for Special Surgery, Weill Medical College of Cornell University, NY, NY).)

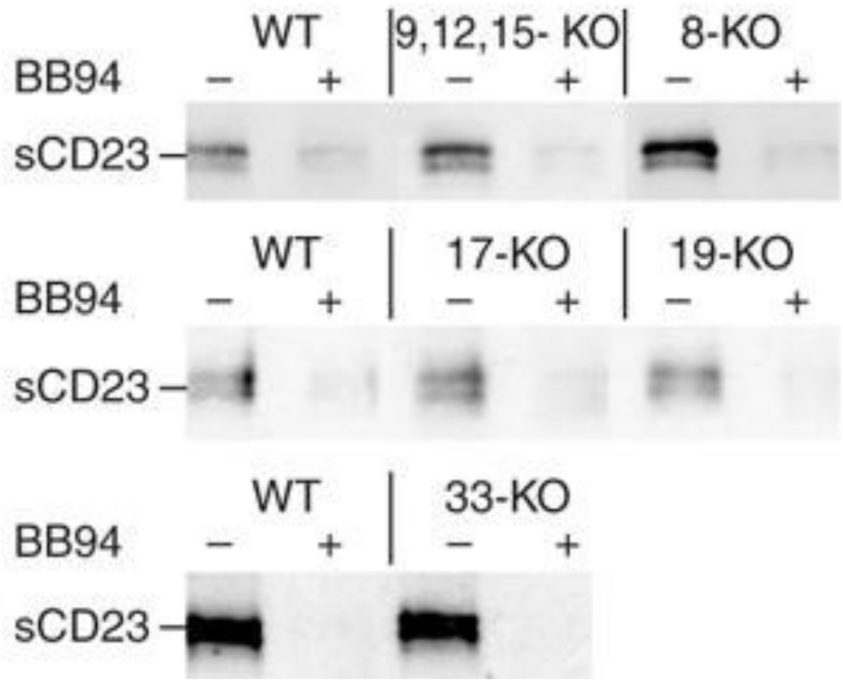
WT
9,12,15- KO
8-KO
BB94
−
+
−
+
−
+
sCD23
WT
17-KO
19-KO
BB94
−
+
−
+
−
+
sCD23
WT
33-KO
BB94
−
+
−
+
sCD23

Figure 3. ADAM10-dependent shedding of CD23 in MEFs.

Immortalized wild-type MEFs (WT), ADAM10 Heterozygous KO MEFs (10-HET), or ADAM10 KO MEFs (10-KO) were transfected with human CD23 cDNA in the presence or absence of BB94 as in Figure 2. sCD23 was detected from cell supernatants as is Figure 2 by western blot. (Right Panel) ADAM10$^{-/-}$ MEFs were co-transfected with human CD23 cDNA and ADAM10 cDNA. sCD23 was detected in supernatants by western blot. (Experiments performed by Gisela Weskamp.)

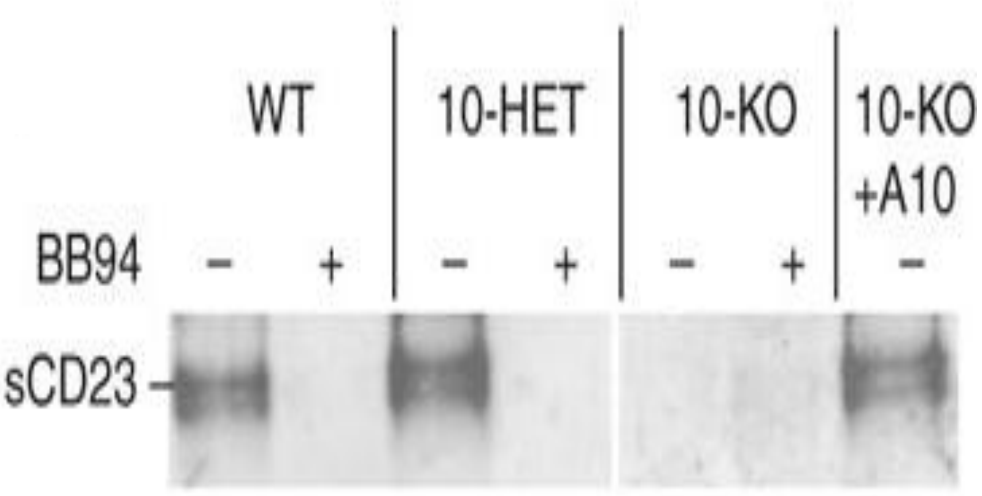
WT
10-HET
10-KO
10-KO +A10
BB94
–
+
–
+
–
+
–
sCD23

Figure 4. Chemical structure of the ADAM10-specific inhibitor GI254023X.

GI254023X is a reverse hydroxamate inhibitor with a large heteroaryl substituent at position R2. This group is thought to fit snuggly within the S1' pocket of ADAM10, thus providing GI254023X with 100-fold more selectivity for ADAM10 than ADAM17. (Taken from 77)

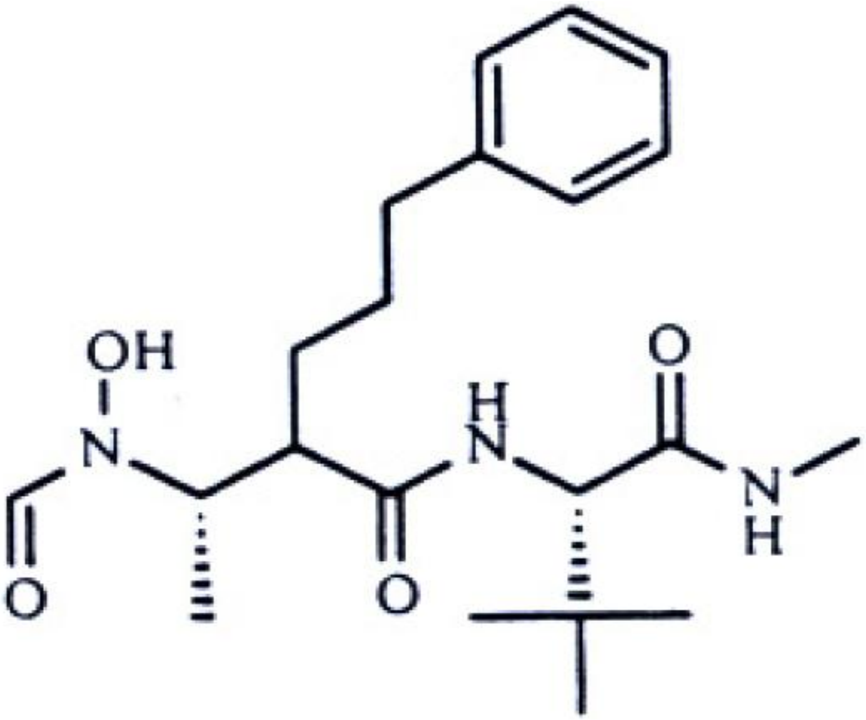
OH
N
O
O
H
N
O
N
H

Figure 5. GI254023X blocks ADAM10 mediated cleavage of CD23 and EGF.

MEF, 8866, and tonsilar B cells were cultured in the presence of varying concentrations of GI254023X or vehicle control (DMSO). 24 hours later, cell free supernatants were analyzed for sCD23 by ELISA. This pattern of inhibition was compared to release of EGF from simian virus 40–immortalized MEFs (EGF) as EGF is a known ADAM10 substrate. Shown is one experiment of three of similar design.

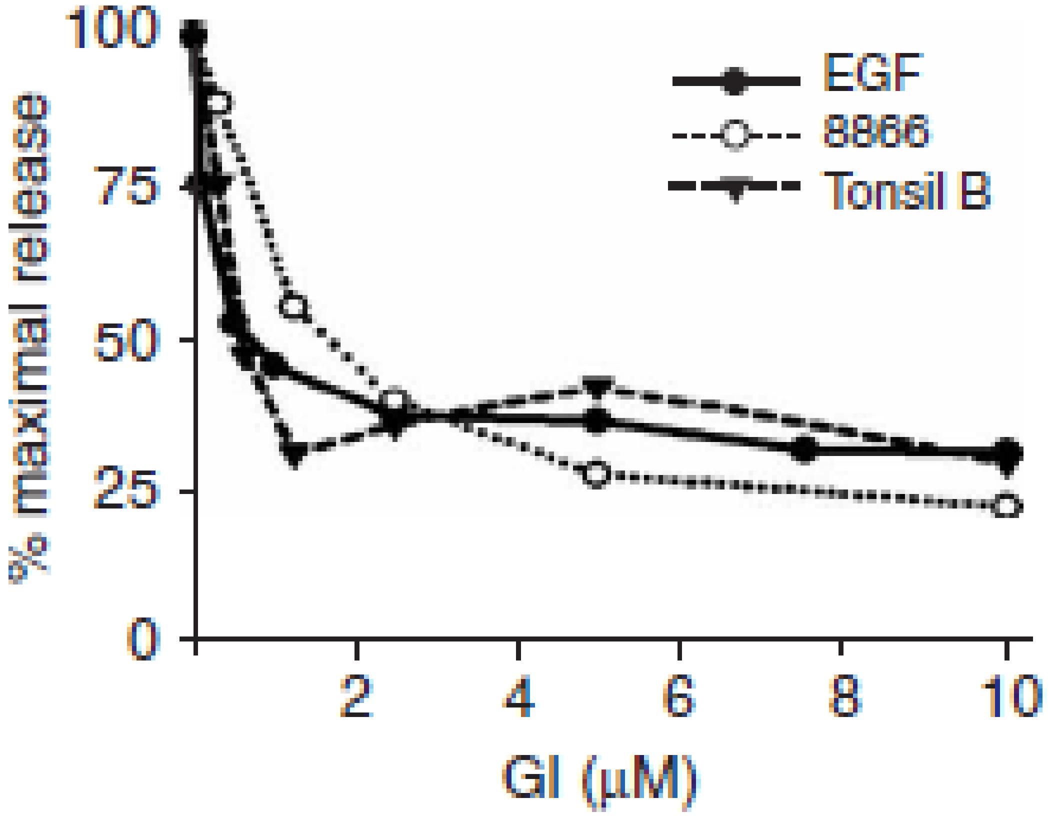
100
75
50
25
0
% maximal release
2
4
6
8
10
GI (μM)
EGF
8866
Tonsil B

Figure 6. siRNA against ADAM10 also inhibits sCD23 release.

8866 were co-transfected with GFP and either a control plasmid or a plasmid containing ADAM10 siRNA via electroporation (AMAXA). 24 hours later cells were sorted by the VCU Flow cytometry core facility to isolate GFP+ cells. These cells were then plated at a concentration of 1 x10^6/mL overnight at 37 degrees. The basis for the dual transfection is that in our hands, 8866 had a maximal transfection efficiency of out 50%, thus we used this GFP as a surrogate marker to enrich our population. After 24 hours post separation, cell free supernatants were harvested and sCD23 was determined via ELISA. Shown is one representative experiment of three of similar design.

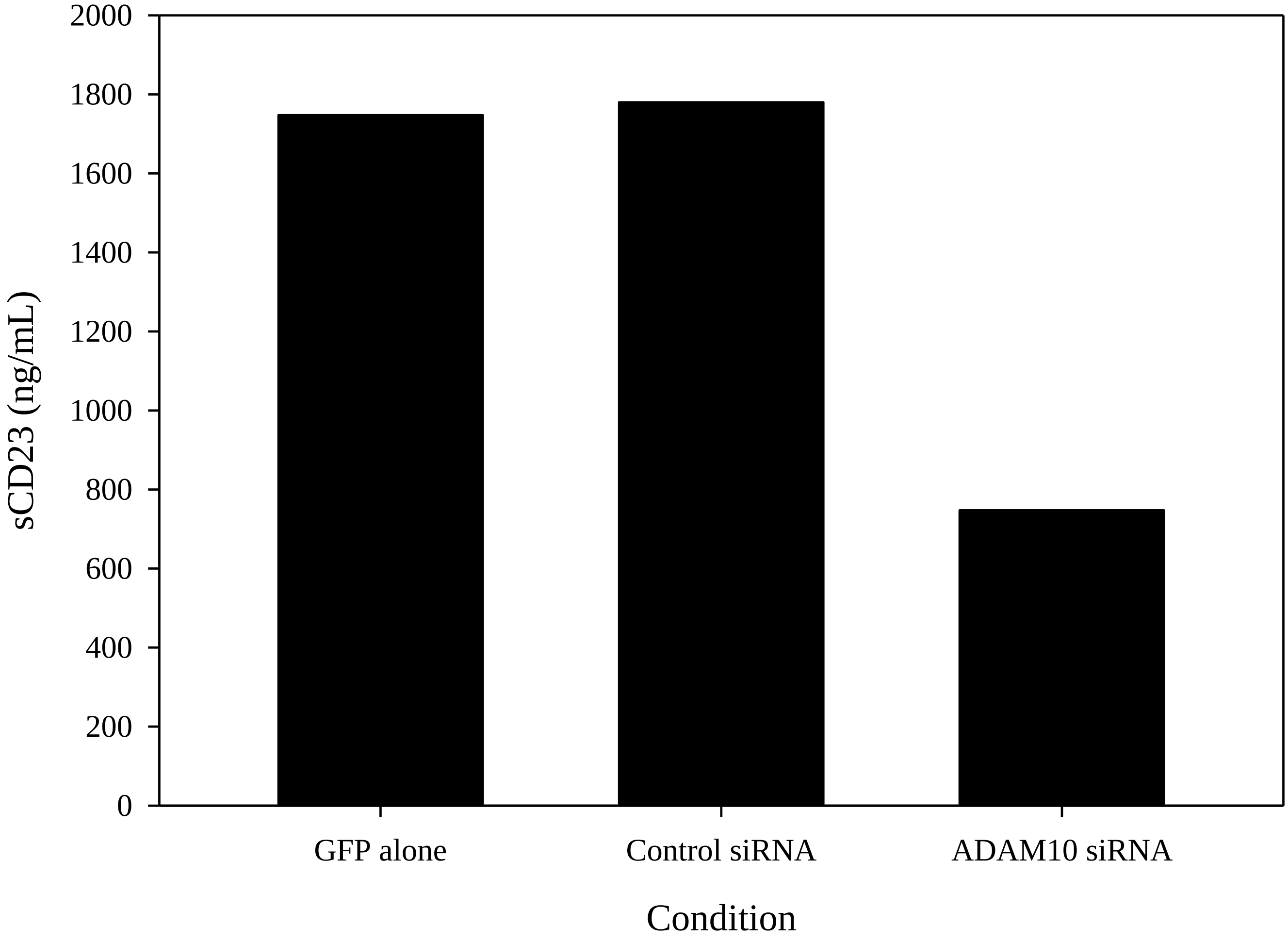
2000
1800
1600
1400
1200
1000
800
600
400
200
0
sCD23 (ng/mL)
GFP alone
Control siRNA
ADAM10 siRNA
Condition

II. Identification of mutations in murine CD23

During the course of the work that led to the identification that ADAM10 was the CD23 sheddase, a serendipitous discovery was made regarding differences among mouse strains and CD23. In separate experiments not listed above, Jill Ford was examining various ADAM KO murine strains for sCD23 levels. Initially, it was thought that ADAM8 was the CD23 sheddase as when ADAM8 KO mice were analyzed, there were no detectable levels of CD23 in their sera. When these studies were repeated however, sCD23 was detected in the sera of ADAM8 KO mice. The reason for these discrepancies is that the ADAM8 KO mice, like many genetically modified mice were initially generated using the 129Sv/J background embryonic stem cells and in their current state were a mixture of the 129Sv/J and C57BL/6J mice. Upon subsequent reexamination of the ADAM8 KO mice, they had been back crossed for several generations onto C57BL/6J background strain in order to develop the ADAM8 KO mice on a true C57BL/6.

This observation begged the question what was unique about the 129Sv/J CD23? The 129 inbred strain of mice originated in 1928 in the laboratory of Leslie Dunn at Columbia University. The 129 colony was established at The Jackson Laboratory in 1948 and at least 8 129 sub-strains are presently available for purchase (83). 129/SvJ mice are frequently used for gene targeting studies due to the availability of several embryonic stem cell lines derived from the parental strain (reviewed in 84). Upon screening mice for sCD23 expression, we observed that sera from mice derived from a 129 background strain, failed to produce soluble CD23 as detected by our standard ELISA techniques.

We first wanted to determine if 129/SvJ CD23 mRNA levels differed from those of WT B cells. We analyzed CD23 message levels in un-stimulated and IL-4 and anti-CD40 stimulated B cells by RT-PCR. CD23 message levels in both 129/SvJ and BALB/c J B cells were similar before and after stimulation (Figure 7) thus indicating that the mechanism for the different levels of sCD23 could not be accounted for at the RNA level.

The reduced levels of sCD23 could be due to reduced protein expression of CD23 or a defect in ADAM10. To further examine CD23, we next analyzed splenic B cells from both 129/SvJ and BALBc/J mice for cell surface expression of CD23. To measure B cell CD23 levels, splenocytes from BALB/cJ or 129/SvJ mice were stained using B3B4, a mab recognizing the lectin domain of CD23, and analyzed by flow cytometry. Less CD23 was observed on B cells from 129/SvJ mice as compared to those from BALB/c J mice (Figure 8). When a polyclonal antibody was used for detection, similar results were obtained (Figure 8B). To determine if 129/SvJ CD23 levels could be up-regulated to BALB/c J levels, we isolated B cells from the spleens of 129/SvJ or BALB/c J mice, stimulated them for 48 hours with IL-4 and anti CD40 and analyzed surface expression by flow cytometry using B3B4. 129/SvJ CD23 expression was increased after stimulation yet remained lower than those observed on stimulated BALB/c JB cells (Figure 9). Because these studies were initiated upon the finding that 129 mice have reduced sCD23, we wanted to determine if it was an effect of the antibody used to determine sCD23. As described in the materials and methods, the mab 2H10 is used to determine murine sCD23 via ELISA. We used this same antibody in a flow cytometric approach and showed that B cells from 129 mice fail to react with 2H10 (Figure 10).

Given the loss of reactivity of 2H10, we next examined the CD23 molecule itself of 129 mice to look for potential mutations. B cells isolated from the spleen of 129/SvJ mice were stimulated for 48 hours as previously described and RNA was then isolated via standard

Figure 7. CD23 message levels are normal in 129/SvJ B cells.

B cells isolated from the spleens of BALB/cJ or 129/SvJ mice were either left untreated or were stimulated with IL-4 and anti CD40 for 48 h. RNA was isolated either immediately (untreated cells) or after the stimulation period via Trizol®, and qPCR was performed using murine CD23 specific primers as described. 18s was amplified as an internal control. No significant difference was observed between the two strains tested. Figure represents three mice per group.

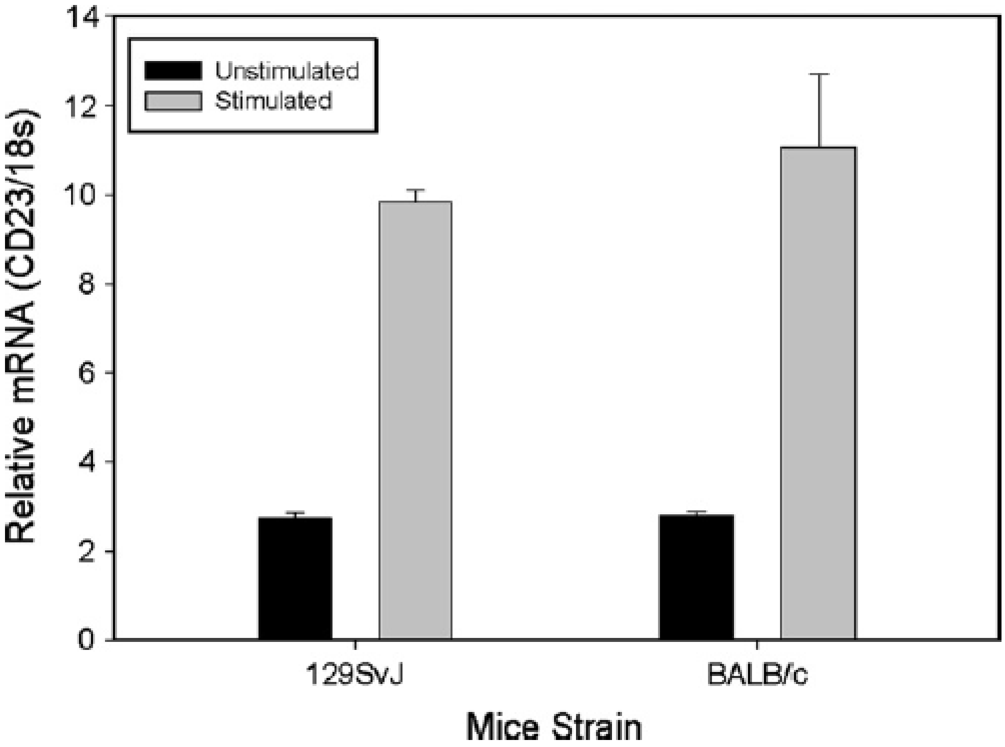
Unstimulated
Stimulated
Relative mRNA (CD23/18s)
0
2
4
6
8
10
12
14
129SvJ
BALB/c
Mice Strain

Figure 8. CD23 surface expression is reduced on 129/SvJ B cells.

B cells isolated from the spleens of BALB/cJ or 129/SvJ mice were stained with B220-APC (B cell marker) in combination with either (A) B3B4-FITC (monoclonal anti-CD23) or (B) Biotinylated Rabbit anti-LZ-CD23 (polyclonal anti-CD23) followed by anti-biotin-FITC. B3B4-FITC and anti-biotin-FITC histograms are shown gated on the APC+ population. Controls in A were stained with B220-APC but left unstained for B3B4-FITC. Controls in B were stained with B220-APC and anti-biotin-FITC in the absence of Rabbit anti-LZ-CD23. Experiment performed by Jill Ford three times with similar results.

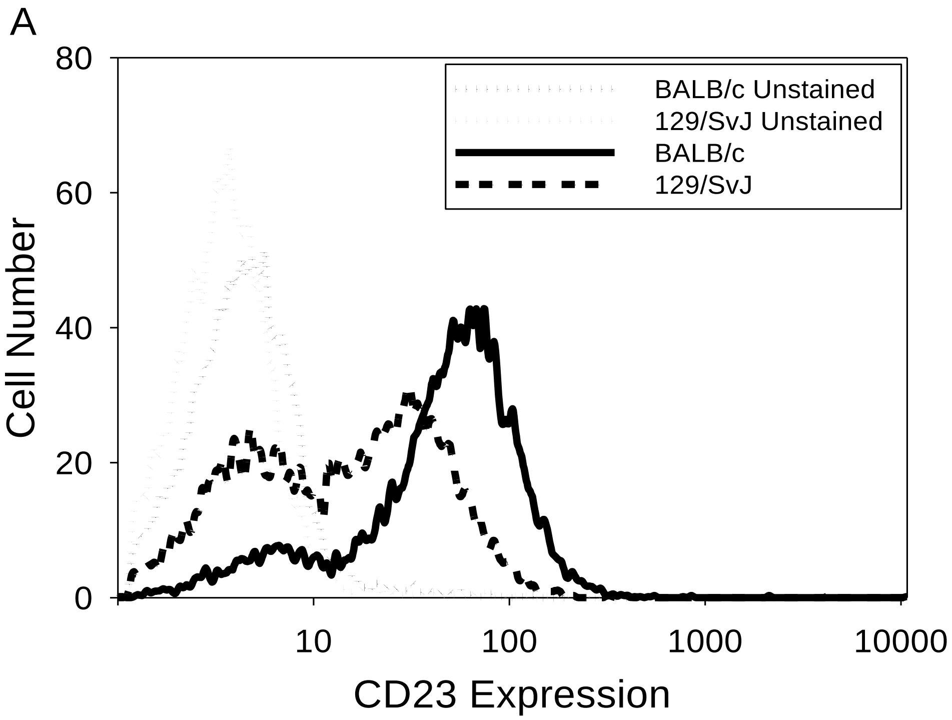
A
BALB/c Unstained
129/SvJ Unstained
BALB/c
129/SvJ
Cell Number
0
20
40
60
80
10
100
1000
10000
CD23 Expression

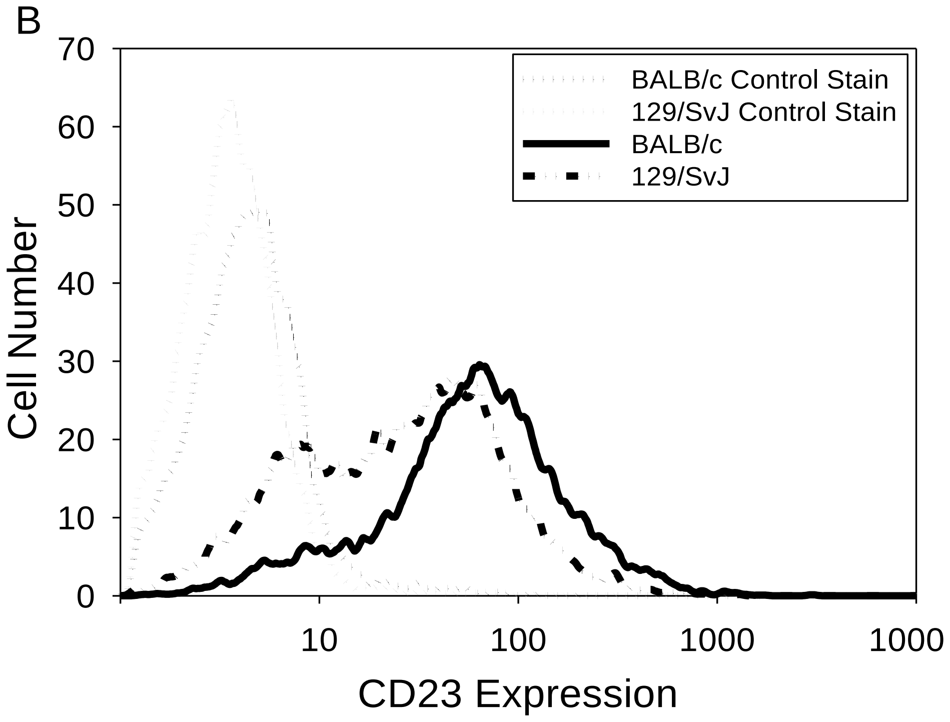
B
BALB/c Control Stain
129/SvJ Control Stain
BALB/c
129/SvJ
Cell Number
0
10
20
30
40
50
60
70
10
100
1000
1000
CD23 Expression

Figure 9. 129/SvJ CD23 surface levels can be up-regulated by stimulation with IL-4 and CD40LT.

B cells isolated from the spleens of BALB/cJ or 129/SvJ mice were stimulated with IL-4 and CD40LT for 48 hours. B cells were then stained with B220-APC (B cell marker) and B3B4-FITC (monoclonal anti-CD23). B3B4-FITC histograms are shown gated on the APC+ population. Controls were stained with B220-APC but left unstained for B3B4-FITC. Experiment performed by Jill Ford three times with similar results.

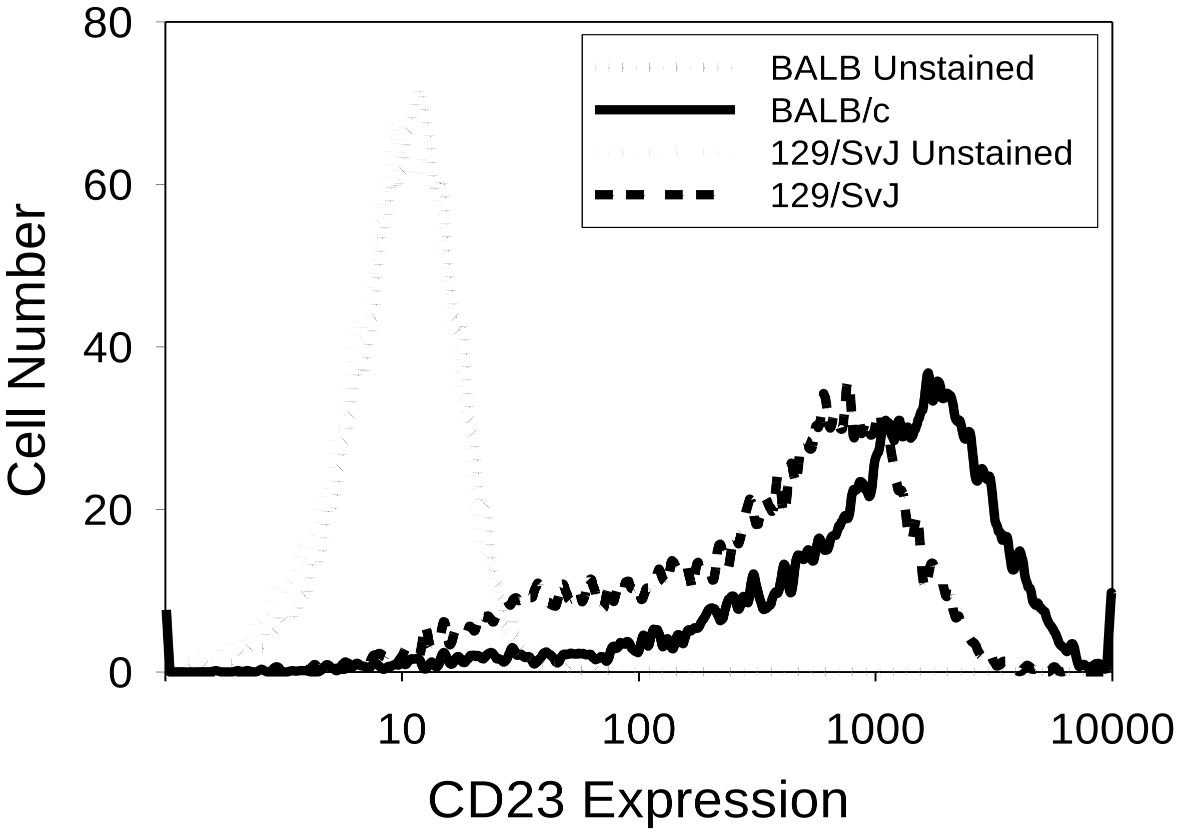
80
60
40
20
0
Cell Number
10
100
1000
10000
CD23 Expression
BALB Unstained
BALB/c
129/SvJ Unstained
129/SvJ

Figure 10. Lack of recognition of 129/SvJ CD23 by the mab 2H10.

Spleen cells isolated from 129/SvJ or BALB/cJ mice were stained with biotinylated 2H10 (anti-lectin-CD23) followed by anti-biotin-FITC and APC-B220. FITC$^+$ cells are shown gated on the B220$^+$ population. BALB/cJ and 129/SvJ CD23 expression is represented by the solid and dotted lines, respectively. Experiment performed by Jill Ford three times with similar results.

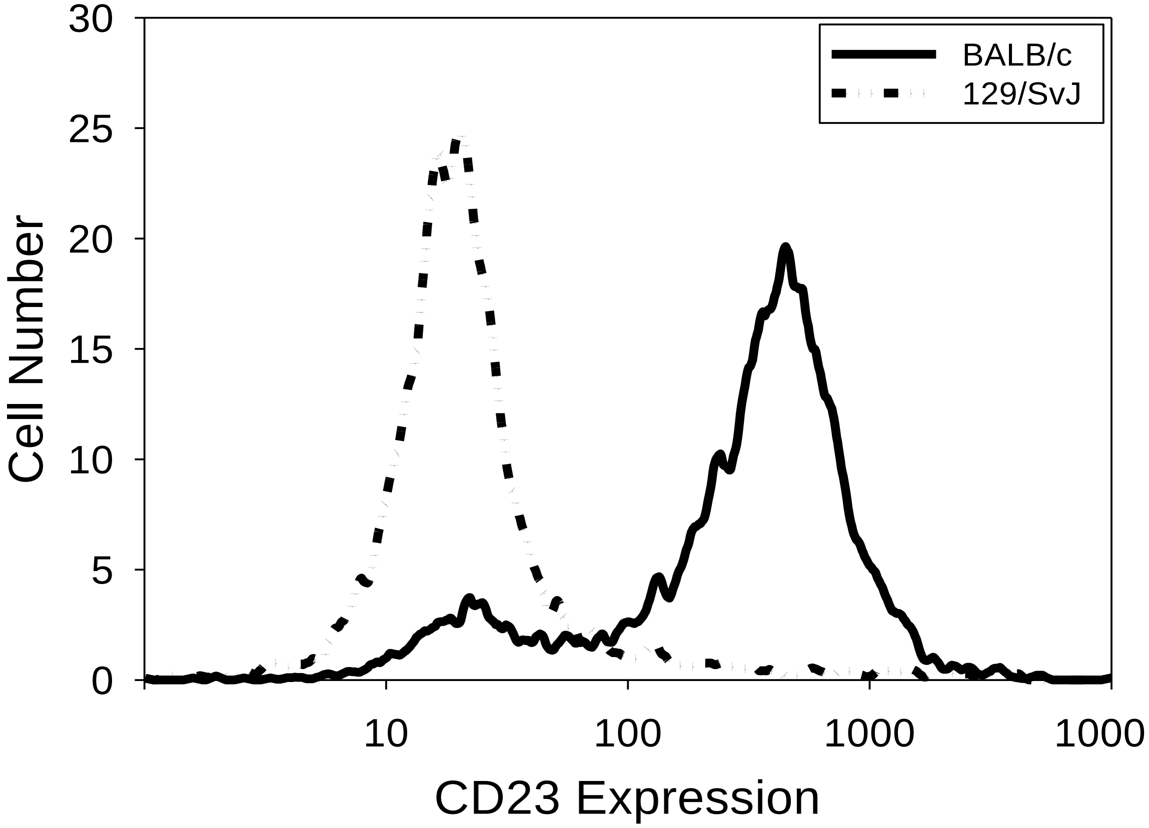
30
25
20
15
10
5
0
Cell Number
10
100
1000
1000
CD23 Expression
BALB/c
129/SvJ

Trizol® procedure. CD23 was then amplified by RT-PCR using the primers indicated and the resultant PCR products were cloned into pCR2.1 and transformed into INVaF' *E.Coli*. *E. coli* were grown overnight and plasmid DNA isolated with the Qiagen DNA extraction kits. Confirmation of positive clones was performed with appropriate DNA digestion to examine product insert size. Plasmids were then sent to the VCU NARF for sequencing. Compared to BALB/c J CD23, 129/SvJ CD23 contained 5 mutations, three in the stalk region (A82T, V87A, and K131E) and two within the lectin domain (S258L and D301N) (Figure 11). The insertion of threonine for alanine at position 82 could disrupt the trimeric structure of CD23 through the addition of the hydrophilic side chain in the core of the coiled-coil domain whereas the substitution of valine for alanine at position 87 is largely neutral and therefore unlikely to be disruptive to the CD23 structure. The third stalk mutation (K131E) replaces lysine with glutamic acid which is a highly unfavored substitution resulting in the exchange of a basic a.a. for an acidic a.a.. The S258L mutation within the lectin domain is also disfavored since it results in a change from a small and polar a.a. to a larger, hydrophobic one. The last mutation (D301N) substitutes an acidic charge for a neutral charge. While this change would not be as unfavorable as the others, it is located in close proximity to two disulphide bridges and thus impact CD23 structure. The examination of published sequences of CD23 from other strains revealed that 4 out of the 5 mutations in the 129/SvJ CD23 were identical to those recently reported for the NZB CD23(85). Given CD23's role as a natural negative regulator of IgE synthesis, 129Sv/J mice were examined for IgE levels. Indeed the 129Sv/J strain exhibited higher levels of IgE both at the basal level and post immunization and cleared *Nippostrongylus brasiliensis* much faster that BALB/c J or C57BL/6J strains (86). Thus, the identification of mutations in the 129Sv/J CD23 further emphasize CD23's role in the regulation of IgE synthesis.

Figure 11. 129/SvJ CD23 is mutated.

CD23 amino acid sequence analysis comparing CD23 from BALB/cJ and 129/SvJ inbred strains. Five mutations, three in the stalk and two in the lectin domain were observed in the 129/SvJ CD23 as compared to the BALB/c JCD23. Four of these mutations (outlined in red boxes) were recently identified in a variant CD23 allele from the NZB inbred strain (87). Sequence analysis was performed multiple times to eliminate the possibility of any sequencing error.

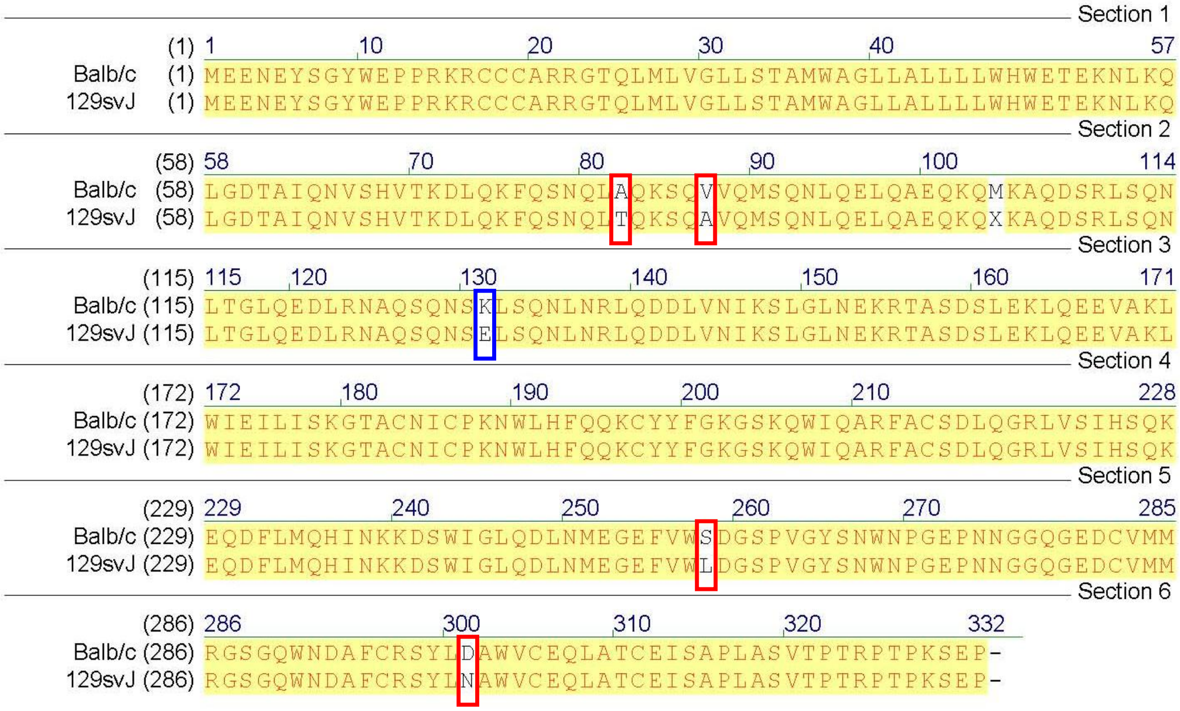

```
                                                                      Section 1
           (1) 1               10              20              30              40                        57
Balb/c     (1) MEENEYSGYWEPPRKRCCCARRGTQLMLVGLLSTAMWAGLLALLLLWHWETEKNLKQ
129svJ     (1) MEENEYSGYWEPPRKRCCCARRGTQLMLVGLLSTAMWAGLLALLLLWHWETEKNLKQ
                                                                      Section 2
          (58) 58                  70              80              90              100                  114
Balb/c    (58) LGDTAIQNVSHVTKDLQKFQSNQLAQKSQVVQMSQNLQELQAEQKQMKAQDSRLSQN
129svJ    (58) LGDTAIQNVSHVTKDLQKFQSNQLTQKSQAVQMSQNLQELQAEQKQXKAQDSRLSQN
                                                                      Section 3
         (115) 115     120             130             140             150             160              171
Balb/c   (115) LTGLQEDLRNAQSQNSKLSQNLNRLQDDLVNIKSLGLNEKRTASDSLEKLQEEVAKL
129svJ   (115) LTGLQEDLRNAQSQNSELSQNLNRLQDDLVNIKSLGLNEKRTASDSLEKLQEEVAKL
                                                                      Section 4
         (172) 172           180             190             200             210                        228
Balb/c   (172) WIEILISKGTACNICPKNWLHFQQKCYYFGKGSKQWIQARFACSDLQGRLVSIHSQK
129svJ   (172) WIEILISKGTACNICPKNWLHFQQKCYYFGKGSKQWIQARFACSDLQGRLVSIHSQK
                                                                      Section 5
         (229) 229                 240             250             260             270                  285
Balb/c   (229) EQDFLMQHINKKDSWIGLQDLNMEGEFVWSDGSPVGYSNWNPGEPNNGGQGEDCVMM
129svJ   (229) EQDFLMQHINKKDSWIGLQDLNMEGEFVWLDGSPVGYSNWNPGEPNNGGQGEDCVMM
                                                                      Section 6
         (286) 286                     300             310             320                   332
Balb/c   (286) RGSGQWNDAFCRSYLDAWVCEQLATCEISAPLASVTPTRPTPKSEP-
129svJ   (286) RGSGQWNDAFCRSYLNAWVCEQLATCEISAPLASVTPTRPTPKSEP-
```

III. Identification of Kainate receptors in the immune system

In view of the recent demonstration that a disintegrin and metalloprotease 10 (ADAM10) is the primary CD23 sheddase, we searched for agents that would modify ADAM10 expression and/or activity. The overall purpose was to test the hypothesis that ADAM10 modulation would, by virtue being the CD23 sheddase, result in IgE modulation. Ortiz *et al.*. showed that when a specific type of glutamate receptor, namely the kainate receptor (KAR), was stimulated with its ligand, ADAM10 mRNA increased (88). KARs are one of three types of multi-subunit, ionotropic glutamate receptors which are named based upon their preferred pharmacological ligand: α-amino-3-hydroxy-5-methyl-4-isoxazole propionic acid (AMPA), N-methyl-D-aspartic acid (NMDA), and kainic acid (KA). KARs are the most recently identified of the three and have been shown to be widely expressed in the central nervous system (89,90) however, little is reported on their presence outside the CNS. Kainic acid, a chemical first isolated from the red algae *Digenea simplex*, is a potent agonist of KARs and is a widely used for the generation of epilepsy in laboratory rodent models and is responsible for neuro-inflammation following epilepsy induction (91-95).

A. Kainate receptors are present on human B cells

KARs are multi-subunit receptors consisting of four distinct subunits. The gene names for these subunit are designated as *GRIK1-5*, whereas the protein names are GluK1, GluK2, GluK3, GluK4, and GluK5 (96). Thus, to form a functional receptor, KARs must consist of GluK1 or GluK2 in combination with GluK3, GluK4, and GluK5. Two of the genes that encode subunit GluK1 (*GRIK1*) and GluK2 (*GRIK2*), can undergo specific RNA editing and thus result in two transcript variants (TVs). From the data shown, we observe the presence of four subunit genes, *GRIK2, GRIK3, GRIK4*, and *GRIK5*, thus, it is evident that message for KARs do exist in human B cells (Figure 12). It appears that the immune type of kainate receptor is the GluK2 (*GRIK2*) containing receptor as evidenced by the presence of this transcript. Furthermore, the fact that four subunits are present would indicate the presence of a functionally active receptor. We confirmed our RT-PCR data by showing protein expression of the kainate receptor subunit GluK4 (*GRIK4*) by Western Blot analysis, using B cell lines and primary human lymphocytes (Figure 13). We focused on the presence of GluK4 (*GRIK4*) as it is required for ligand binding. In addition, flow cytometric analysis confirmed that KARs are cell surface expressed on both 8866 and primary human leukocytes from PBMC and tonsils (Figure 14).

B. KAR activation increases ADAM10 mRNA and activity

Based upon the publication by Ortiz *et al.*, KAR stimulation in the CNS led to an increase in ADAM10 mRNA. In order to determine if kainic acid (KA), an exogenous ligand, or glutamate (Glu), an endogenous ligand, has the ability to increase ADAM10 message levels in the human immune system, purified human B cells were cultured in the presence of KA or Glu for 30 minutes and then RNA analyzed by qPCR for ADAM10 expression. As evidenced in Figure 15, there is a significant increase in the mRNA levels for ADAM10 after KAR activation in primary B cells. In keeping with ADAM10's newly identified role as the CD23 sheddase, it was anticipated that KAR activation would increase soluble CD23 release. For these studies, the CD23$^+$ human B cell line 8866 was utilized and experiment was performed as outlined in Materials and Methods. As shown in Figure 16, a significant elevation in the amount of sCD23 released was seen following KAR activation by either KA or glutamate. We also wanted to determine if this same increase in sCD23 release is observed in primary human B cells. B cells were cultured in the presence of IL-4, anti-CD40, +/- 5mM glutamate for 48 hours. The reason that primary cells are cultured longer than 8866 is that CD23 first needs to be up-regulated, which takes approximately 24 hours, before it can be cleaved. Figure 17 shows that sCD23 release is also appreciably increased in primary human B cells in the presence of glutamate.

Figure 12. Kainate receptor mRNA is expressed in the human immune system.

Human B cells were analyzed for the presence of kainate receptor subunits at the RNA level. The human cell line 8866 was examined by RT-PCR for the presence of multiple subunits of the kainate receptor. A representative TBE agarose gel stained with Ethidium Bromide of three performed is shown. GRIK = Glutamate receptor, ionotropic kainate which is the gene name as appearing in Genbank. TV = transcript variant. Similar results obtained with Jiyoye and primary B cells (data not shown)

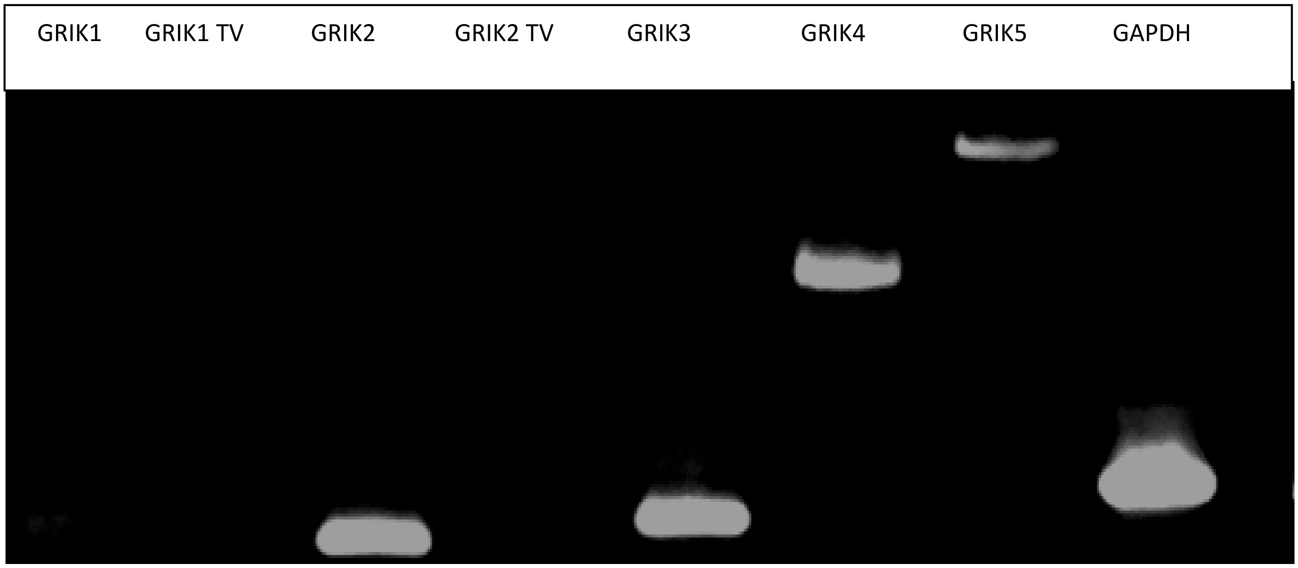
GRIK1
GRIK1 TV
GRIK2
GRIK2 TV
GRIK3
GRIK4
GRIK5
GAPDH

Figure 13. Kainate receptor protein is expressed in the human immune system.

Human B cells were analyzed for the presence of kainate receptor subunits at the protein level. B cell lines as well as human primary B cells were analyzed by Western Blot as described. Western blot shows presence of GluK4 (*GRIK4*) protein in multiple B cell sources. Shown is one representative Western out of 3 performed. Ponceau staining was performed to ensure equal loading.

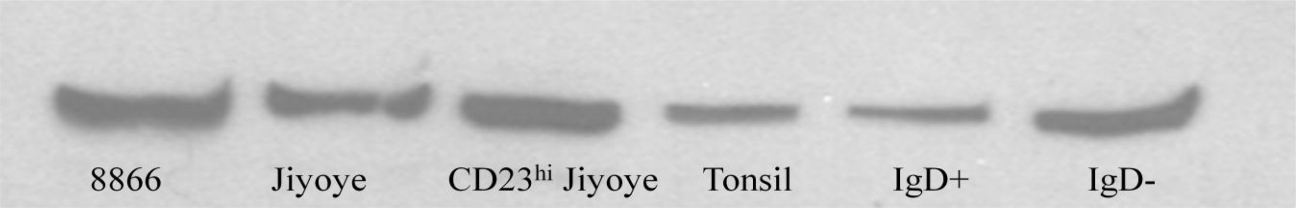
8866
Jiyoye
CD23hi Jiyoye
Tonsil
IgD+
IgD-

Figure 14. Kainate Receptors are cell surface expressed in the human immune system. Cells were subjected to flow cytometric analysis as described. Briefly, cells were stained with rabbit anti GluK4 followed by a goat anti rabbit PE. Cell specific stains were FITC labeled. Shown here is one representative tonsil and PBMC preparation out of three of similar design. Human 8866 cells also display high levels of KAR expression (data not shown)

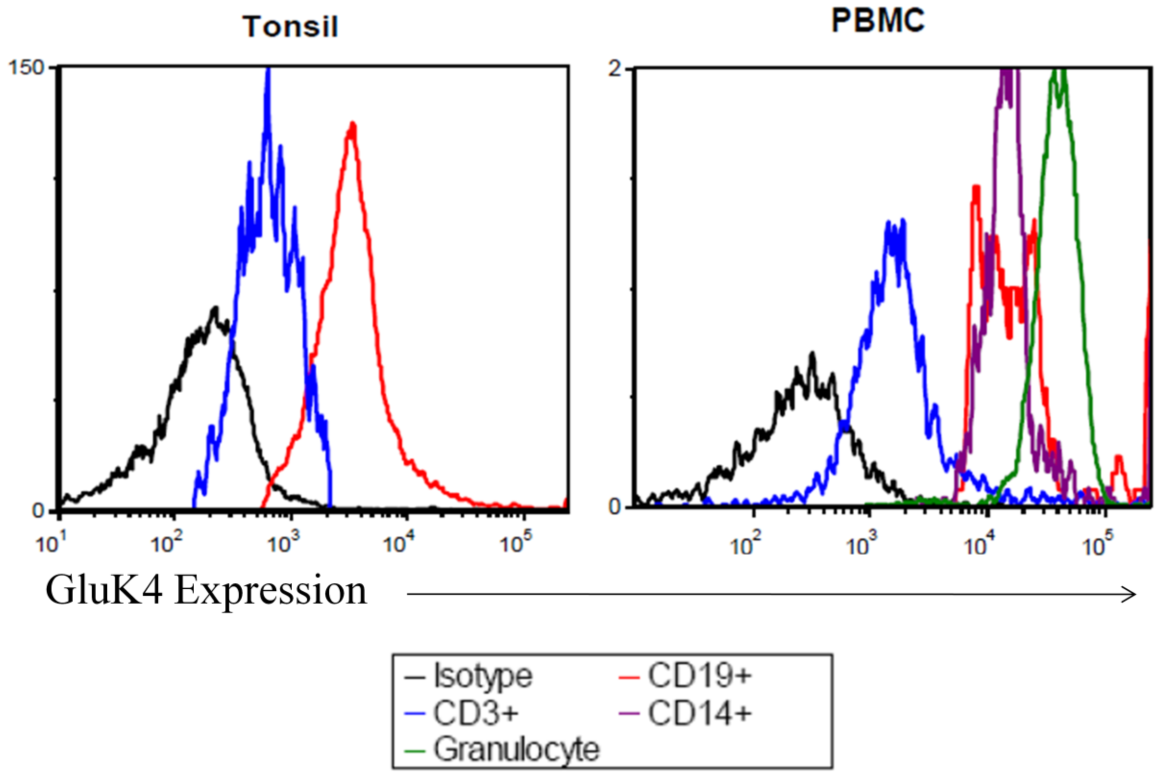
Tonsil
PBMC
150
0
2
0
10^1
10^2
10^3
10^4
10^5
10^2
10^3
10^4
10^5
GluK4 Expression
Isotype
CD19+
CD3+
CD14+
Granulocyte

Figure 15. Kainate receptor activation increases ADAM10 mRNA levels.

Primary B cells were cultured in CDMEM-10 alone, 5mM glutamate, or 5mM kainic acid for 30 minutes. RNA was then isolated by Trizol® and subjected to qPCR analysis as described. Levels are normalized to human beta-actin and shown as fold increase over cells in media alone. Shown is the average of 3 separate donors. * indicates a p value less than 0.05 as compared to media alone.

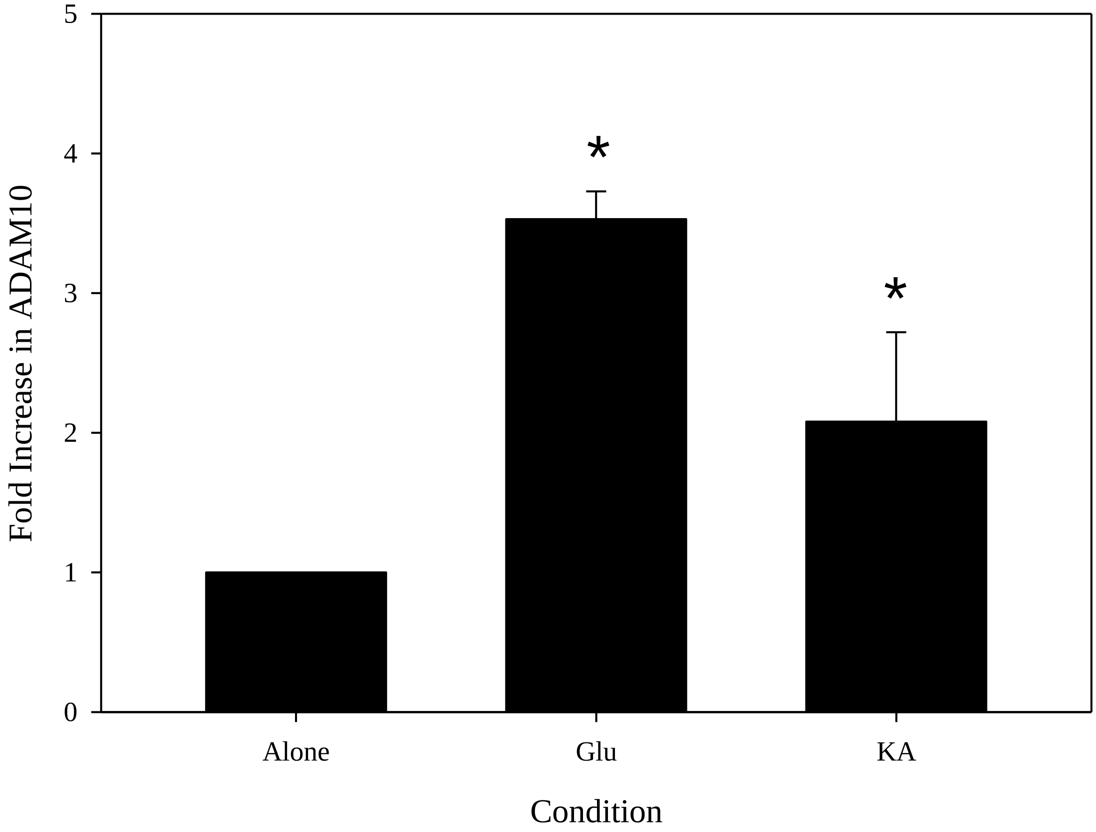
5
4
3
2
1
0
Fold Increase in ADAM10
*
*
Alone
Glu
KA
Condition

As stated earlier, three types of ionotropic glutamate receptors, NMDAR, AMPAR, and KAR exist. High doses of kainic acid can activate AMPA receptors and both AMPA and NMDA receptors have been described on other immune cells (97,98, 99). Therefore, receptor antagonists were used to confirm that the KAR was indeed responsible for the enhanced CD23 cleavage. NS102 is a specific KAR antagonist (100,101), NBQX is antagonist of the AMPA receptor (102) and topiramate (TPM) is a NMDA antagonist (103). The soluble CD23 release assays were performed as before, except the 8866 cells were incubated with 50µM of the antagonist for 1hr prior to the addition of KA or Glu. Figure 18 shows that none of the antagonists have any effect on baseline sCD23 release. Furthermore, only NS102, the KAR specific antagonist, can prevent the significant increase observed in the presence of KAR stimulation. Verdoorn *et al.* showed that NS102 selectively antagonizes GluR6 containing KARs (101). This fact is in agreement with our data in that we do observe the GluR6 subtype of receptor in the immune system and indeed NS102 does block. This shows that this phenomenon is KAR specific due to the fact that no change is observed in the presence of the AMPAR or NMDAR antagonists. Thus, we are confident that the observations made are a direct result of KAR activation on the human B cells. Ortiz originally reported that KAR activation increased ADAMs other than ADAM10 and KAR activation has been linked to the increase in several other matrix metalloproteinases (104,105). Hence we next wanted to determine if the KAR mediated increase in sCD23 was

Figure 16. Kainate receptor activation increases sCD23 shedding.

Soluble CD23 release is increased post KAR activation. 8866 cells were cultured at a concentration of 1 x10^6/mL either alone or in the presence of 5mM kainic acid (KA) or 5mM glutamate (Glu). 24 hours later cell free supernatants were harvested and analyzed for soluble CD23 release via ELISA. Shown is the average +/- SE of three individual experiments. *Significant at p<.05 as determined by Oneway Anova using the JMP software.

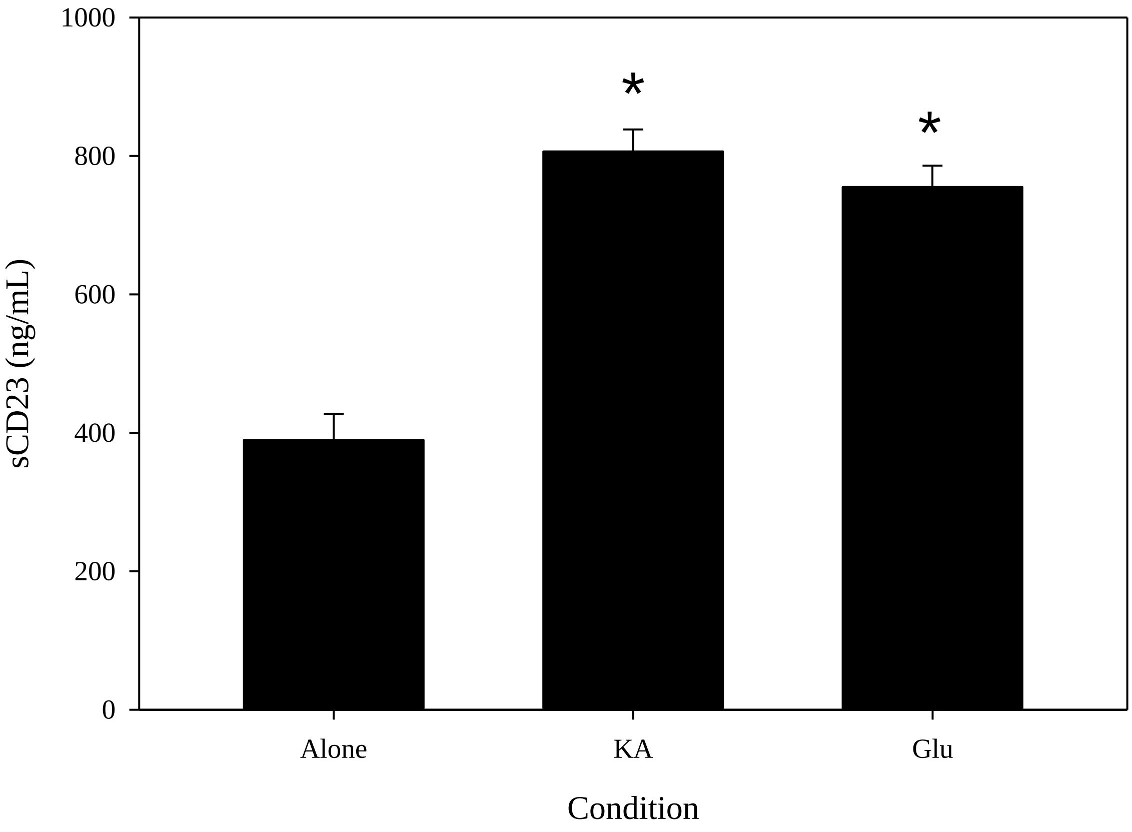
1000
800
600
400
200
0
sCD23 (ng/mL)
*
*
Alone
KA
Glu
Condition

Figure 17. Soluble CD23 release is increased in the presence of glutamate in primary B cells.

Naïve B cells were cultured in the presence of 10ng/mL IL-4, 1 µg/mL anti-CD40, +/- 5mM glutamate at a concentration of 1 x10^6/mL. 48 hours later cell free supernatants were harvested and analyzed for soluble CD23 release via ELISA. Shown here is the result of four individual donors. Data is graphed in terms of sCD23 release as compared to media alone control. Bars indicate the average +/- SE. * indicated p <0.05.

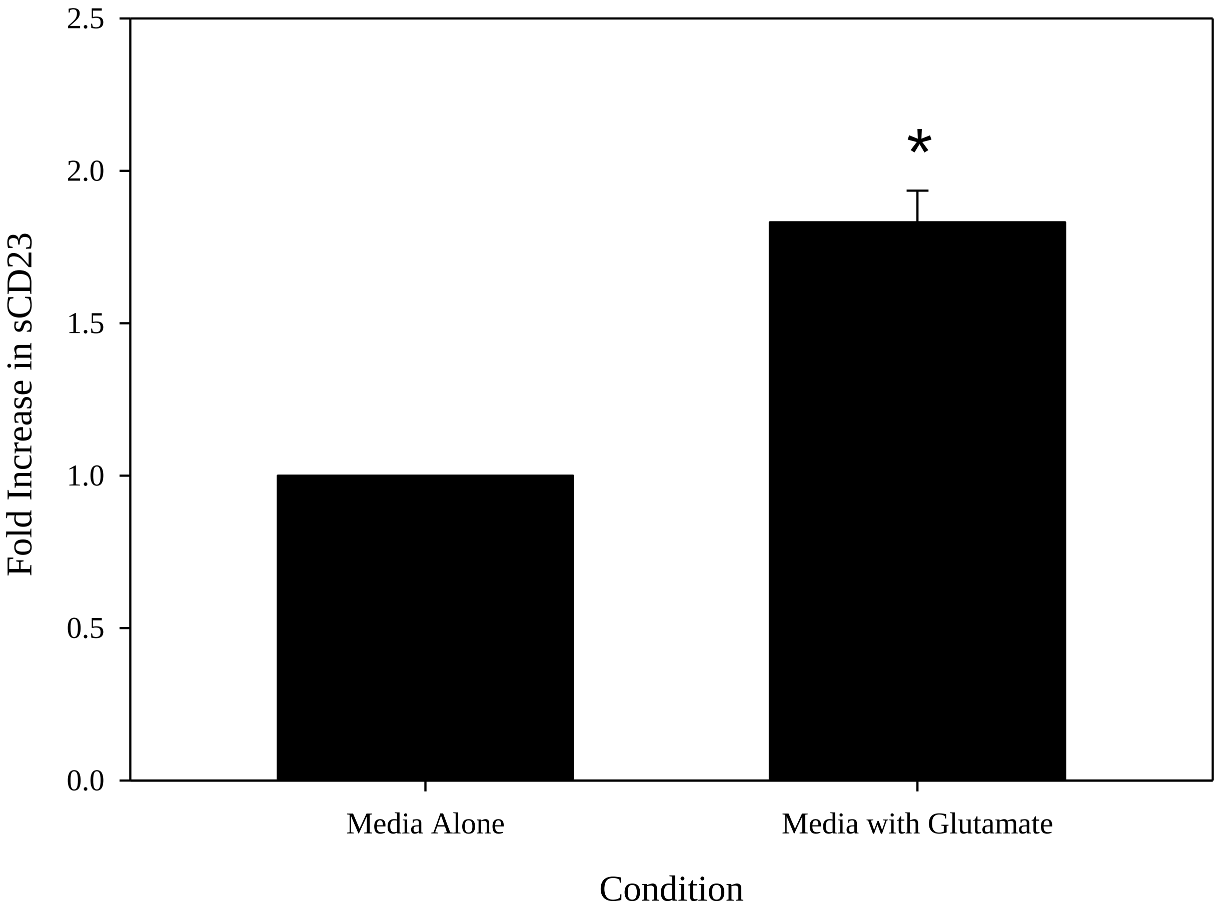
2.5
2.0
1.5
1.0
0.5
0.0
Fold Increase in sCD23
*
Media Alone
Media with Glutamate
Condition

Figure 18. The increase in soluble CD23 release is specifically mediated through KAR activity.

8866 cells were pretreated with either vehicle control (DMSO), NBQX (AMPA antagonist), TPM (NMDA antagonist), or NS102 (KAR antagonist) at a concentration of 50µM each for one hour prior to the addition of 5mM glutamate or 5mM KA. 24hours later, sCD23 levels were determined as described. Shown is the average +/- SE of three individual experiments. *Significant at $p<.05$; NS – not significant as determined by ANOVA using JMP software.

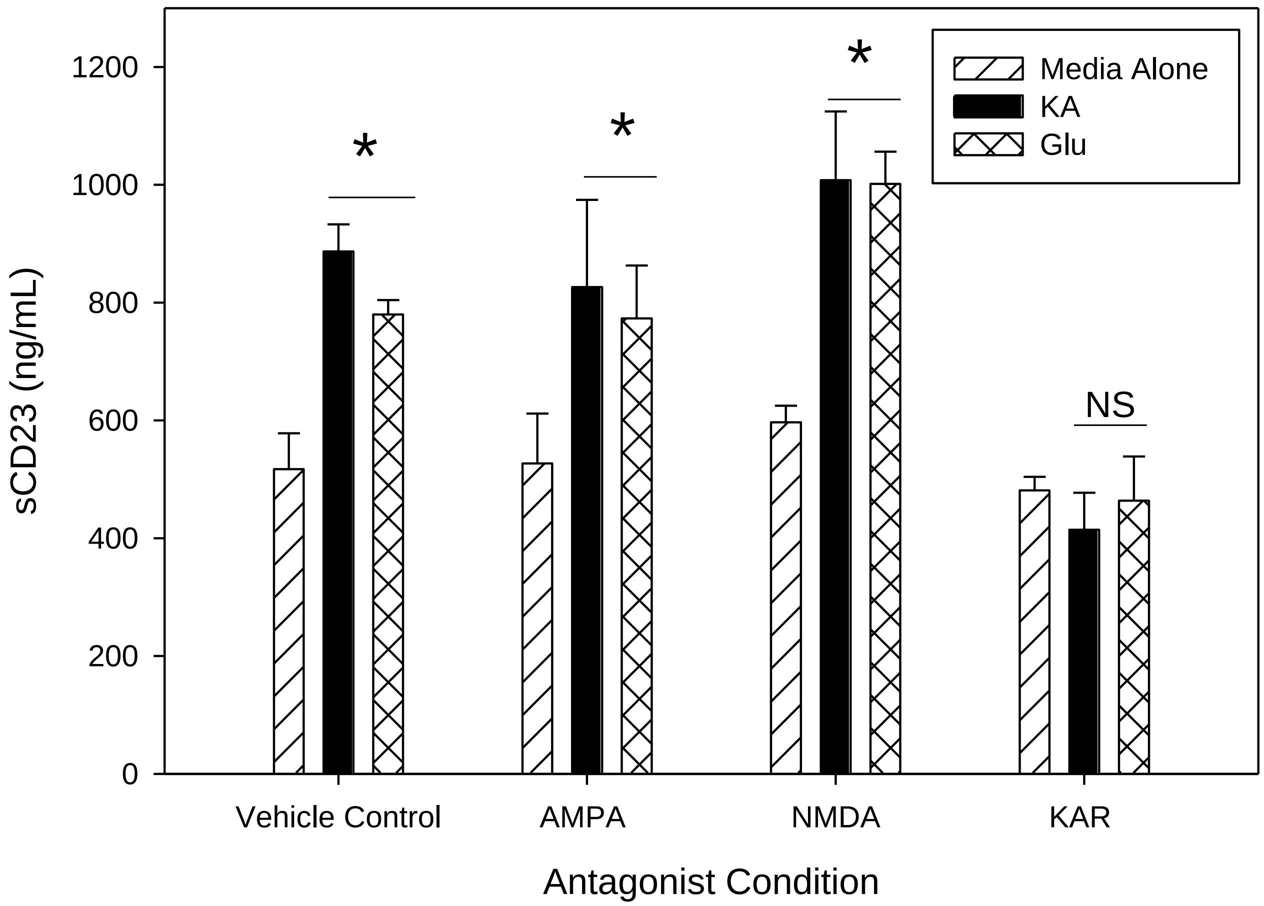
sCD23 (ng/mL)
0
200
400
600
800
1000
1200
Vehicle Control
AMPA
NMDA
KAR
Antagonist Condition
Media Alone
KA
Glu
*
*
*
NS

Figure 19. The KAR mediated increase in sCD23 release is ADAM10 specific.

Prior to the addition of 5mM glutamate, 8866 were cultured as described and were incubated with 10 µM ADAM10 specific inhibitor (INCB08765) for one hour. 24 hours later, cell free supernatants were harvested and sCD23 was determined by ELISA. Shown is the average +/- SE of three individual experiments. NS - not significant.

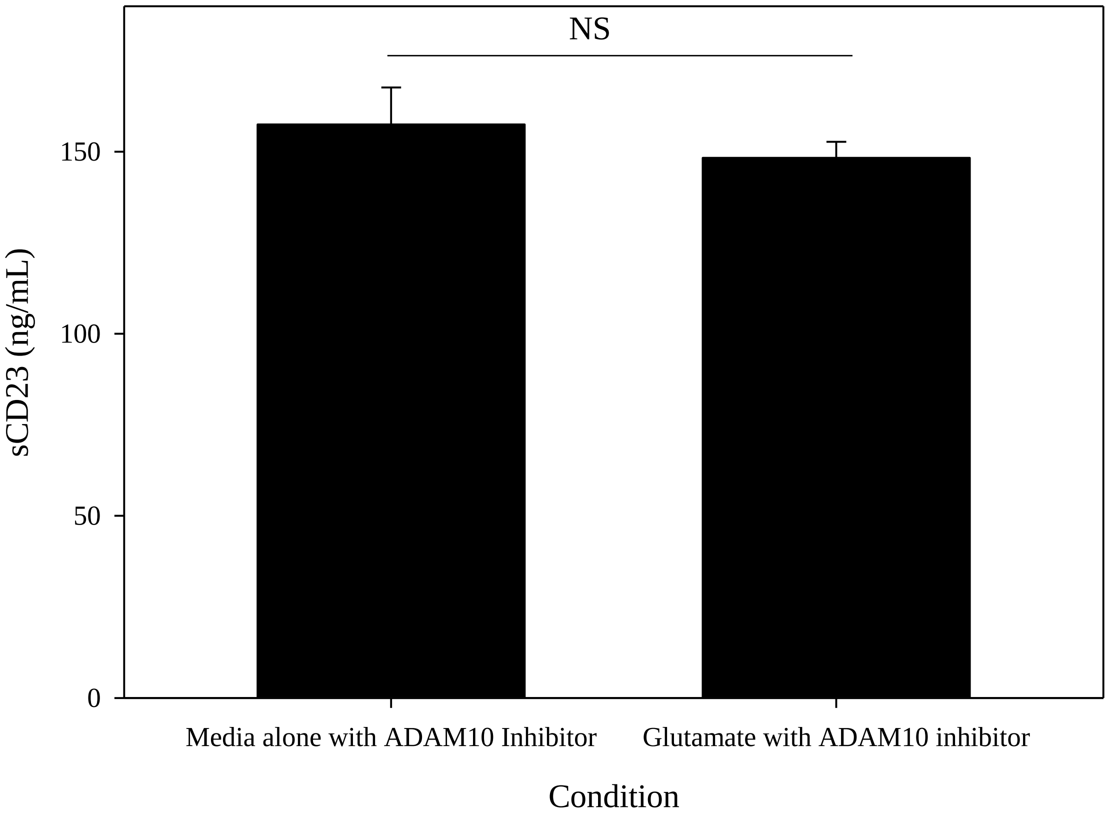
NS
sCD23 (ng/mL)
0
50
100
150
Media alone with ADAM10 Inhibitor
Glutamate with ADAM10 inhibitor
Condition

due to ADAM10 activation. Prior to the addition of glutamate, 8866 were incubated with 10µM ADAM10 specific inhibitor. Figure 19 shows that glutamate cannot overcome the ADAM10 mediated inhibition of sCD23 further indicating that the increase in sCD23 observed in the presence of glutamate is mediated through a KAR specific activation of ADAM10.

C. KAR activation increases IgE synthesis

Because there was a significant increase in sCD23 released from the cell surface, the natural extension of these studies was to look at IgE synthesis as CD23 is a regulator of IgE production. Primary human B cells were stimulated with IL-4 and anti-CD40 to stimulate IgE production and cultured in the presence or absence of KA. When KA is present in the media, there is a strong and statistically significant increase in the amount of IgE produced (Figure 20A). The cultures were performed at multiple cell concentrations as our laboratory has previously reported that cell density inversely correlates with IgE production (74, 71). To determine physiological relevance, the studies were repeated with the natural ligand glutamate. A similar increase in the amount of IgE synthesized from purified human B cells in the presence of glutamate (Figure 20B) was seen. Thus, we chose to utilize the natural ligand for the remainder of the studies.

Our laboratory, as well as others, has previously shown that the addition of IL-21 can enhance IgE production in the human system (106) due to the fact that IL-21 augments plasma cell development in human *in vitro* cultures. Thus, we decided to add IL-21 into our culture system to determine if the glutamate mediated effect on IgE synthesis was still seen even in the presence of the additional cytokine stimuli. This effect is illustrated by the fact that cultures with IL-21 and glutamate make much more IgE than either IL-21 alone or with glutamate alone as indicated by the scale on the y axis of the ELISA graphs.

RPMI-1640, the primary media most utilized for lymphocyte culture, contains 0.1mM glutamate. To better control for and determine the actual role of the glutamate mediated increase in IgE, we switched these studies to using DMEM based media, which lacks any glutamate. In the DMEM based media we observed a pronounced increase in the amount of IgE generated in the presence of glutamate and IL-21(Figure 20C). Thus all remaining studies will employ the use of DMEM based media.

To confirm that the glutamate mediated increase in IgE is mediated through the kainate receptor, the antagonists that were used in the soluble CD23 studies were employed. As evidenced in Figure 20D, we see no effect with either vehicle (DMSO) or the AMPA antagonist, NBQX. However the KAR antagonist, NS102, almost completely blocks the glutamate mediated increase in IgE production. While the IgE production in wells containing both Glu and NS-102 is still significantly higher than the control wells lacking Glu the amount of IgE produced is dramatically reduced ($p<.00001$) when compared to Glu containing cultures. In separate experiments, TPM also did not influence IgE production (Figure 21), further confirming the KAR specificity.

D. KAR Activation leads to an increase in cell proliferation

Hasbold *et al.* (107) reported that cell proliferation is directly related to Ig production, thus B cells were cultured in the presence or absence of Glu to examine changes in proliferation. Our laboratory has shown that B cell proliferation and human IgE synthesis are correlated and increased in the presence of IL-21, thus extending upon the Hasbold study (71). In order to examine if this phenomenon held true in the presence of KAR agonism,

Figure 20. Kainate receptor activation increases IgE synthesis.

Primary B cells were cultured in the presence of 10 ng/mL IL-4 and 1 µg/mL anti-CD40 in CRPMI-10 in the presence or absence of 5mM KA (A) or 5mM Glu (B). After 14 days of culture, cell free supernatants were analyzed via ELISA for IgE levels. (C)Primary B cells were cultured in the presence of IL-4 and anti-CD40 as in (A) plus 200ng/mL IL-21 in the presence or absence of 5mM glutamate in CDMEM-10. After 14 days of culture, cell free supernatants were analyzed via ELISA for IgE levels. (D) Before culture primary B cells were treated with 10µM vehicle (DMSO), NBQX, or NS102. Primary B cells were then cultured in similar conditions as in C. After 14 days, ELISA analysis performed. Part A, B, and C represent three different individuals that serve as a representative donor. Part D is the cell concentration in which maximum Ig production was observed (9,000 cells/well) either in the presence or absence of antagonist from another donor. Both the RPMI and DMEM culture experiments have been performed a minimum of 3 times with similar results. * indicated $p<0.05$ as compared to indicated control. # indicates $p<0.01$ as compared to indicated control.

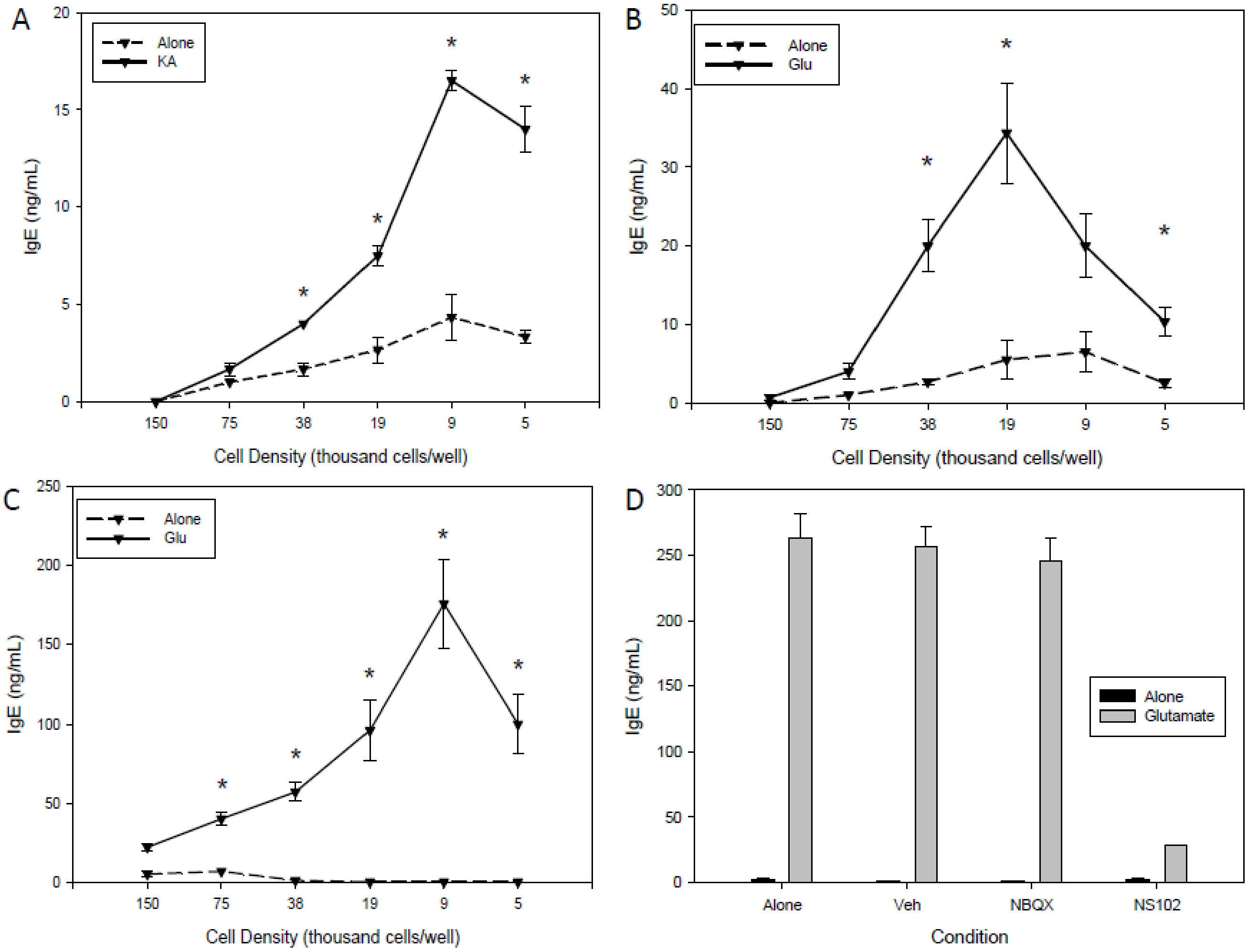
A
Alone
KA
IgE (ng/mL)
0
5
10
15
20
150
75
38
19
9
5
Cell Density (thousand cells/well)
*
B
Alone
Glu
IgE (ng/mL)
0
10
20
30
40
50
150
75
38
19
9
5
Cell Density (thousand cells/well)
C
Alone
Glu
IgE (ng/mL)
0
50
100
150
200
250
150
75
38
19
9
5
Cell Density (thousand cells/well)
D
Alone
Glutamate
IgE (ng/mL)
0
50
100
150
200
250
300
Alone
Veh
NBQX
NS102
Condition

Figure 21. The glutamate mediated increase in IgE synthesis is not through the NMDA receptor.

Primary B cells were cultured in the presence of 10 ng/mL IL-4, 1 µg/mL anti-CD40, and 200ng/mL IL-21 in the presence or absence of 5mM glutamate in CDMEM-10. Before culture primary B cells were treated with 10µM vehicle (DMSO) or Topiramate (TPM) for one hour prior to the addition of glutamate. After 14 days of culture, cell free supernatants were analyzed via ELISA for IgE levels. Shown is the cell concentration in which maximum Ig production was observed (9,000 cells/well). Experiments have been performed a minimum of 3 times with similar results. There is no statistical difference between the group treated with vehicle control or TPM indicating that TPM is not capable of reducing the glutamate mediated effect on IgE production.

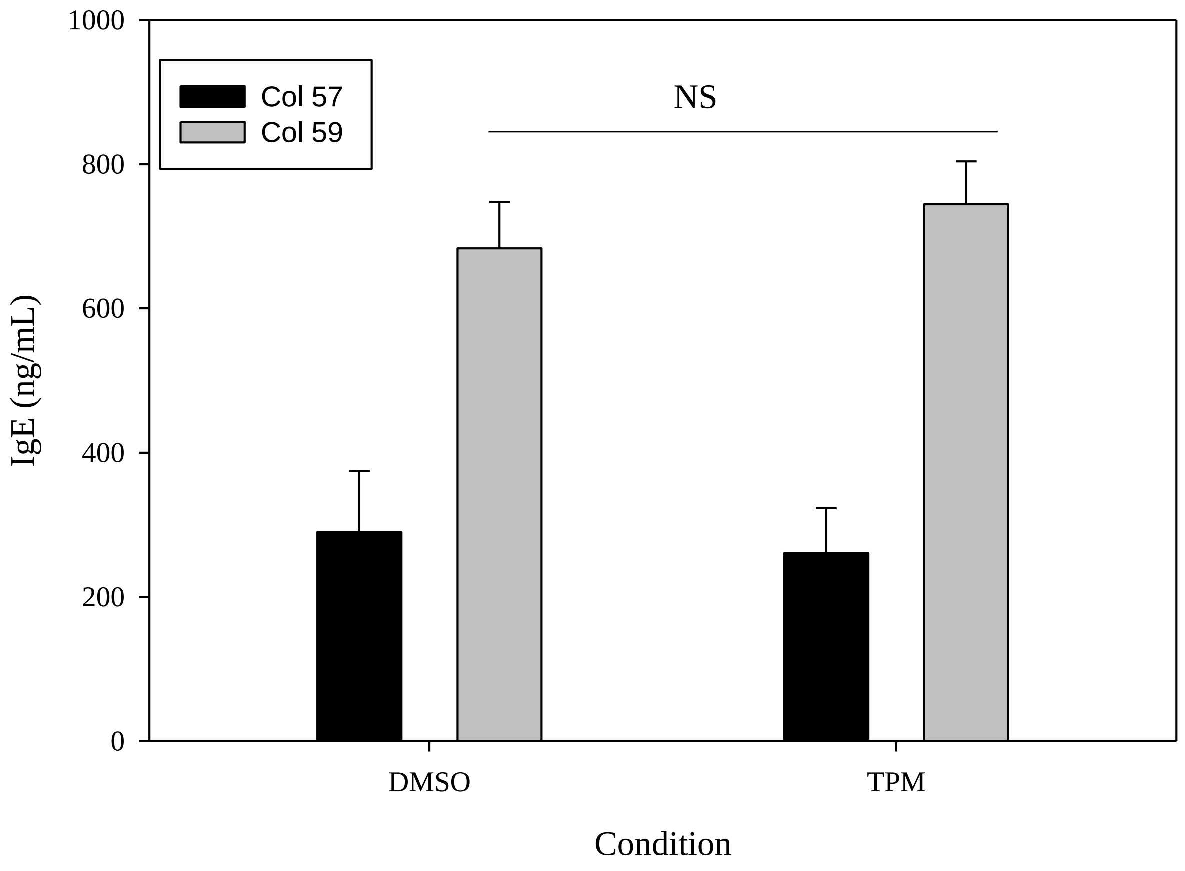
1000
800
600
400
200
0
IgE (ng/mL)
Col 57
Col 59
NS
DMSO
TPM
Condition

primary human B cells were grown in the presence/absence of glutamate and cell proliferation was determined. From the data shown, KAR activation leads to a significant increase in proliferation (Figure 22 and 23) which is prevented in the presence of NS102. Taken together, our data coupled with previous data shown by other groups indicating the need for a proliferative response required for IgE synthesis clearly strengthens the argument that KAR activation via glutamate signaling can promote an enhanced humoral response and the enhanced IgE production would be anticipated to enhance an atopic phenotype.

E. KAR activation increases IgG synthesis but has no effect on IgM synthesis

To determine if glutamate stimulation through the KAR would enhance other immunoglobulin isotypes, we examined total IgG and IgM secretion from B cell cultures. A similar phenomenon in terms of IgG production was observed as compared to the glutamate mediated IgE enhancement and this enhancement was also blocked by the KAR antagonist, NS102, but was unaffected by either vehicle control or the AMPA antagonist, NBQX (Figure 24). However, total IgM levels were not influenced. The IgM data is shown at a single concentration (150,000 cells/well) but no enhancement of IgM was seen at any cell concentration (Figure 25).

F. Glutamate enhancement is also seen in PBMC cultures.

The aforementioned studies used purified B cells. In order to determine if the enhancement was still effective with the cellular milieu that closely mimics the immune system, we examined effect of KAR agonists on IgE production using PBMC. As can be seen in Figure 26A, addition of glutamate to the PBMC cultures that are stimulated with anti-CD40 and IL-4 again resulted in a very strong enhancement of IgE synthesis. Other immunoglobulins (total IgG and IgM) were also tested and while IgG enhancement was seen

Figure 22. Kainate receptor activation increases cellular proliferation.

Primary B cells were cultured as in Fig 20C in CDMEM-10 in the presence or absence of 5mM glutamate at a concentration of 150,000 cells/well. Prior to the addition of glutamate, cells were pretreated for 1 hour with 10µM vehicle (DMSO) or NS102. After 96 hours, cells were pulsed for 24 hrs with [^{3}H]-thymidine. Shown is one representative donor of three performed. * indicates $p<0.05$ as compared to vehicle alone.

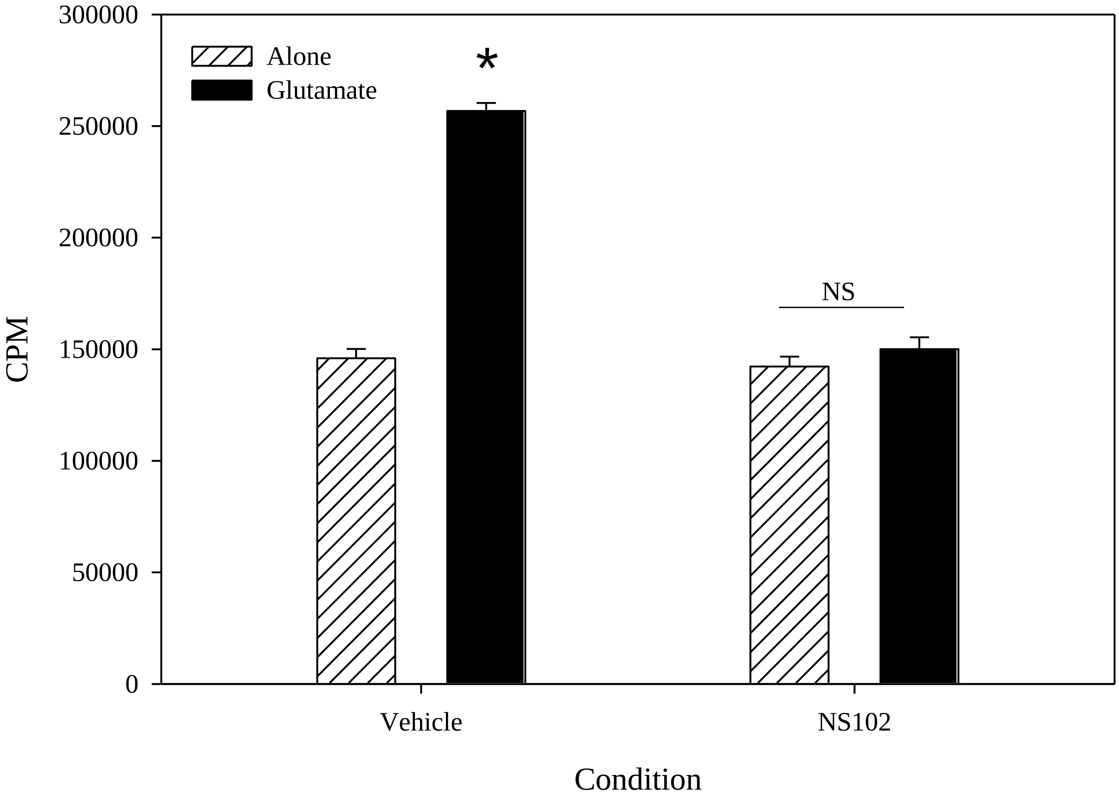
300000
250000
200000
150000
100000
50000
0
CPM
▨ Alone
■ Glutamate
*
NS
Vehicle
NS102
Condition

Figure 23. Kainate receptor activation increases cellular proliferation.

Primary B cells (10^4 /well) were labeled with CFSE as indicated in Materials and methods and were cultured with IL-4, anti-CD40, IL-21 in CDMEM-10 alone (▬▬) or in the presence of 5mM glutamate (−·−·−).CFSE fluorescence was determined on day 5 post culture initiation**.** Shown is a representative of two of similar design

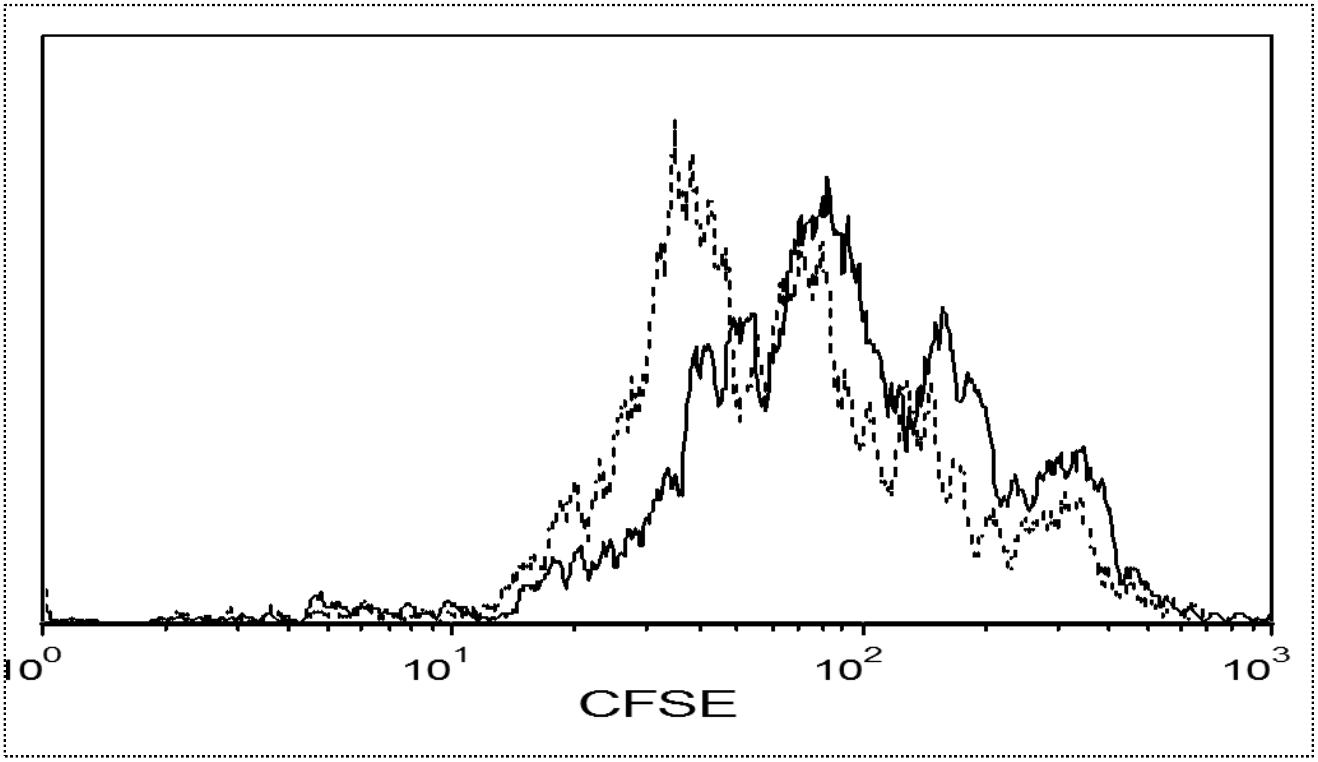
10^0
10^1
10^2
10^3
CFSE

Figure 24. Kainate receptor activation increases total IgG synthesis.

Primary B cells were cultured as in Fig 20C in CDMEM-10 in the presence or absence of 5mM glutamate. After 14 days of culture, cell free supernatants were analyzed via ELISA for IgG levels. Before culture primary B cells were treated with 10µM vehicle (DMSO), NBQX, or NS102 for one hour prior to the addition of glutamate. After 14 days, ELISA analysis performed. Shown is one cell concentration with highest Ig production (38,000 cells/well) and is one representative donor of three with similar results. * indicated $p<0.05$ as compared to alone.

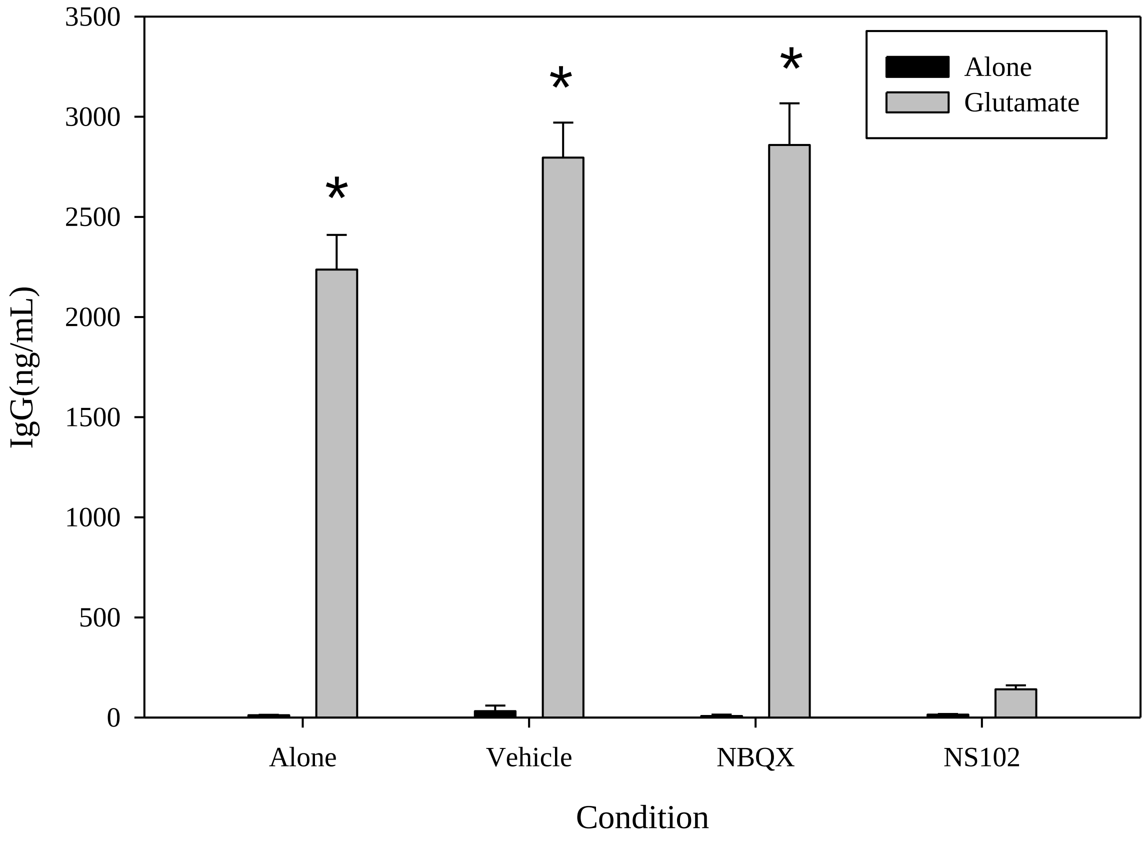
3500
3000
2500
2000
1500
1000
500
0
IgG(ng/mL)
*
*
*
Alone
Glutamate
Alone
Vehicle
NBQX
NS102
Condition

Figure 25. Kainate receptor activation does not affect IgM synthesis.

Primary B cells were cultured as in Figure 20C in CDMEM-10 in the presence or absence of 5mM glutamate. After 14 days of culture, cell free supernatants were analyzed via ELISA for IgM levels. Experiment shown is one of three with similar outcomes. NS – not significant.

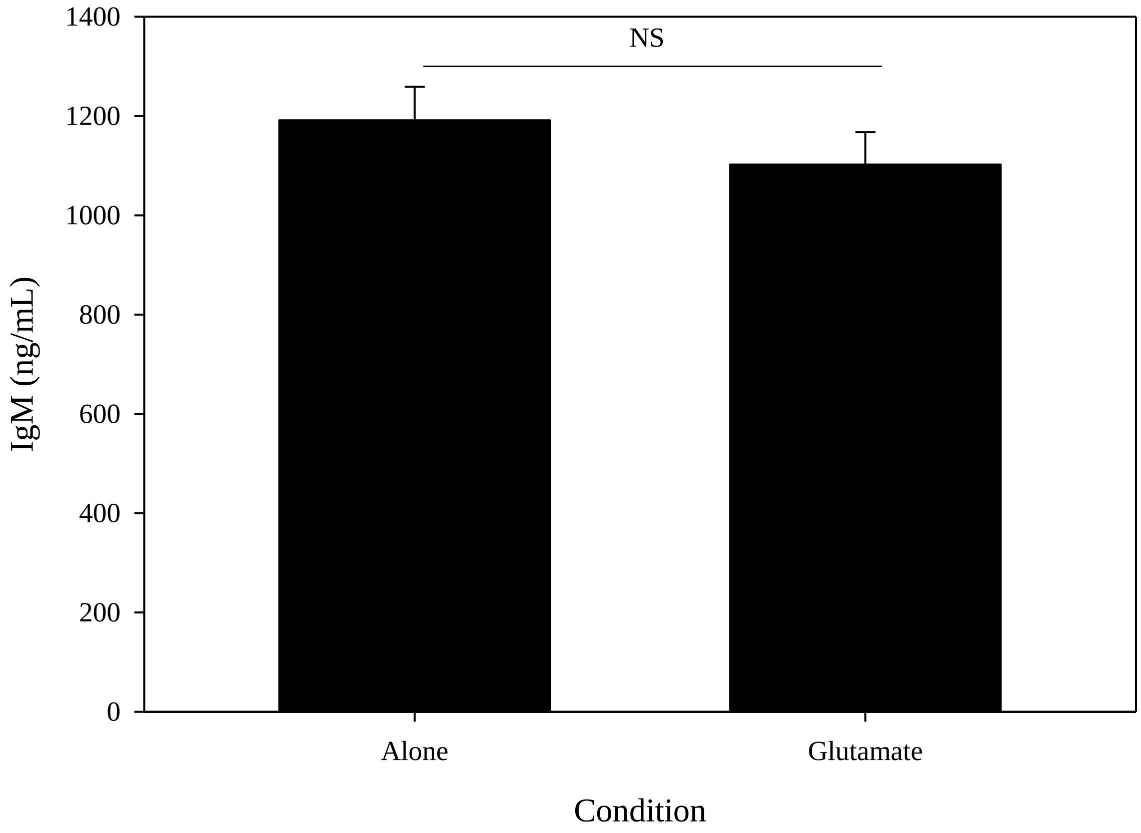

1400
1200
1000
800
600
400
200
0
IgM (ng/mL)
NS
Alone
Glutamate
Condition

(Figure 26B), IgM production in the PBMC cultures, as with purified B cells, was not significantly influenced (Figure 26C). The KAR specific antagonist, NS-102, again strongly blocked the increase in IgE and IgG production. Note that the cell concentrations used for the NS102 were where maximum Ig production was seen. In a similar fashion as with purified B cells, proliferation was also affected by the addition of glutamate (Figure 26D).

G. KARs are also expressed in the murine immune system.

After the discovery that KARs were expressed in the human immune system and that stimulation of this receptor had a dramatic impact on Ig production, we next wanted to determine if this phenomenon held true in the mouse. Utilizing mouse models allows for more genetic control as well as *in vivo* examination of the role KARs play in humoral immunity. We first wanted to determine if the KAR was expressed on mouse immune cells. Flow cytometric analysis of mouse splenocytes was performed in an identical fashion as with human PBMC and tonsilar cells and indeed we do see expression of KARs on all immune cells examined (Figure 27)

H. IgE Production is enhanced in murine B cells via KAR stimulation.

Our next step was to determine if the KAR functioned similarly in the mouse immune system as in the human. Naïve mouse splenic B cells were cultured with IL-4 and anti-CD40 stimulation in the presence or absence of 5mM glutamate. As shown in Figure 28, we see a pronounced increase in the amount of IgE produced *in vitro.* To confirm that the glutamate mediated increase is a result of KAR stimulation, we once again employed the use of NS102. When mouse B cells were pretreated with 1 µM of NS102, prior to the addition of 5mM glutamate, the increase in glutamate mediated IgE production is abrogated (Figure 28).

Figure 26. Kainate receptor activation in human PBMC model.

Human PBMC were cultured in the presence of 10ng/mL IL-4, 1 µg/mL anti-CD40, and 200 ng/mL IL-21 in CDMEM-10. Prior to the addition of glutamate, cells were pretreated for 1 hour with 10µM vehicle (DMSO) or NS102. After 14 days of culture, cell free supernatants were analyzed for IgE (A), total IgG (B), or IgM (C). The cell concentration showing maximum Ig production is shown in the presence or absence of Glu. These cell concentration values were 18,000 cells/well (A), 38,000 cells/well (B) and 300,000 cells/well (C). Separate, identical cultures (150K/well) were plated to analyze cellular proliferation (D). Shown in each is one representative donor. A total of 3 PBMC cultures have been examined in this manner with similar results. * indicated $p<0.05$ as compared to alone. # indicates $p<0.01$ as compared to indicated control. NS – not significant.

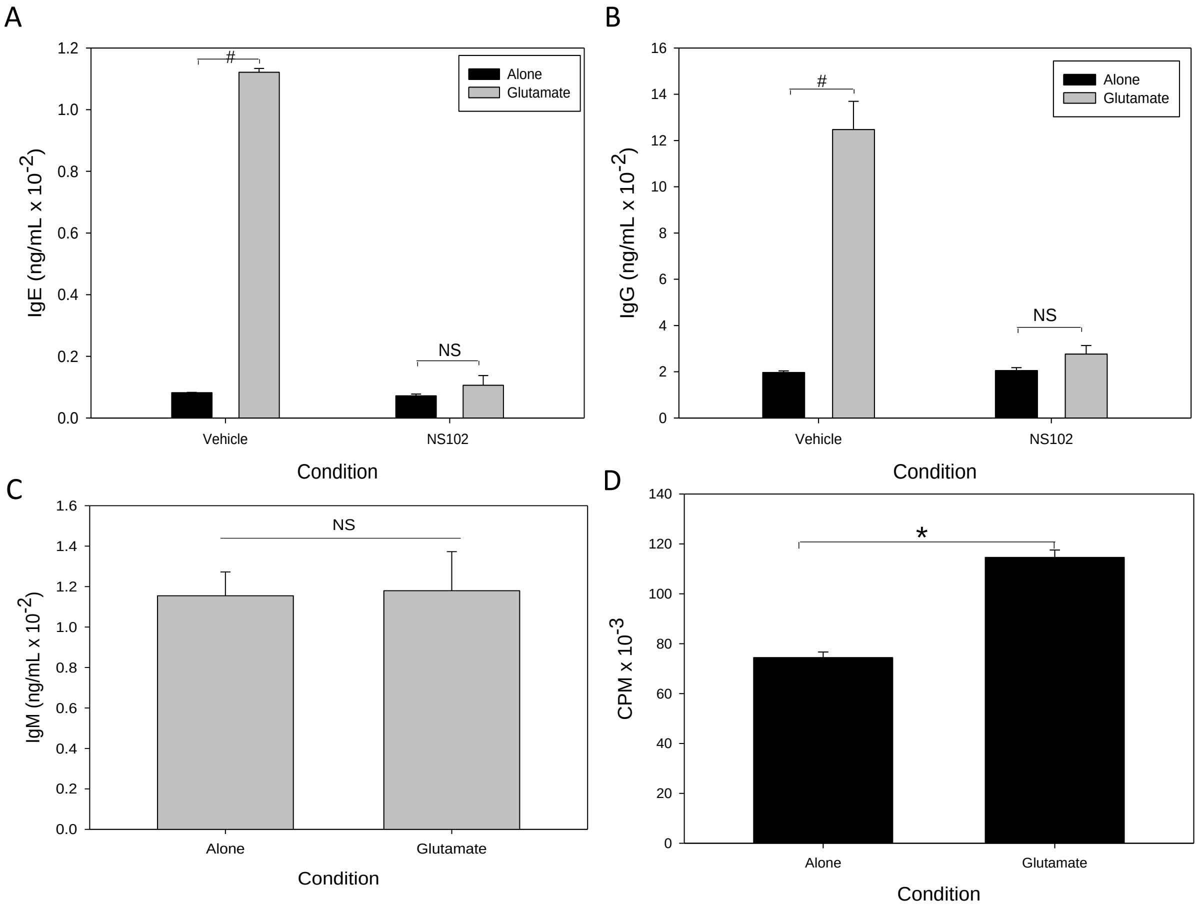
A
1.2
1.0
0.8
0.6
0.4
0.2
0.0
IgE (ng/mL x 10^{-2})
#
NS
Alone
Glutamate
Vehicle
NS102
Condition
B
16
14
12
10
8
6
4
2
0
IgG (ng/mL x 10^{-2})
#
NS
Alone
Glutamate
Vehicle
NS102
Condition
C
1.6
1.4
1.2
1.0
0.8
0.6
0.4
0.2
0.0
IgM (ng/mL x 10^{-2})
NS
Alone
Glutamate
Condition
D
140
120
100
80
60
40
20
0
CPM x 10^{-3}
*
Alone
Glutamate
Condition

Figure 27. Kainate Receptors are cell surface expressed in the mouse immune system. Cells were subjected to flow cytometric analysis as described. Briefly, cells were stained with rabbit anti GluK4 followed by a goat anti rabbit PE. Cell specific stains were FITC labeled. Natural Killer cells were stained with NK1.1, monocytes were stained with Mac-1, T cells were stained with Thy1.1, and B cells were stained with B220. Shown here is one representative spleen preparation out of three of similar design.

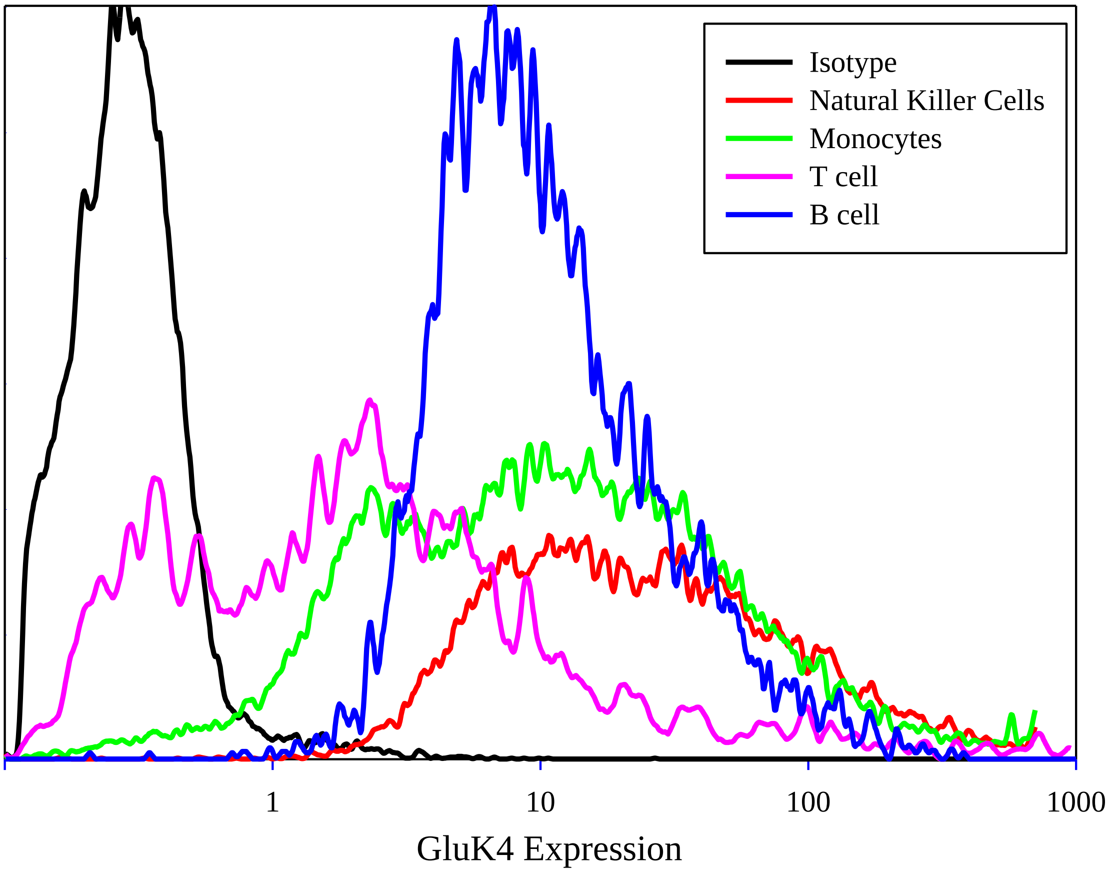
Isotype
Natural Killer Cells
Monocytes
T cell
B cell
1
10
100
1000
GluK4 Expression

Figure 28. IgE Production is enhanced in murine B cells via KAR stimulation.

Naïve mouse B cells were cultured with 10,000U/mL IL-4 and 25 µg/mL anti-CD40 stimulation in the presence or absence of 5mM glutamate. To confirm that the glutamate mediated increase is a result of KAR stimulation, we once again employed the use of NS102 or DMSO as a vehicle control. Shown is one representative mouse *in vitro* experiment of three of similar design.

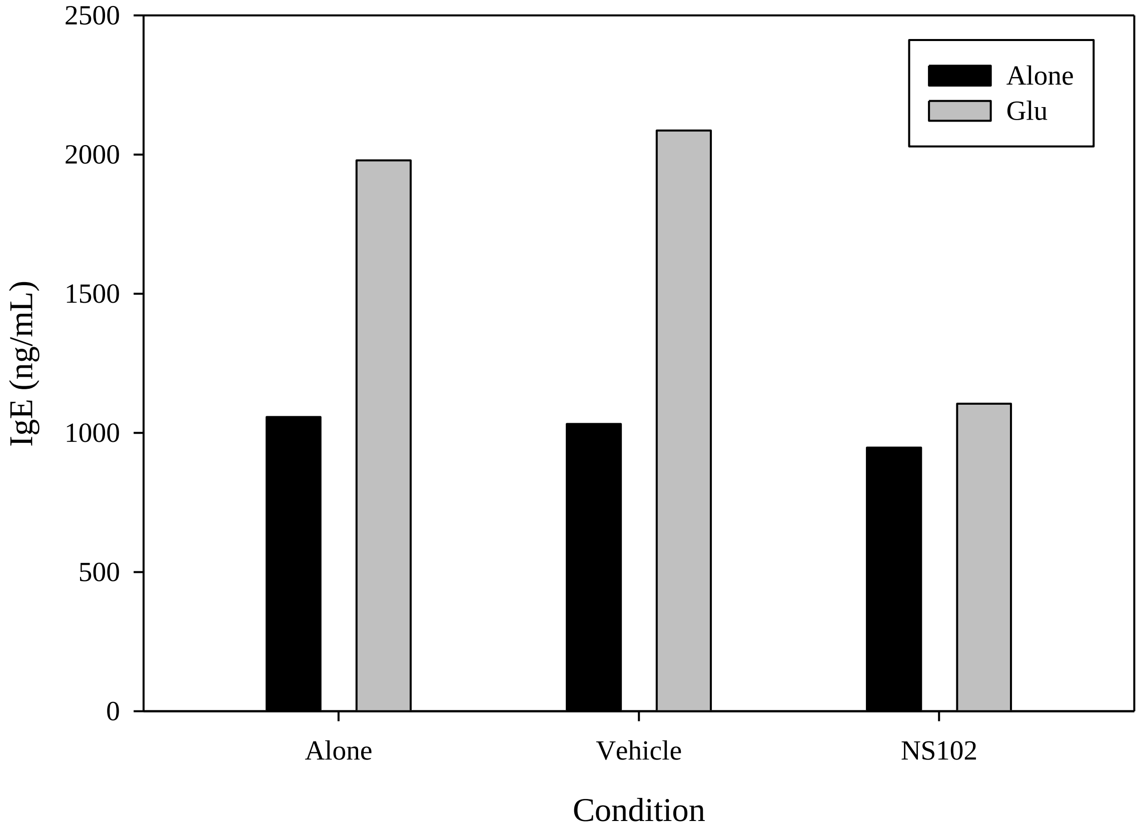
2500
2000
1500
1000
500
0
IgE (ng/mL)
Alone
Glu
Alone
Vehicle
NS102
Condition

I. Immunophenotyping and *in vitro* experimentation with GluK2 KO mouse

As with the case of any inhibitor, there is always the question of specificity. Thus far we have utilized NS102 as a specific inhibitor of the GluK2 containing KAR, as this is the subtype evidenced by our data to exist in the immune system. In the literature, most inhibitor studies are confirmed with eloquent genetic manipulations such as siRNA or shRNA to "knockdown" the gene target in question in order to recapitulate the results seen in the presence of the inhibitor. While knockdown studies are useful, we are limited by the fact we are using primary lymphocytes which are notoriously hard to transfect by conventional means. Furthermore, our endpoints of KAR blockade are 14 days in the human and 8 days in the mouse, much longer than the normal time frame for transient transfections. To confirm that indeed the GluK2 containing KAR receptor is important in the immune system, we obtained GluK2 deficient mice from Anis Contractor (Northwestern University, Chicago, IL). These mice were engineered by a neomycin disruption of the GRIK2 gene and have been characterized and extensively studied in the CNS field (67). It is important to note that in the absence of this subunit, a functional kainate receptor fails to form, thus these mice are sometimes referred to as KAR KO. However, to our knowledge nothing has been reported about the immune systems of these mice.

We received 2 male homozygous knockout (KO) and one female heterozygous knockout. These mice are on a mixed 129-C57BL/6J background. Given the novel finding that the CD23 is mutated in the 129 mouse strain (as described above), we want to backcross these mice onto a pure C57BL/6 strain. Thus mice were mated with C57BL6/J (Jackson Laboratories, Bar Harbor ME) and resultant offspring were typed as described. Because it takes at least 7 generations to completely move a genetically modified mouse from one strain to another, we began to utilize the progeny produced here at VCU but were also careful to use appropriate littermate controls.

As little is known about these mice, we first wanted to immunophenotype them to discern if there were any differences between mice that express or lack GluK2. We note no gross differences in size or weight of the mice. The only outwardly visible difference is that GluK2 mice appear more docile in our hands. We observe no noticeable difference in spleen size, weight, or cellular distribution (Figure 29 and data not shown). Furthermore, we detect no difference in baseline IgE in the sera (data not shown).

We next wanted to determine if B cells isolated from these mice fail to respond to glutamate *in vitro*. Spleens were isolated and B cells were purified by negative selection as described. B cells were cultured with IL-4 and anti-CD40 in the presence or absence of 5mM glutamate. We detect no increase in soluble CD23 released from the cell surface (Figure 30), no increase in IgE production (Figure 31), or no increase in cellular proliferation (Figure 31) in the KO mice in the presence of glutamate. These studies corroborate data in the human system which utilized NS102 and further emphasize that the GluK2 subtype KAR is the sole glutamate receptor involved in the glutamate mediated enhancement seen on humoral immunity in both man and mouse.

J. *In vivo* experimentation with GluK2 KO

Not only do the GluK2 KO mice allow for a system to determine the role the KAR plays in the absence of chemical inhibition *in vitro,* they allow for further examination of the role that the KAR plays *in vivo.* Using an ovalbumin immunization challenge we can determine if KAR are critical for IgE production *in vivo*. Prior to any immunization, mice were bled by tail nick with a surgical scalpel (Feather #11 Fisher Scientific). Blood was collected in

Figure 29. Immunophenotyping the GluK2 KO mouse.

Spleens were isolated from either KO or littermate (LM) control mice and subjected to either flow cytometric analysis or immunohistochemistry. Flow cytometry shows that the average B cell percentage in KO vs. LM is 41 +/- 7% vs. 45 +/- 6% whereas the T cell percentage is 50 +/- 2% vs. 48 +/- 2%. (N=3, p>0.05, data not shown). Immunohistochemical analysis was performed by Rebecca Martin and shows no histological difference in either spleens or lymph nodes (not shown) of KO

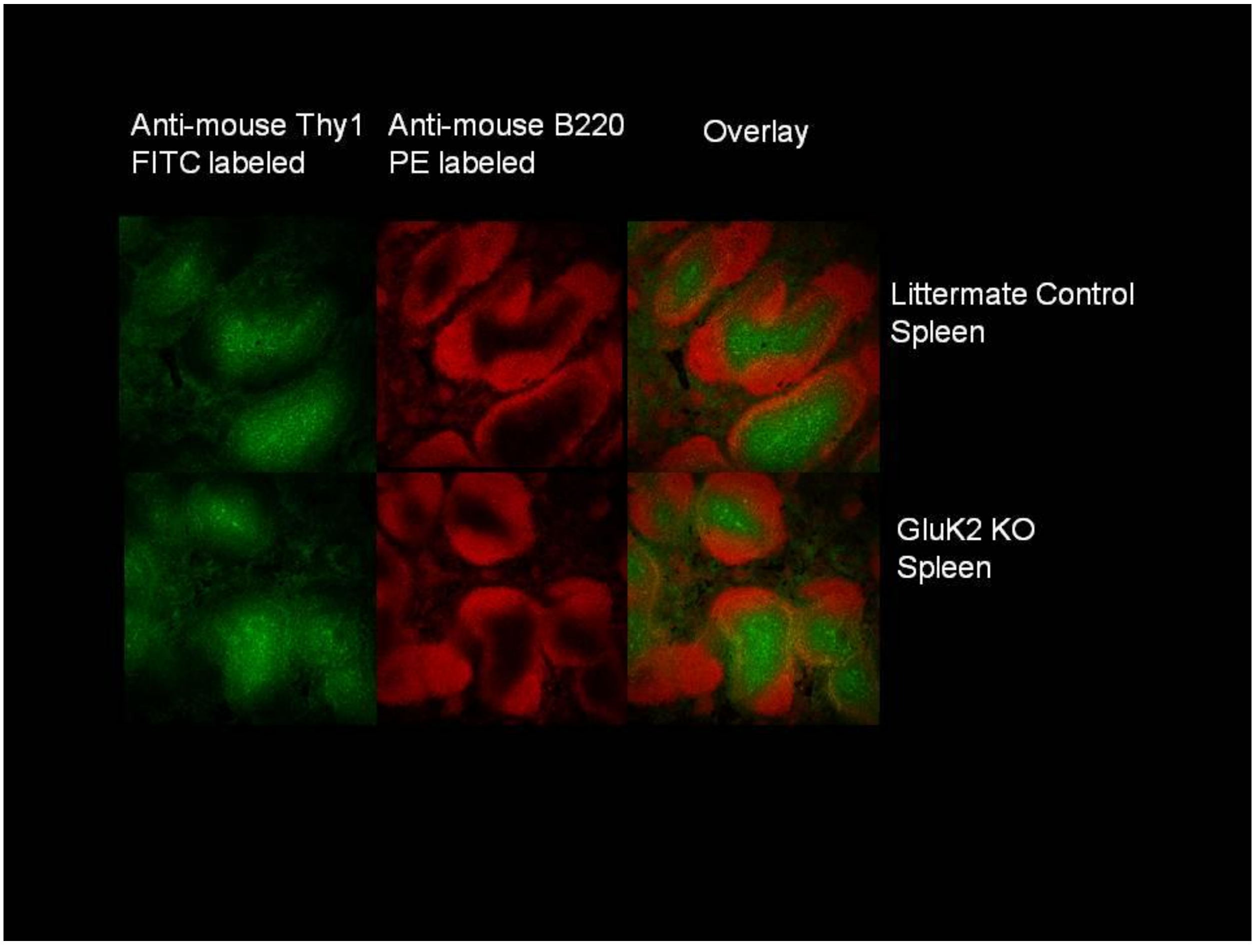
Anti-mouse Thy1
FITC labeled
Anti-mouse B220
PE labeled
Overlay
Littermate Control
Spleen
GluK2 KO
Spleen

Figure 30. Glutamate mediated enhancement of soluble CD23 is not observed in GluK2 KO mice.

1 x10^6 naïve B cells/ mL were cultured in the presence of 10,000U IL-4 and 25ug anti CD40 in the presence or absence of 5mM glutamate. 24 hours later, cell free supernatants were harvested and sCD23 was determined via ELISA. The polyclonal ELISA was used as these mice are on a 129 mixed background and contain a mutation in CD23 that prevents 2H10 binding. Shown is one representative mouse per group. Experiment has been repeated once with similar design.

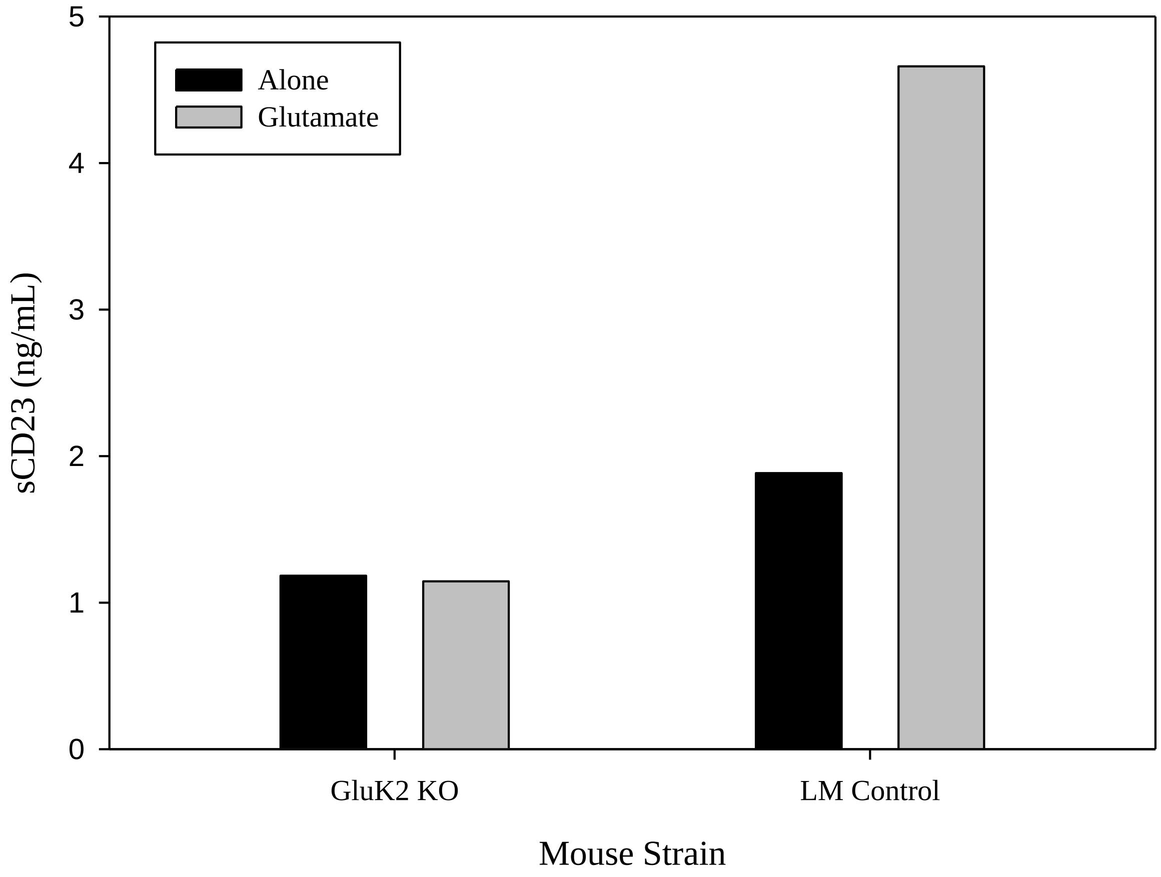
5
4
3
2
1
0
sCD23 (ng/mL)
Alone
Glutamate
GluK2 KO
LM Control
Mouse Strain

Figure 31. Glutamate mediated enhancement of IgE is not observed in GluK2 KO mice. Naïve B cells/ mL were cultured in the presence of 10,000U IL-4 and 25ug anti CD40 in the presence or absence of 5mM glutamate. Eight days later, cell free supernatants were harvested and IgE was determined via ELISA. Shown is one representative mouse per group. Experiment has been repeated twice with similar design. Data is represented as fold increase over media alone.

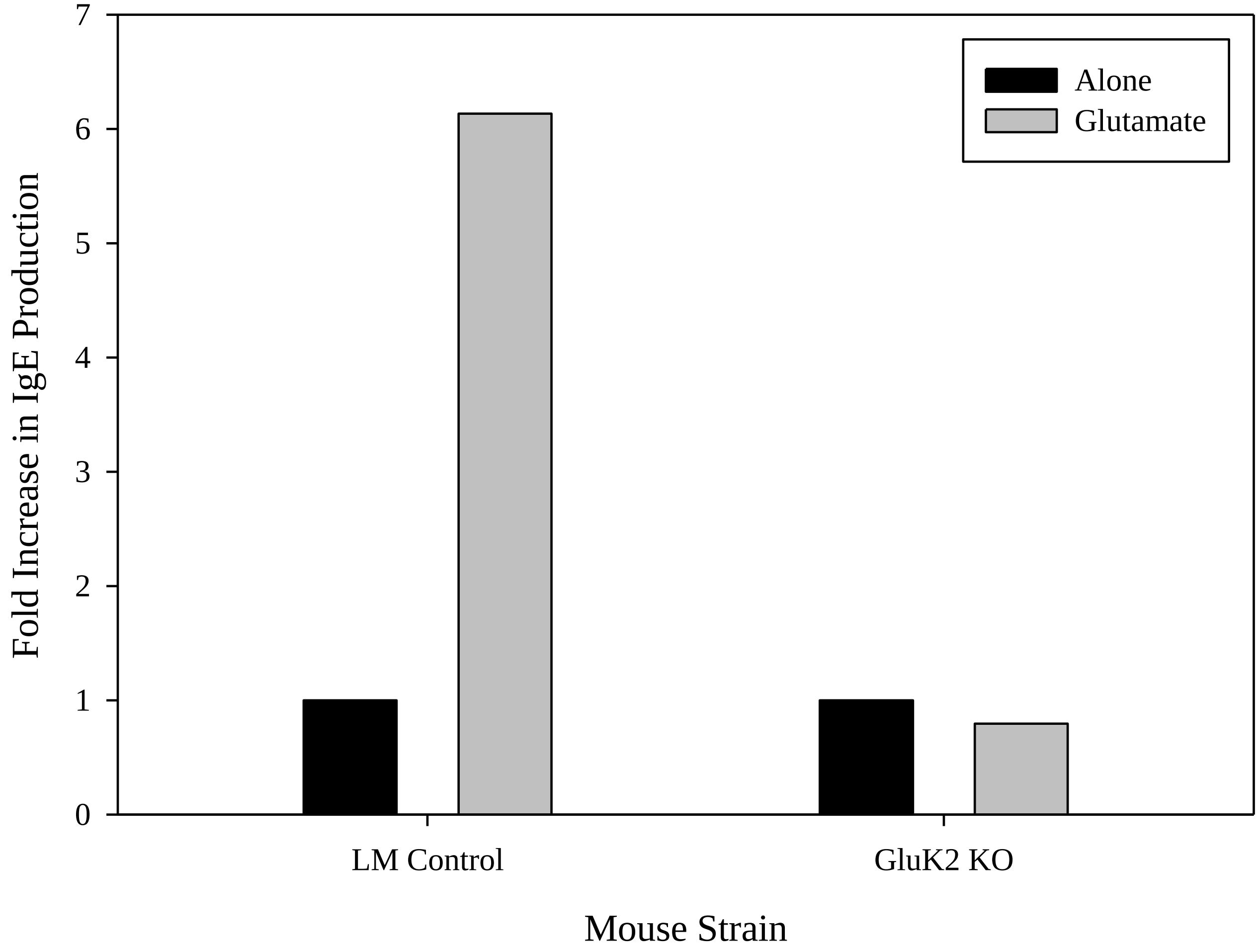
7
6
5
4
3
2
1
0
Fold Increase in IgE Production
Alone
Glutamate
LM Control
GluK2 KO
Mouse Strain

Figure 32. Glutamate mediated enhancement of proliferation is not observed in GluK2 KO mice.

Naïve B cells/ mL were cultured with 10,000U IL-4 and 25ug anti CD40 in the presence or absence of 5mM glutamate at a concentration of 25,000 cells/well. After 96 hours, cells were pulsed for 24 hrs with [^{3}H]-thymidine. Shown is average experiment of three mice per group. * indicates $p<0.05$ NS – not significant.

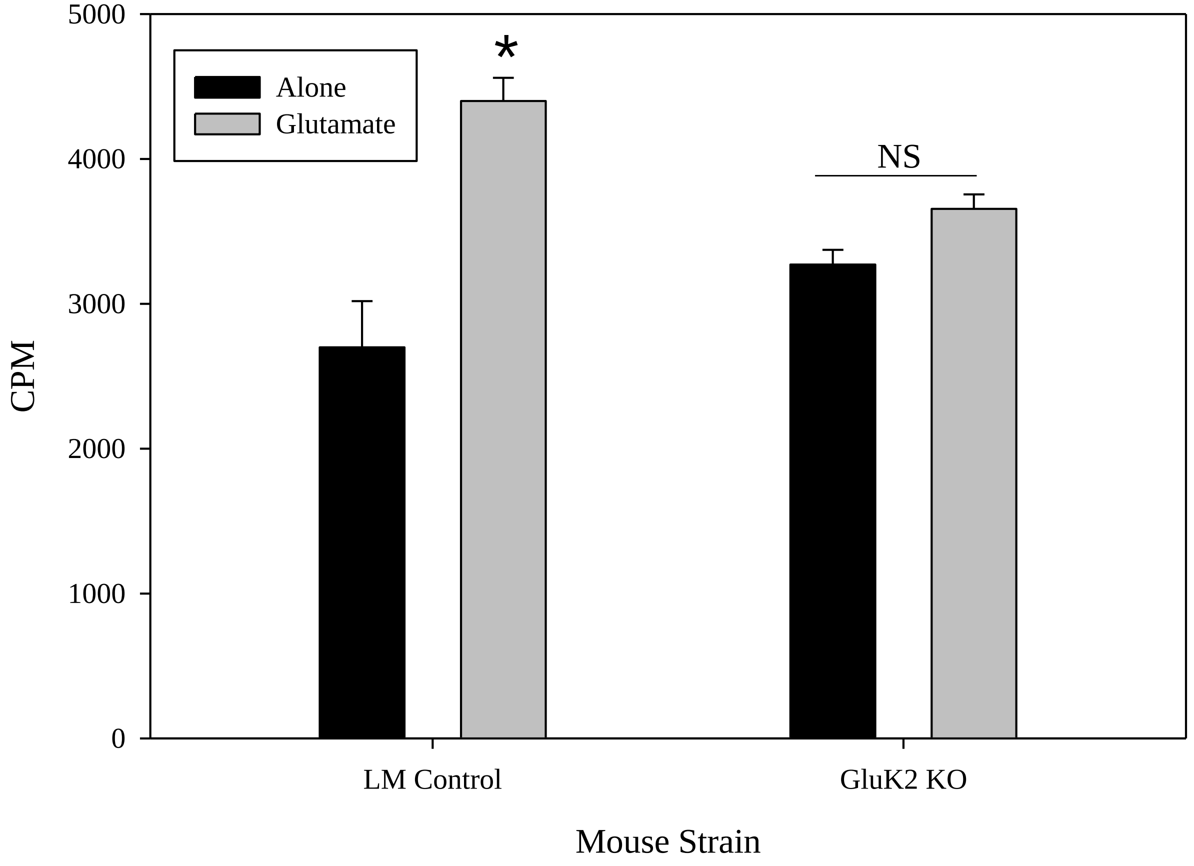
5000
4000
3000
2000
1000
0
CPM
Alone
Glutamate
*
NS
LM Control
GluK2 KO
Mouse Strain

heparin coated capillary tubes, transferred to 1.5mL eppendorf tubes, and spun at 10,000 RPM for 10 minutes to separate serum from cellular components. Mice were injected s.c. with 100µg ovalbumin (Sigma) in 4mg Imject Alum (Pierce) or alum in PBS as a control. On day 15, mice were boosted with 100µg ova in alum or alum in PBS i.p. On day 22, mice were sacrificed by isoflurane inhalation, cardiac punctured for blood collection, and spleens were saved for analysis. Figure 33 shows that the GluK2 mice have significantly reduced IgE levels on day 22 post immunization.

Because the IgE post antigen challenge with ovalbumin showed a reduced amount of IgE in GluK2 KO mice, we next wanted to utilize the *Nippostrongylus brasillensis* infection model. *Nippostrongylus brasillensis* (Nippo) is an intestinal nematode used to invoke a strong T_H2 response in laboratory rodents. We injected 3 mice per group with 500 L3 larvae. Ten days later, mice were bled by cardiac puncture and IgE was analyzed by ELISA. There is a clear reduction in the amount of IgE produced in the GluK2 KO mice post Nippo challenge (Figure 34). However one caveat of this study is that we chose to examine IgE on day 10 rather than the traditional end-point of day 14. The reasoning for this is that we previously reported that mice on a 129 background clear Nippo much faster than C57BL/6 (86). Although the data presented does show a difference, it should be noted that further more thorough kinetic analysis and clearance studies should be performed to determine if indeed GluK2 KO mice have a different response to Nippo infection.

Figure 33. GluK2 mice have reduced IgE post immunization.

Mice were injected s.c. with 100µg ovalbumin (Sigma) in 4mg Imject Alum (Pierce) or alum in PBS as a control. On day 15, mice were boosted with 100µg ova in alum or alum in PBS i.p. On day 22, mice were sacrificed by isoflurane inhalation, cardiac punctured for blood collection, and spleens were saved for analysis. Shown is ELISA examining total IgE levels on day 22. One experiment N=3 mice per group. Data is total IgE with pre-bleed values subtracted. There were no differences in pre-bleed values or alum alone between the two groups of mice. * indicates p value less than 0.05.

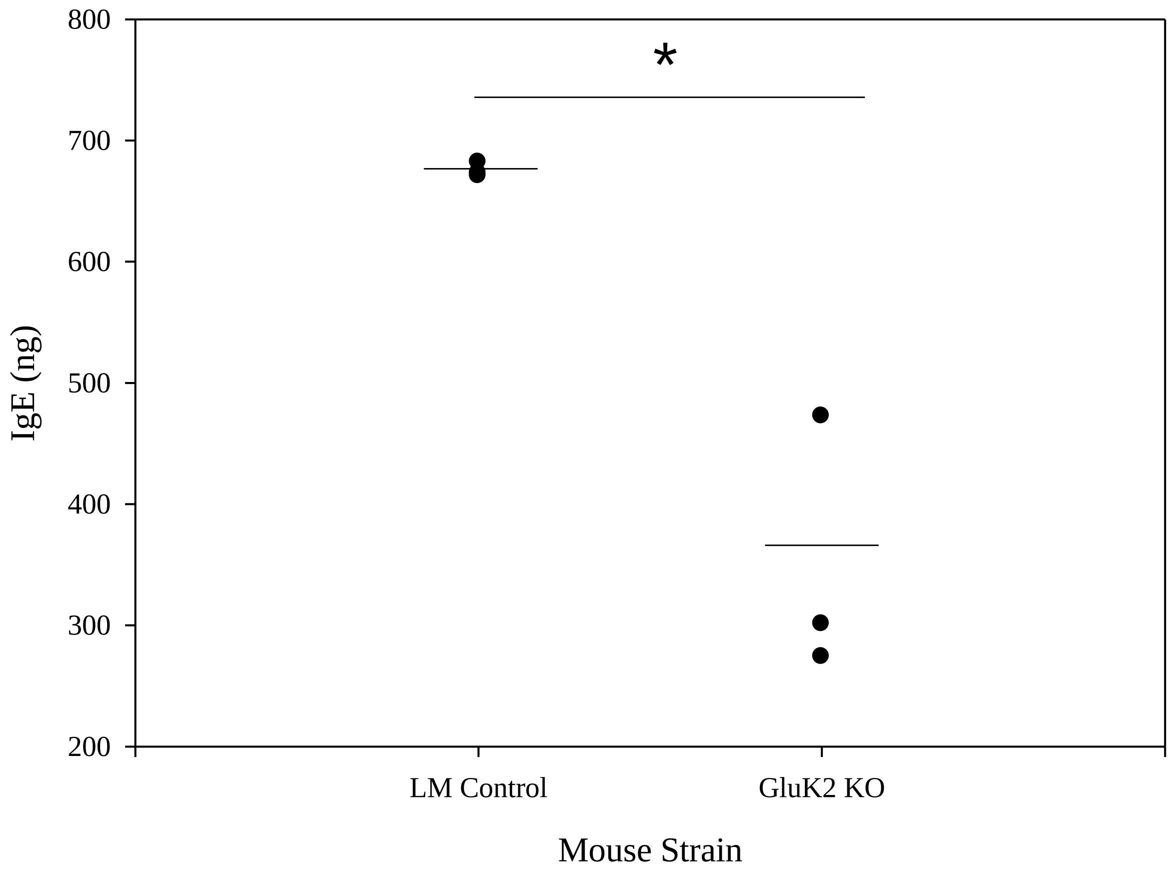
800
700
600
500
400
300
200
IgE (ng)
*
LM Control
GluK2 KO
Mouse Strain

Figure 34. GluK2 mice have reduced IgE post *Nippostrongylus brasillensis* challenge

500 *Nippostrongylus brasillensis* L3 larvae were injected s.c.. Ten days later, mice were bled by cardiac puncture and IgE was analyzed by ELISA. Shown is ELISA examining total IgE levels on day 10. One experiment N=3 mice per group. Data is total IgE with pre-bleed values subtracted. There were no differences in pre-bleed values between the two groups of mice. * indicates p value less than 0.05.

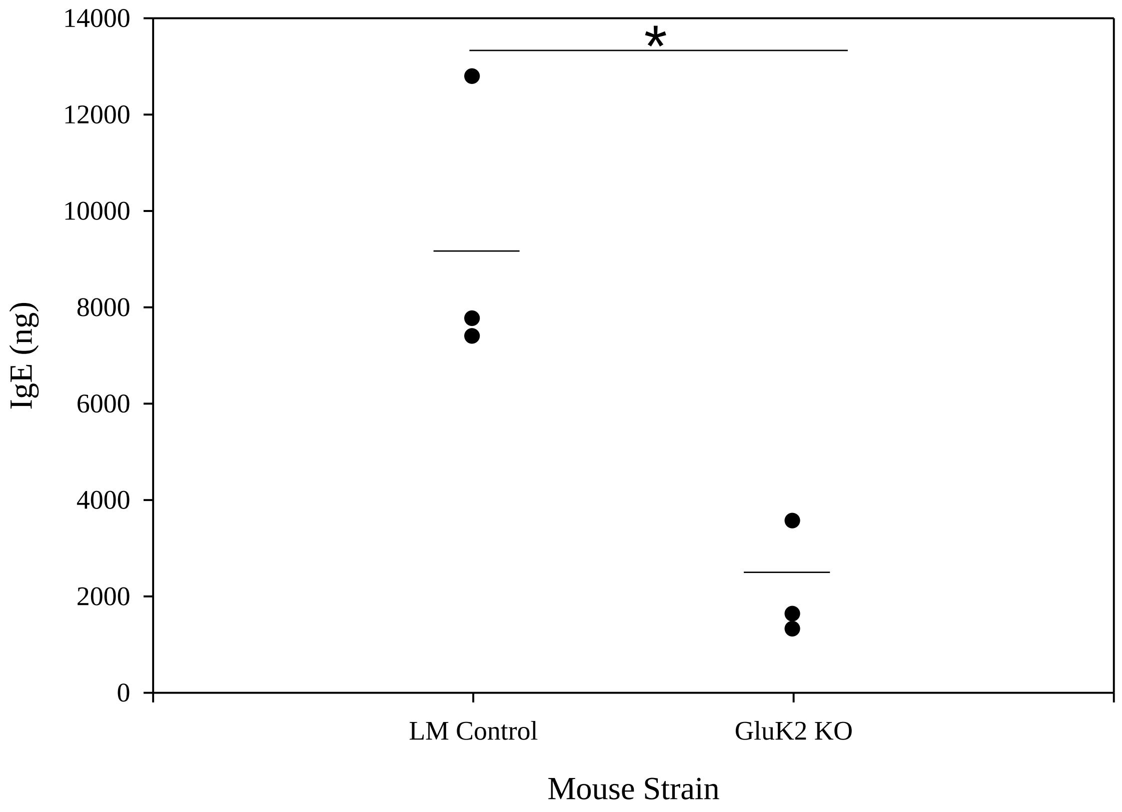
14000
12000
10000
8000
6000
4000
2000
0
IgE (ng)
*
LM Control
GluK2 KO
Mouse Strain

IV. Identification of ADAM10 as a novel therapeutic target in B cell chronic lymphocytic leukemia

Chronic lymphocytic leukemia (CLL) is one of four main types of leukemia and is the most common type seen in the North American and European populations. According to the National Cancer Institute, it is estimated that approximately 14,990 American men and women will be diagnosed with CLL and of those, 4,390 will die of this disease in 2010. This equates to a relative lifetime risk that 1 in every 210 Americans will be diagnosed with this disease. In addition, more people are living with CLL than any other type of leukemia today. In 95% of cases, CLL is a disorder of B lymphocytes (BCLL) thus making a specific treatment to target this type of malignant cell would certainly be warranted as CLL is currently considered incurable.

BCLL is characterized by an accumulation of monoclonal CD5+/CD19+/CD23+ resting B cells. Patients with BCLL not only have increased levels of membrane CD23 they also exhibit elevated levels of sCD23. This solubilized CD23 in the sera of BCLL patients has historically been used as a negative prognostic indicator for clinical outcomes (108). Thus, CD23 in either its membrane or soluble form is a logical target for novel BCLL treatment. Given our long standing history in the field of CD23 biology, we chose to examine the CD23 axis in BCLL.

With the discovery that ADAM10 was the CD23 sheddase, this opened the door for further examination of the CD23-ADAM10 interaction in the context of malignant disease. Upon further investigation, ADAM10 has also been implicated in various malignancies including colon, pancreatic, breast, and prostate cancers as well as gliomas (109), however little is known about its role in leukemia, let alone BCLL. Therefore, we performed a pilot study to determine if ADAM10 is over-expressed in BCLL and is perhaps responsible for the highly elevated levels of soluble CD23 seen in BCLL patients. Both BCLL patients and normal donors were identified by the VCU TDAAC or in collaboration with Charles Chu (North Shore-Long Island Jewish Research Institute Manhasset, NY). Peripheral blood was obtained with informed consent per approved VCU IRB. The experimental design is outlined in Figure 35.

From the samples examined to date, we have analyzed 35 BCLL samples, 17 of these from patients here at VCU, and 35 normal donors (ND), all from VCU. The VCU BCLL patients were identified by having a current WBC count >20 and lymphocyte percentage >70 and been diagnosed as BCLL with a high CD23 expression in previous pathology reports. Normal donors are defined to have a WBC within normal range and no history of any malignancy. Sample hematological parameters are shown in Figure 36.

We first examined PBMC for expression of CD23 and as indicated there is a significant elevation in the amount of cell surface expressed CD23 in the BCLL population (Figure 37). Using a standard sandwich ELISA technique, we are able to detect a statistically significant difference between plasma sCD23 levels in the two populations (Figure 38). While this finding is not novel, we corroborate previously reported data by Safarti *et al.* and show that our patient population also exhibits dramatic differences in both mCD23 and sCD23 levels (108). We then analyzed mRNA levels of ADAM10 via qPCR. RNA was isolated from whole PBMC preparations via standard Trizol® procedure. RNA was then sent to the VCU Nucleic Acid Research Facility (NARF) and subjected to quantitative PCR (qPCR). All quantitative qPCR reactions were performed in the Applied Biosystems Prism® 7900 Sequence Detection System (AB, Foster City, Ca) using the TaqMan® One Step PCR Master Mix Reagents Kit and all the samples were tested in triplicate under the conditions recommended by the fabricant. We observed a statistically significant increase in the amount of ADAM10 mRNA expressed in the BCLL samples when compared to normal donor PBMC tested thus far (Figure 39). We next wanted to determine if the over-expression of ADAM10 mRNA translated to a corresponding increase in ADAM10 protein levels. Flow cytometric analysis was performed on both ND and BCLL samples and indeed we see a large increase in the amount of ADAM10 protein expressed in the PBMC preparations (Figure 40). However one caveat to these studies is that we are comparing ND PBMC, which is compromised of about 10-20% lymphocytes, only half of which are B cells, to BCLL PBMC which is compromised of upwards to 80% B cells. To account for this difference, we compared ADAM10 protein expression on BCLL samples to normal B cell subsets. Tonsils were obtained from routine tonsillectomies here at VCU and single cell suspensions were made. T cells were depleted using anti-CD3 beads from Miltenyi to enrich for B cells. These enriched B cells were subjected to dual labeled flow cytometric analysis so that each population was identified by its unique marker and in turn ADAM10 levels could be assessed. As depicted in Figure 41, BCLL B cells still have a higher level of ADAM10 expression when compared to either total B cells (CD19+), memory B cells (CD27+), B1 B cells (CD5+), or normal CD23+ B cells. Thus, making ADAM10 both a unique phenotypic marker for BCLL cells as well as a novel therapeutic target.

Upon the discovery that ADAM10 was indeed over-expressed in BCLL, we wanted to pursue potential pharmacological methods as a means of ADAM10 inhibition. We first chose to examine a compound known as marimastat (kindly provided by Ouathek Ouerfelli, Memorial Sloan Kettering Cancer Center) a second generation matrix metalloproteinase

Figure 35. Experimental Outline for B cell chronic lymphocytic cancer studies. BCLL patients were identified by VCU TDAAC or provided in collaboration with Dr. Charles Chu (North Shore-Long Island Jewish Research Institute Manhasset, NY). Whole blood was received in an EDTA containing tube. Blood was transferred to a 15mL tube and subjected to centrifugation. Plasma was saved for soluble CD23 analysis via ELISA. Peripheral blood mononuclear cells were isolated for RNA and protein analysis via qPCR and flow cytometry respectively or used in other *in vitro* analysis.

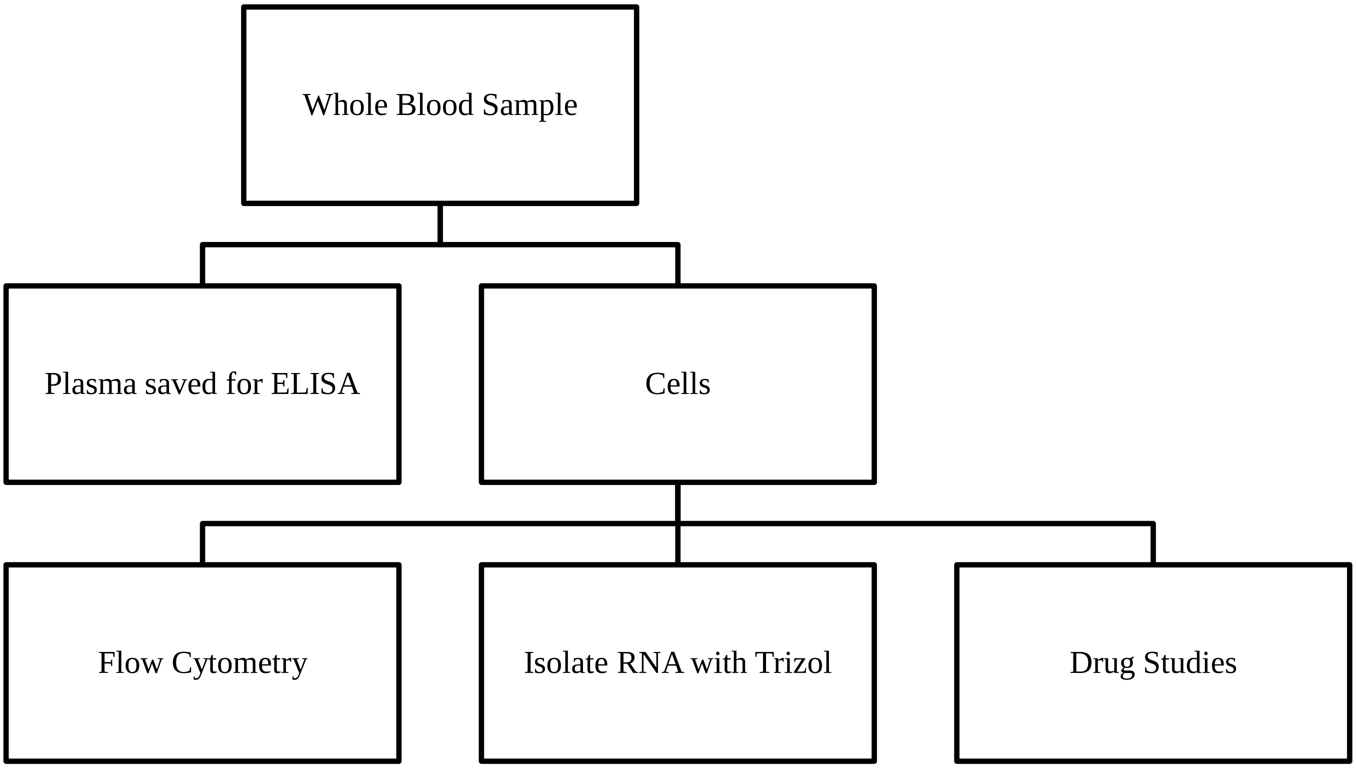
Whole Blood Sample
Plasma saved for ELISA
Cells
Flow Cytometry
Isolate RNA with Trizol
Drug Studies

Figure 36. Hematological Parameters of the VCU Subjects.

VCU BCLL patients were identified by having a current WBC count >20 and lymphocyte percentage >70 and been diagnosed as BCLL with a high CD23 expression in previous pathology reports. Normal donors are defined to have a WBC within normal range and no history of any malignancy. Complete blood counts with automated differentials were performed by the VCU Department of Pathology Hematology laboratory. * indicates $p < 0.0001$.

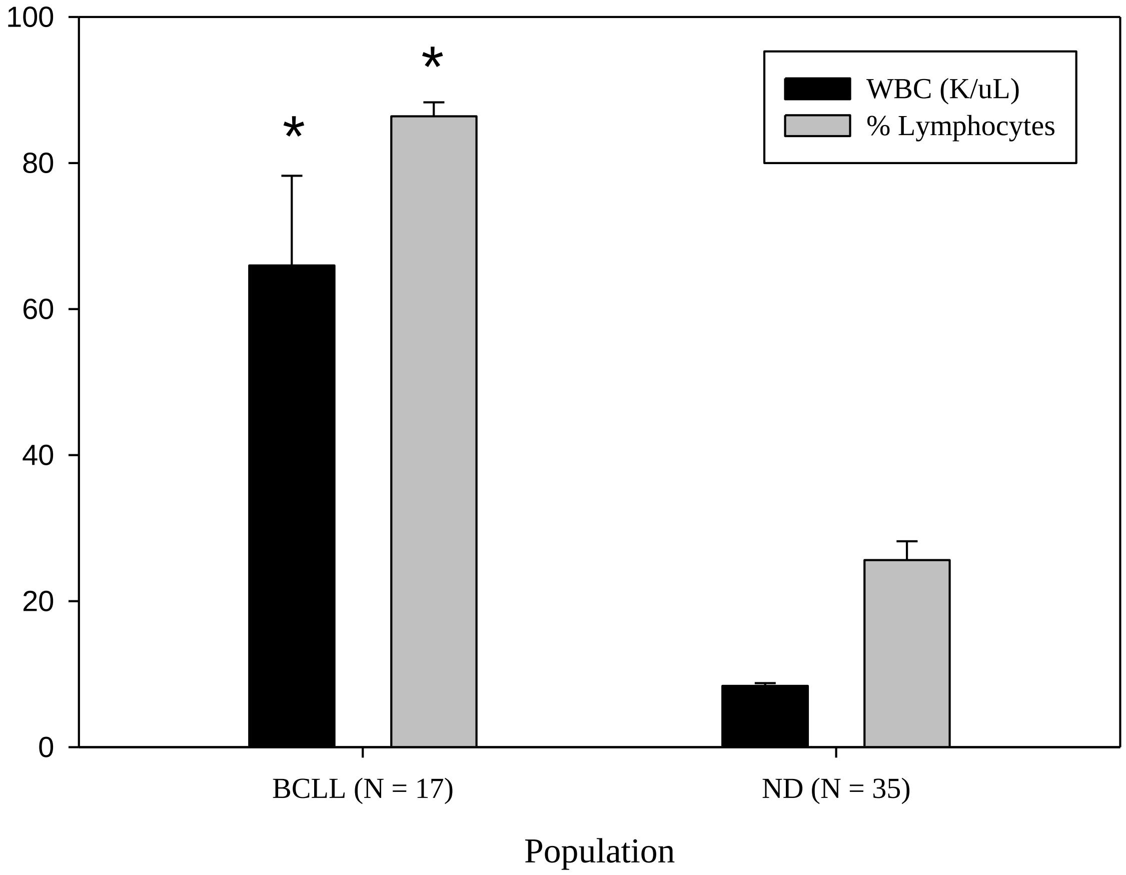
100
80
60
40
20
0
*
*
WBC (K/uL)
% Lymphocytes
BCLL (N = 17)
ND (N = 35)
Population

Figure 37. Peripheral blood mononuclear cells from BCLL patients have higher levels of membrane bound CD23.

Peripheral blood mononuclear cells were isolated from either normal donor (ND) or BCLL patients and subjected to flow cytometric analysis. Cells were Fc receptor blocked prior to staining. Isotype control staining was performed (not shown). Shown here is one representative sample from each patient population however experiment has been repeated numerous times with similar results.

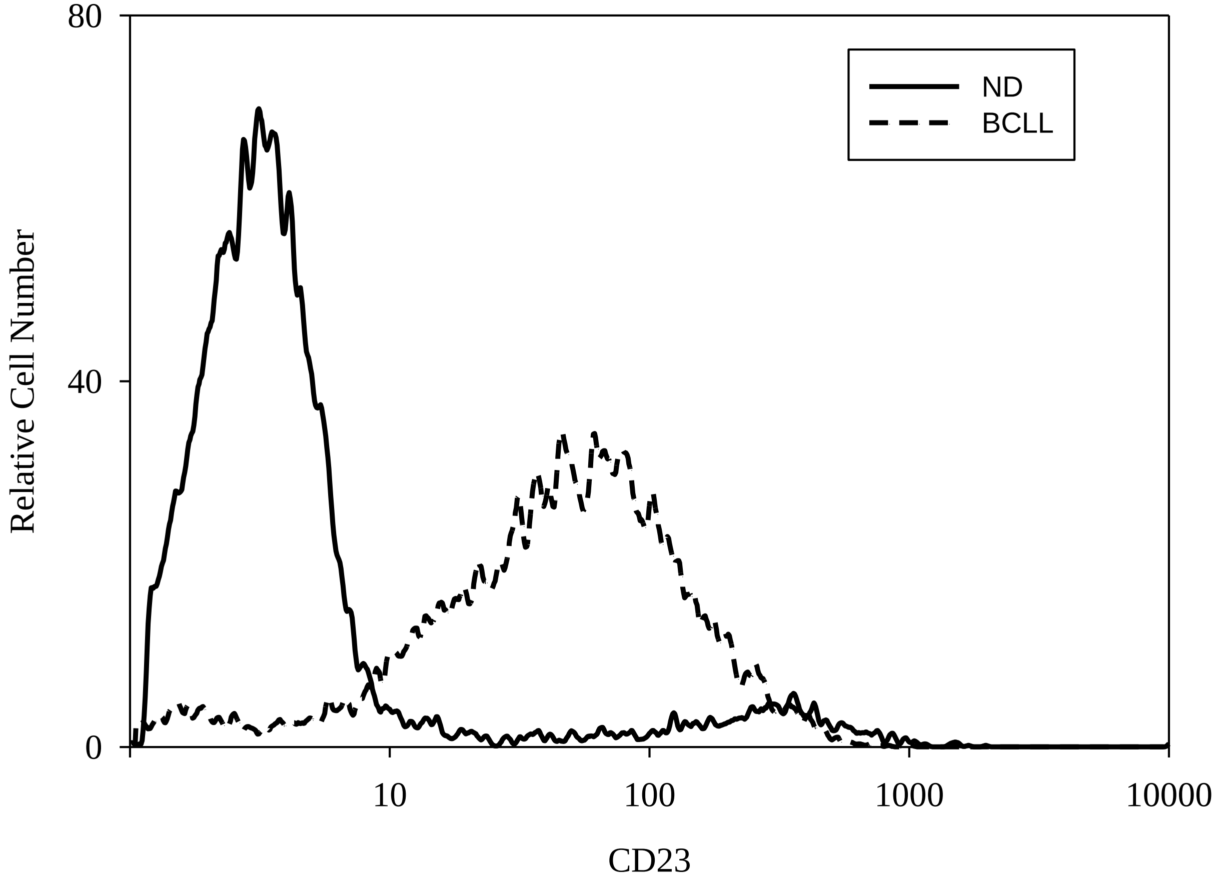
80
40
0
Relative Cell Number
10
100
1000
10000
CD23
ND
BCLL

Figure 38. BCLL patients have significantly higher levels of sCD23 than controls.

Using a standard sandwich ELISA technique, we examined plasma samples from 35 BCLL and 35 normal donors for the presence of sCD23. Clone BU38 was used for coating and detection was determined using a sheep anti human CD23 mab followed by a goat anti-sheep HRP. Appropriate dilutions of each sample were analyzed so that all data fell on the linear portion of the standard curve. * indicates a $p < 0.001$.

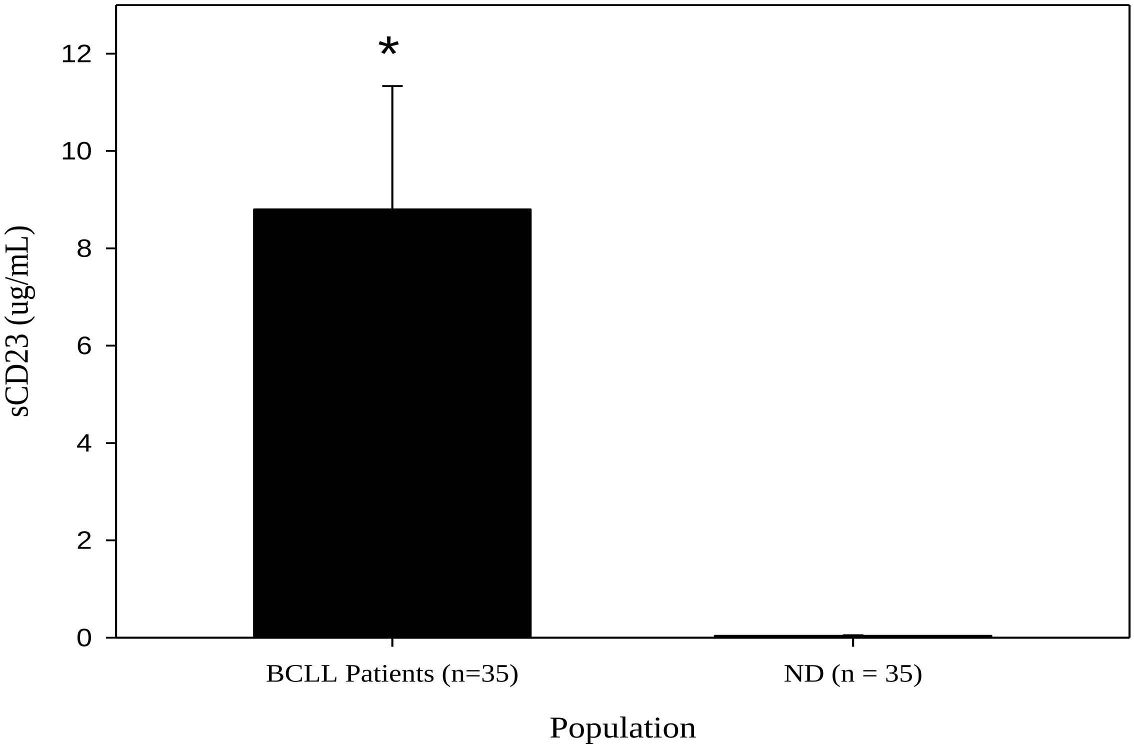

*
12
10
8
6
4
2
0
sCD23 (ug/mL)
BCLL Patients (n=35)
ND (n = 35)
Population

Figure 39. BCLL Samples have elevated ADAM10 mRNA.

RNA was isolated from whole PBMC preparations from either BCLL or ND samples via standard Trizol® procedure. RNA was then sent to the VCU Nucleic Acid Research Facility (NARF) and subjected to quantitative PCR (qPCR). All quantitative qPCR reactions were performed in the Applied Biosystems Prism® 7900 Sequence Detection System (AB, Foster City, Ca) using the TaqMan® One Step PCR Master Mix Reagents Kit. Primers for both ADAM10 and GAPDH were obtained from ABI and all the samples were tested in triplicate under the conditions recommended by the fabricant. * indicates a p value less than 0.009. Although not all 35 samples from each population have been analyzed, appropriate power analysis was performed (JMP software) and enough samples were utilized for the study to obtain statistical power.

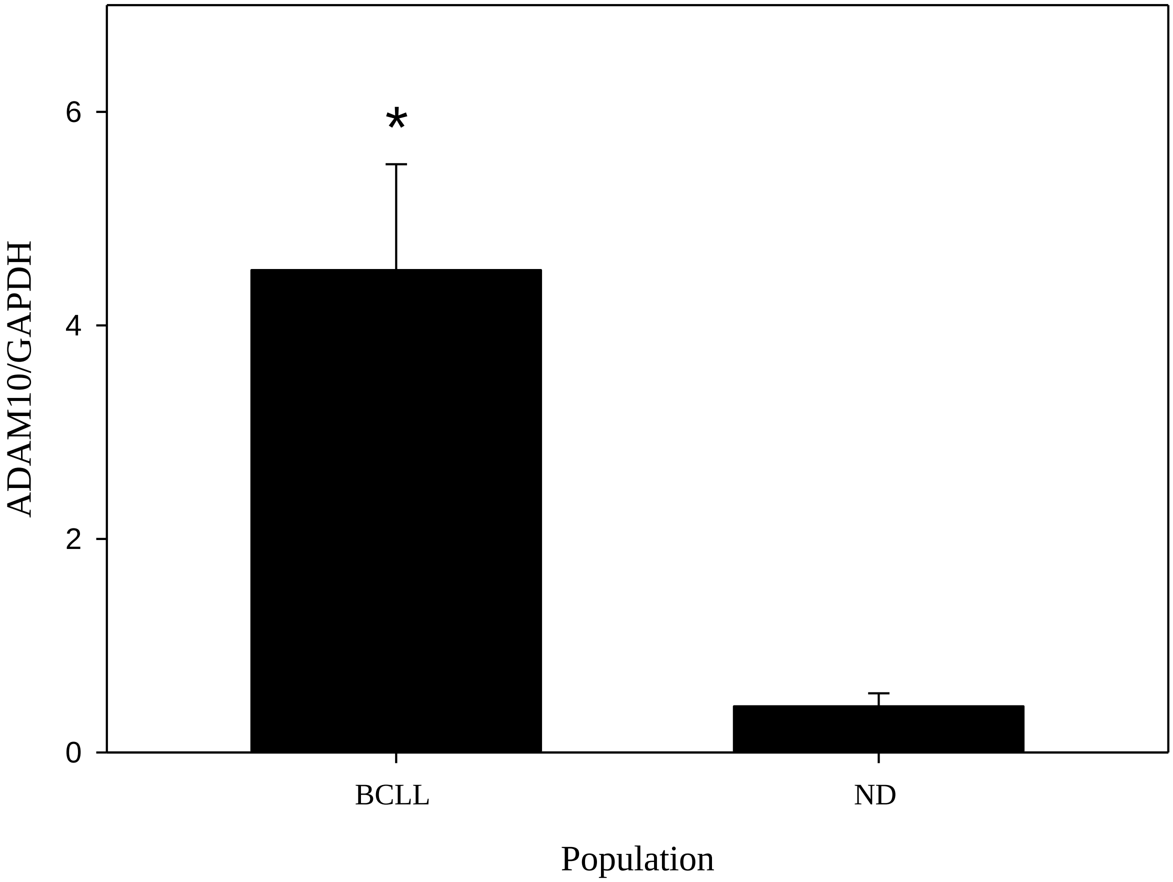
6
4
2
0
ADAM10/GAPDH
*
BCLL
ND
Population

Figure 40. BCLL Samples express high levels of ADAM10 Protein.

Peripheral blood mononuclear cells were isolated from either normal donor (ND) or BCLL patients and subjected to flow cytometric analysis. Cells were Fc receptor blocked prior to staining. Isotype control staining was performed (not shown). Shown here are two representative samples from each patient population however experiment has been repeated numerous times with similar results.

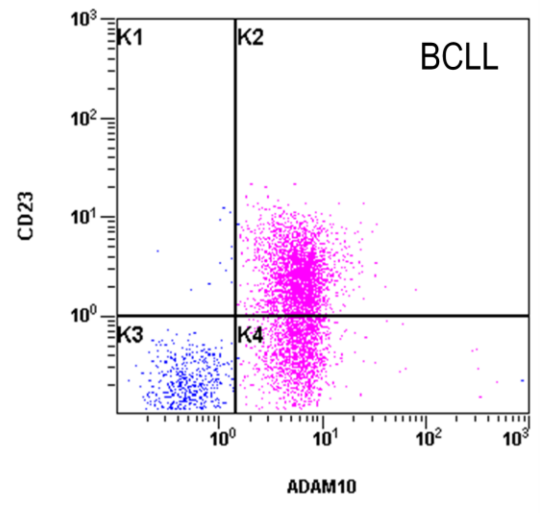
BCLL
K1
K2
K3
K4
CD23
ADAM10
10^0
10^1
10^2
10^3

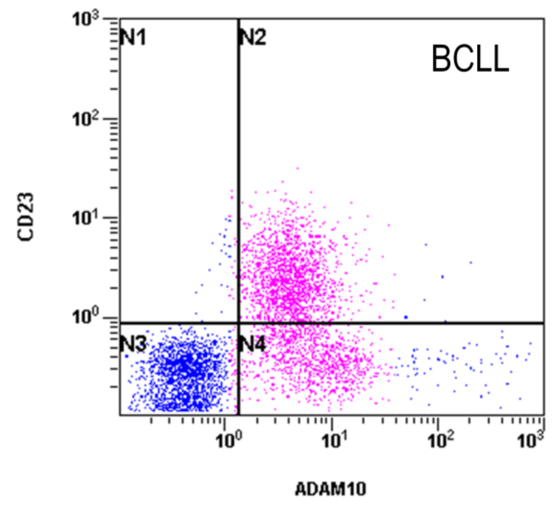
BCLL
N1
N2
N3
N4
CD23
ADAM10
10^0
10^1
10^2
10^3

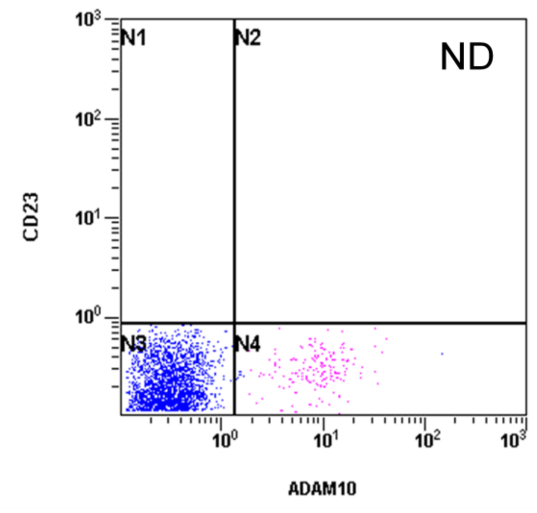
ND
N1
N2
N3
N4
CD23
ADAM10
10^0
10^1
10^2
10^3

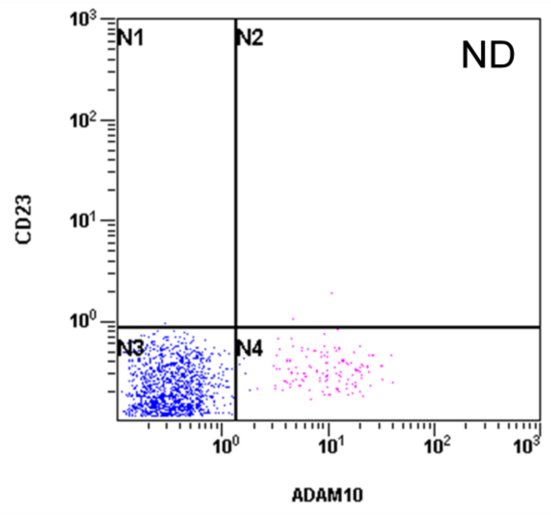
ND
N1
N2
N3
N4
CD23
ADAM10
10^0
10^1
10^2
10^3

Figure 41. ADAM10 over-expression is unique to BCLL B cells.

Peripheral blood mononuclear cells were isolated from BCLL patients. B cells were from tonsils obtained from routine tonsillectomies here at VCU. Dual labeling was employed so that each B cell subset could be identified and ADAM10 levels determined. Cells were Fc receptor blocked prior to staining. Isotype control staining was performed as shown. Shown here are representative samples from each population however experiment has been repeated with similar results.

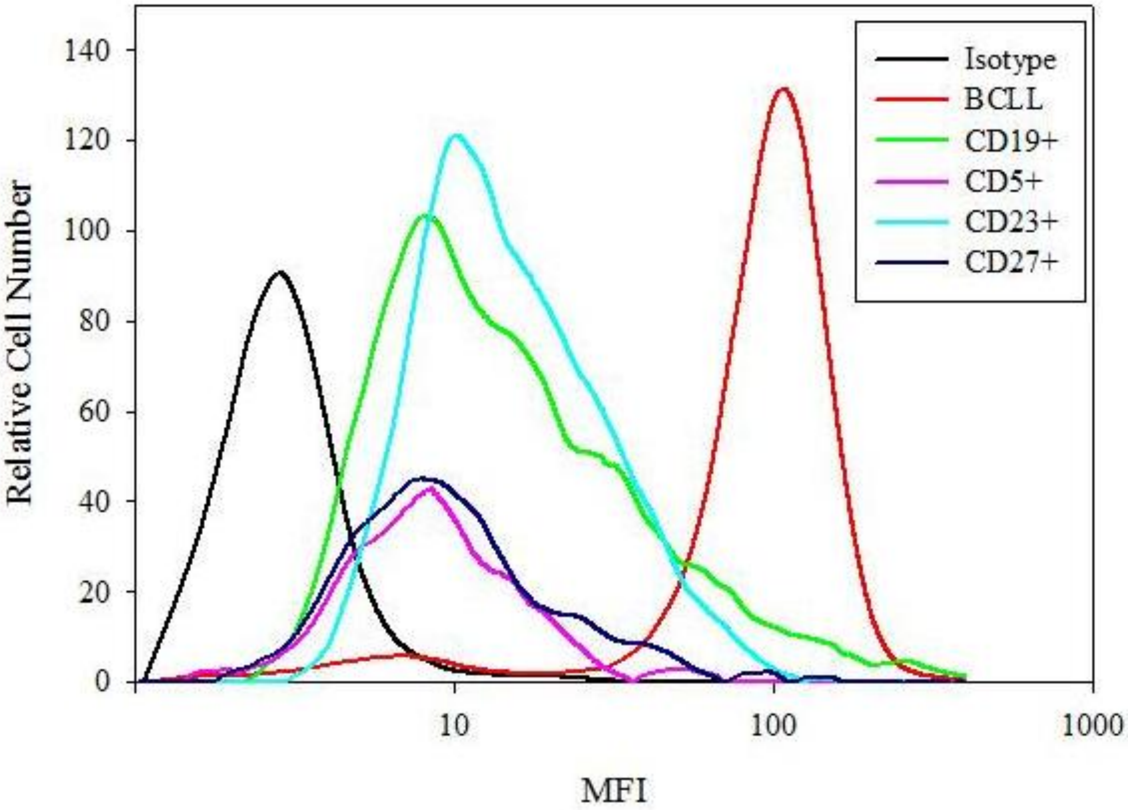

Relative Cell Number
0
20
40
60
80
100
120
140
10
100
1000
MFI
Isotype
BCLL
CD19+
CD5+
CD23+
CD27+

(MMP) inhibitor (110). Although not a specific ADAM10 inhibitor, marimastat is currently approved for human use and would serve as a logical candidate for easy movement into the clinical realm. In contrast to its first generation counterpart, batimastat, it is orally available and is renally excreted thus making it a more attractive drug. More importantly it has completed Phase III trials in US, Europe and Canada for solid tumor malignancies and was not considered cytotoxic when tested on healthy donors. Despite its disappointing results in solid tumors, according to the NCI clinical trial database, there have been no studies evaluating its effectiveness in treating leukemic cells in the US. Using an *in vitro* system which employs the leukemic B cell lines 8866, we observe that in the presence of marimastat as compared to vehicle control, sCD23 levels are considerably reduced in a concentration dependent manner (Figure 42).

To confirm that marimastat is working via ADAM10, we utilized ADAM10 specific inhibitors obtained from either Peggy Scherle (Incyte) or Neil Broadway (GlaxoSmithKline). Because two of the Incyte Inhibitors were against ADAM10 and ADAM17, we used an ADAM17 specific inhibitor as well. From Figure 43, it is evident that ADAM10 is clearly involved in CD23 ectodomain shedding as when INCB012998, the ADAM17 specific inhibitor is added, no change in sCD23 release is observed. To determine if the efficacy of ADAM10 inhibition is limited to 8866, we employed the use of another human CD23+ leukemic B cell line, Jiyoye. Using an identical experimental design as with the 8866, we observe similar results with Jiyoye verifying that ADAM10 is involved in sCD23 cleavage and that this phenomenon is not limited to the cell line initially used (Figure 44).

Figure 42. Marimastat prevents the release of sCD23 in a concentration dependent manner. 8866, a human B cell leukemia line which expresses high levels of CD23, were cultured in CRPMI-10 at a concentration of $1x10^6$ cells/mL in the presence of vehicle control (DMSO) or various amounts of Marimastat. 24 hours later cell free supernatants were harvested and analyzed for the presence of sCD23 via ELISA. * indicates a p value less than 0.01.

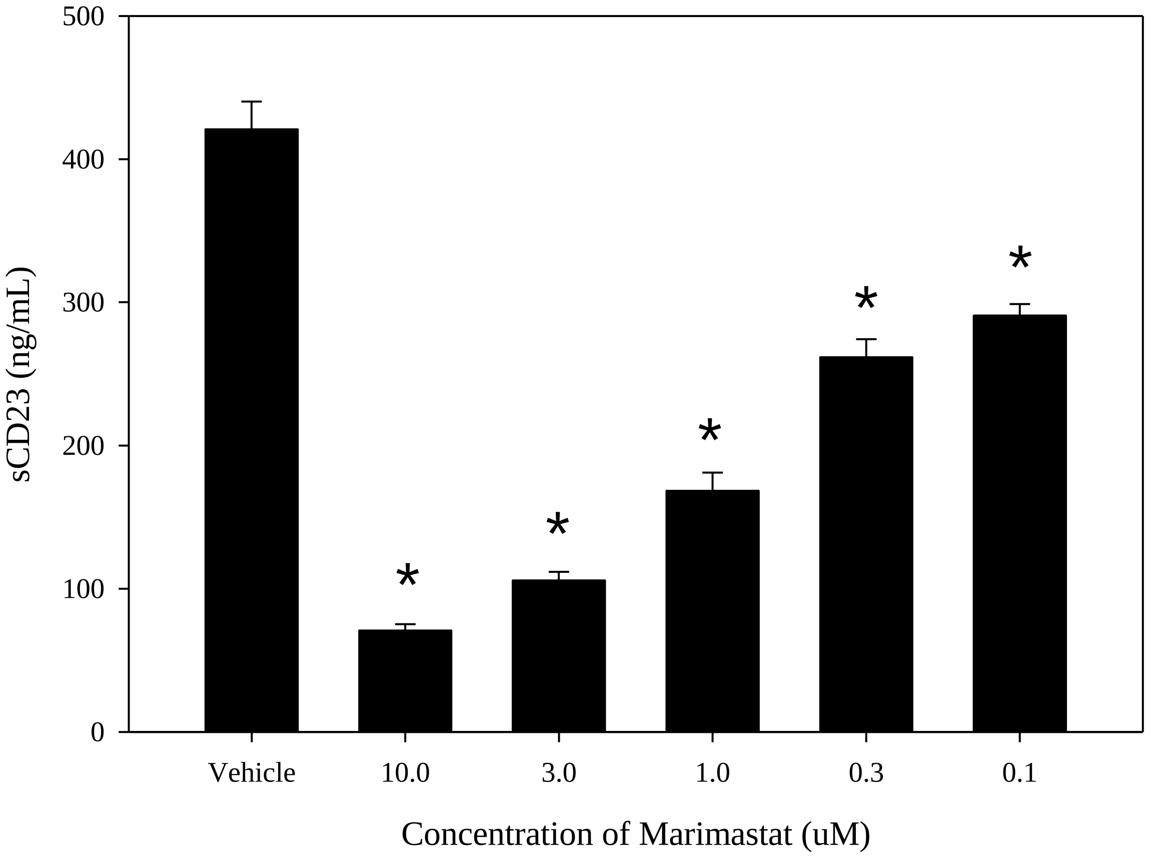
500
400
300
200
100
0
sCD23 (ng/mL)
*
*
*
*
*
Vehicle
10.0
3.0
1.0
0.3
0.1
Concentration of Marimastat (uM)

Figure 43. ADAM10 is clearly involved in CD23 ectodomain shedding in BCLL.

8866 were cultured in CRPMI-10 at a concentration of $1x10^6$ cells/mL in the presence of vehicle control (DMSO) or the various inhibitors. 24 hours later cell free supernatants were harvested and analyzed for the presence of sCD23 via ELISA. The ADAM10 selective inhibitor GI254023X is designated as GI and was used at a concentration of 10 µM. The Incyte inhibitors are designated with the numerical portion of the name assigned. The ADAM10 selective inhibitor INCB008765, the ADAM10/ADAM17 selective inhibitors INCB003919 and INCB009588, and the ADAM17 selective inhibitor INCB012998 were all used at 10 µM. Marimastat was used at 10 µM as well. * indicates a p value less than 0.01.

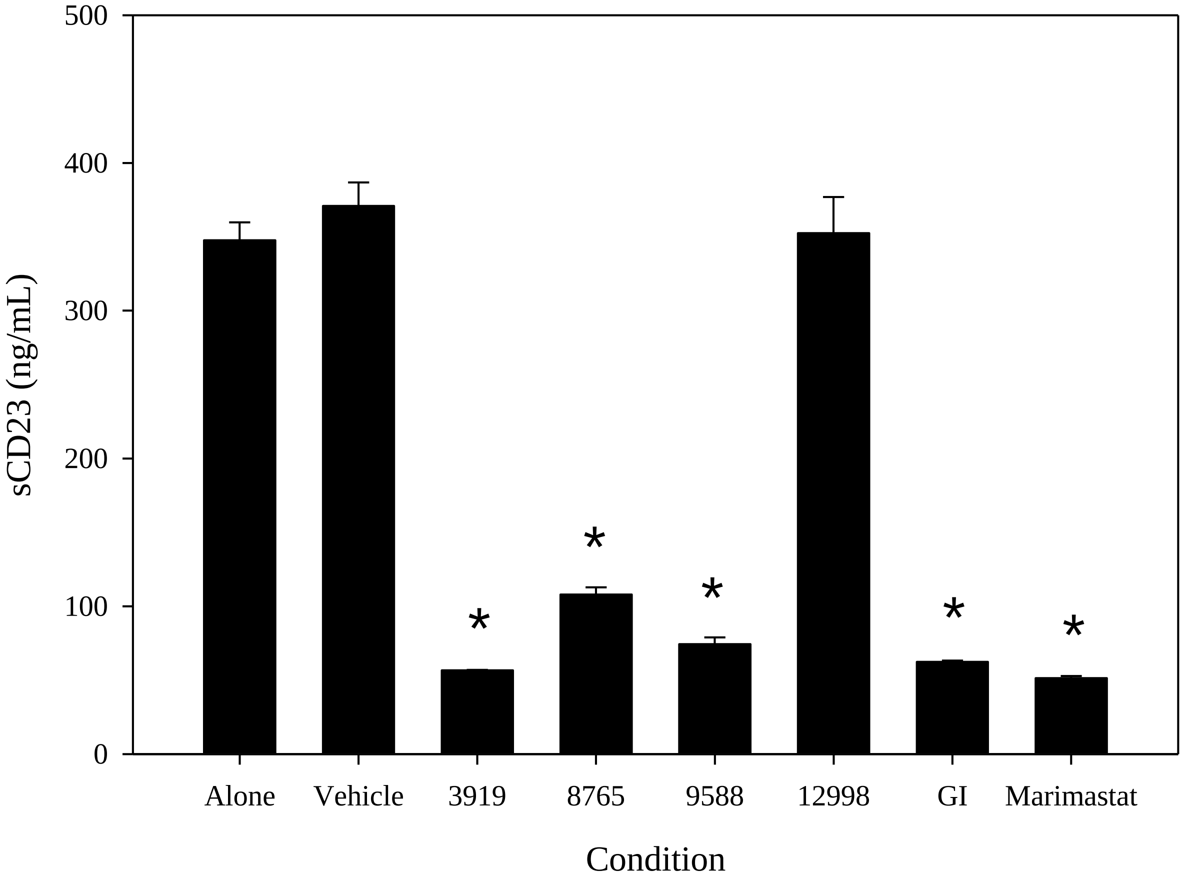

500
400
300
200
100
0
sCD23 (ng/mL)
*
*
*
*
*
*
Alone
Vehicle
3919
8765
9588
12998
GI
Marimastat
Condition

Figure 44. ADAM10 is involved in CD23 ectodomain shedding in another CD23+ leukemic cell line.

Jiyoye were cultured in CRPMI-10 at a concentration of 1x10^{6} cells/mL in the presence of vehicle control (DMSO) or the various inhibitors. 24 hours later cell free supernatants were harvested and analyzed for the presence of sCD23 via ELISA. The ADAM10 selective inhibitor GI254023X is designated as GI and was used at a concentration of 10 µM. The Incyte inhibitors are designated with the numerical portion of the name assigned. The ADAM10 selective inhibitor INCB008765, the ADAM10/ADAM17 selective inhibitors INCB003919 and INCB009588, and the ADAM17 selective inhibitor INCB012998 were all used at 10 µM. Marimastat was used at 10 µM as well. * indicates a p value less than 0.01.

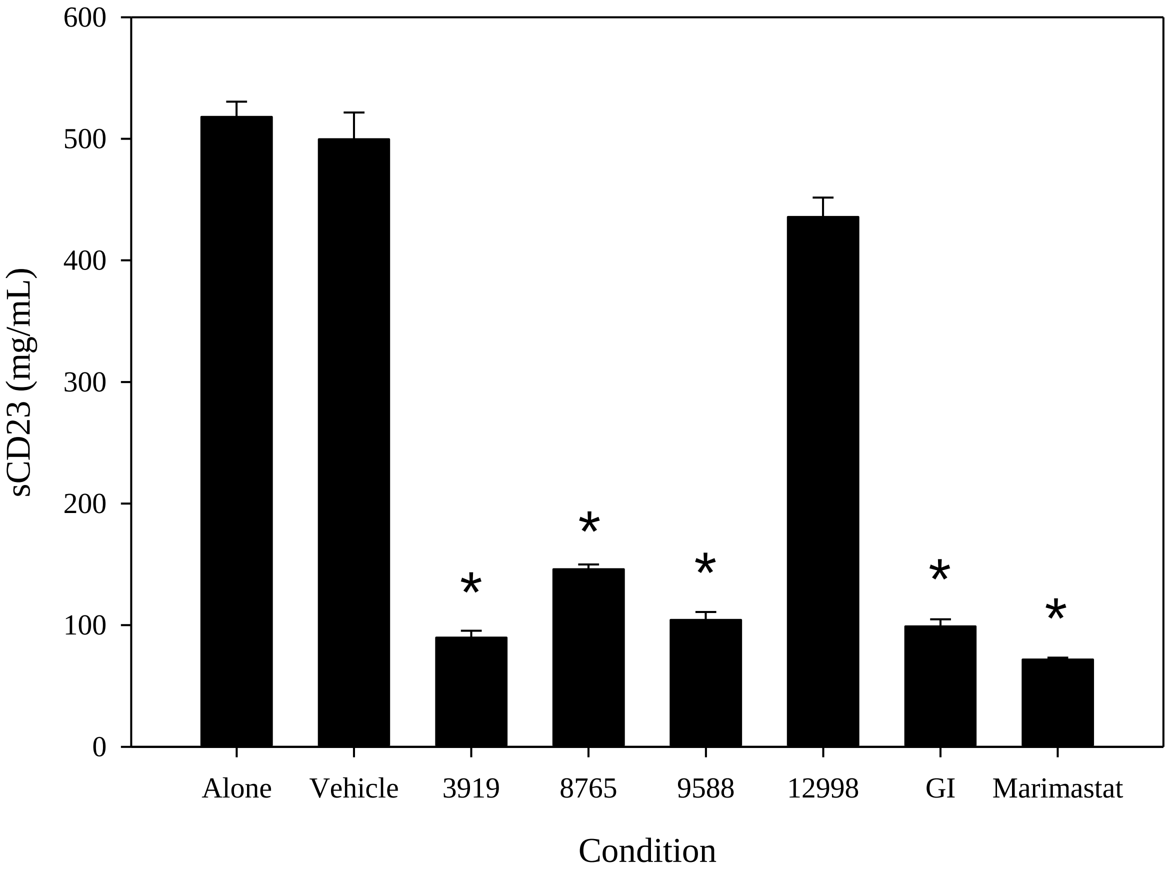
600
500
400
300
200
100
0
sCD23 (mg/mL)
*
*
*
*
*
*
Alone
Vehicle
3919
8765
9588
12998
GI
Marimastat
Condition

Currently, the first line therapy for BCLL is the use of chemotherapeutic agents. Fludarabine (Fludara ®) is used as the initial treatment for CLL as it yields higher response rates and a longer duration of remission and progression-free survival than the previously used drug, chlorambucil (111). We wanted to determine if fludarabine had any effect on ADAM10 as measured by sCD23 release. We observe no inhibition of sCD23 release from 8866 cells in the presence of fludarabine at any concentration tested (Figure 45). Thus targeting ADAM10 and the resultant sCD23 release could serve as a novel avenue for therapeutic intervention.

We next wanted to examine cellular proliferation in the presence of ADAM10 inhibition. We first cultured 8866, normal donor PBMC, or BCLL PBMC in the presence of varying concentrations of marimastat. Cells were grown in sterile 96-well culture plates in complete media. The primary cells from both cancer and normal donors were stimulated with 10ng/mL IL-4 and 1 µg/mL aCD40. After 96 hours of growth, a 24 hr pulse [H^3]-thymidine was used. Plates were then harvested using a Packard Filtermate 196 cell harvester onto Unifilter GFC 96 well plates. Plates were counted on a TopCount plate reader in order to determine CPM. Although at high concentrations of marimastat, inhibition of proliferation of all cell types is observed, the lowest concentration used for these studies (16 µM) results in marked inhibition of both the BCLL and 8866 cells yet has no adverse effect on the ND cells (Figure 46). One limitation of these types of studies is that human primary cells require stimulation for *ex vivo* proliferation but these stimulatory conditions do not necessarily mimic actual physiology. To try to avoid these confounding variables, we have optimized a media that will allow us to grow primary BCLL cells in the absence of supplementary cytokines and/or anti-CD40 stimulation. We feel that this system is better approach to

Figure 45. Fludarabine has no inhibitory effect on ADAM10 in BCLL.

8866 were cultured in CRPMI-10 at a concentration of $1x10^6$ cells/mL in the presence of vehicle control (DMSO) or various concentrations of fludarabine. 24 hours later cell free supernatants were harvested and analyzed for the presence of sCD23 via ELISA. There is clearly no inhibition seen in sCD23 release with any concentration of fludarabine tested.

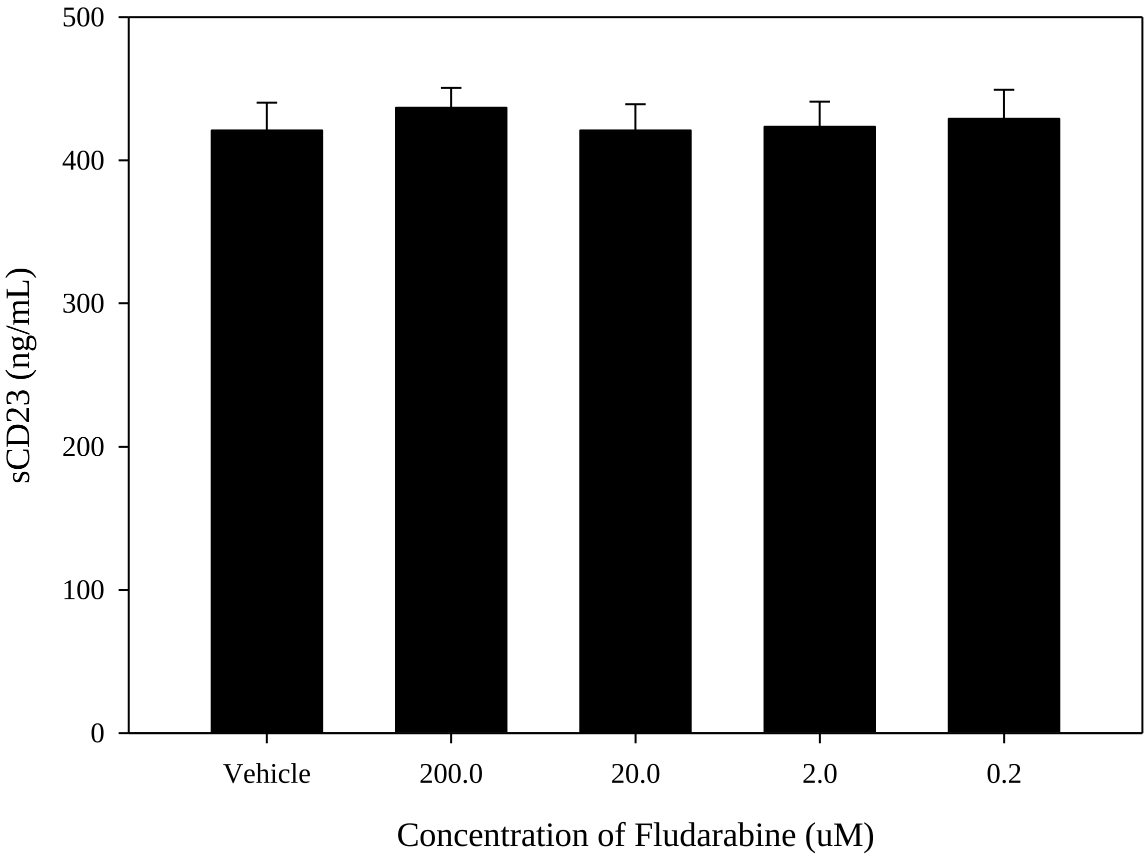
500
400
300
200
100
0
sCD23 (ng/mL)
Vehicle
200.0
20.0
2.0
0.2
Concentration of Fludarabine (uM)

Figure 46. Marimastat inhibits proliferation of both 8866 and BCLL PBMC in a concentration dependent manner.

8866, normal donor PBMC, or BCLL PBMC were cultured in the presence of varying concentrations of marimastat. Cells were grown in sterile 96-well culture plates in complete media. The primary cells from both cancer and normal donors were stimulated with 10ng/mL IL-4 and 1 µg/mL aCD40. After 96 hours of growth, a 24 hr pulse [H^3]-thymidine (Perkin Elmer, Waltham, MA) was used. Plates were then harvested using a Packard Filtermate 196 cell harvester (Packard Instrument Co, Meriden CT) onto Unifilter GFC 96 well plates (Perkin Elmer). 24 hours later, a plastic backing was added to the plates, 40µL of Microscint-20 (Perkin Elmer) was added to each well, and plates were counted using a Topcount Scintillation MicroPlate Counter (Perkin Elmer). Shown is one representative experiment of three with similar design.

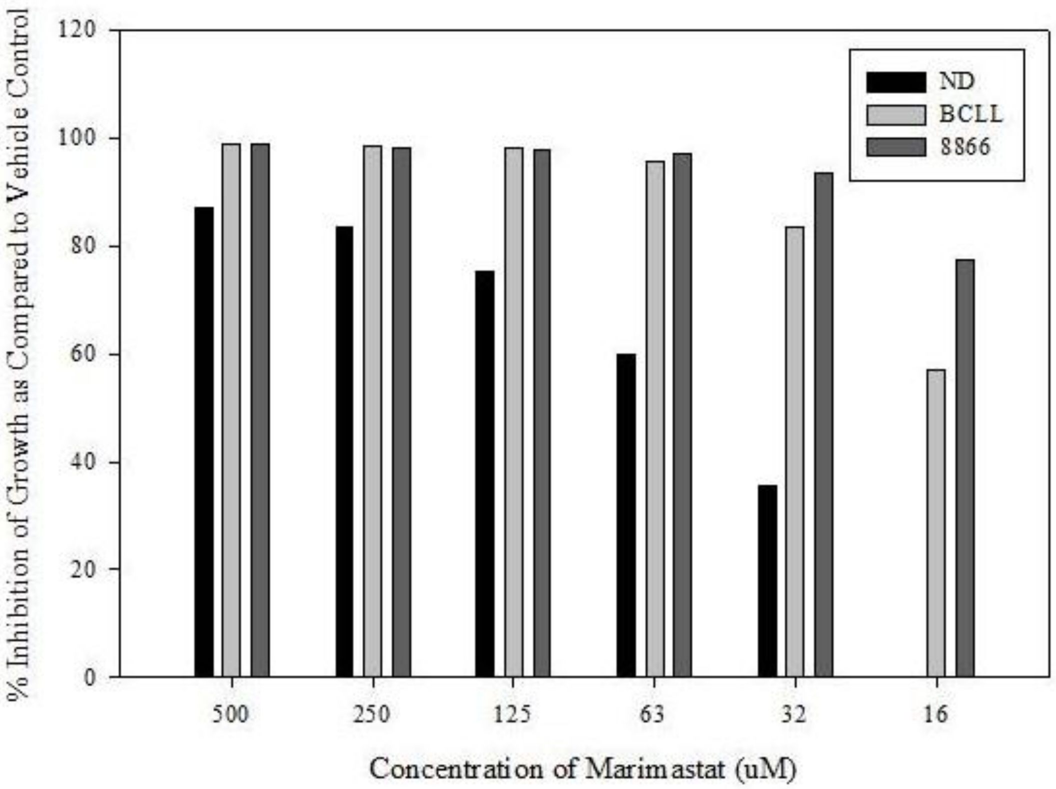
% Inhibition of Growth as Compared to Vehicle Control
120
100
80
60
40
20
0
ND
BCLL
8866
500
250
125
63
32
16
Concentration of Marimastat (uM)

analyze growth inhibition. Primary BCLL cells were grown in the presence of vehicle alone, marimastat, or specific ADAM10 inhibitors. In all cases of ADAM10 inhibition, cellular proliferation is noticeably reduced (Figure 47).

BCLL is historically hard to treat as it is highly resistant to apoptosis induction. Thus, we examined apoptosis via annexin/PI staining in the presence of marimastat, specific ADAM 10 inhibitor, 8765, or vehicle control and do indeed observe an apoptosis induction as evidenced by an increase in Annexin + cells (Figure 48). However it is interesting to note that the broad spectrum inhibitor marimastat does induce more apoptosis that the ADAM10 specific inhibitor.

Figure 47. ADAM10 Inhibition reduced cellular proliferation in BCLL cells.

BCLL PBMC were grown in modified ACL4 media in sterile 96-well culture plates. After 96 hours of growth, a 24 hr pulse [H^3]-thymidine (Perkin Elmer, Waltham, MA) was used. Plates were then harvested using a Packard Filtermate 196 cell harvester (Packard Instrument Co, Meriden CT) onto Unifilter GFC 96 well plates (Perkin Elmer). 24 hours later, a plastic backing was added to the plates, 40μL of Microscint-20 (Perkin Elmer) was added to each well, and plates were counted using a Topcount Scintillation MicroPlate Counter (Perkin Elmer). All inhibitors used were at 10 μM. Shown is one representative experiment of three with similar design.

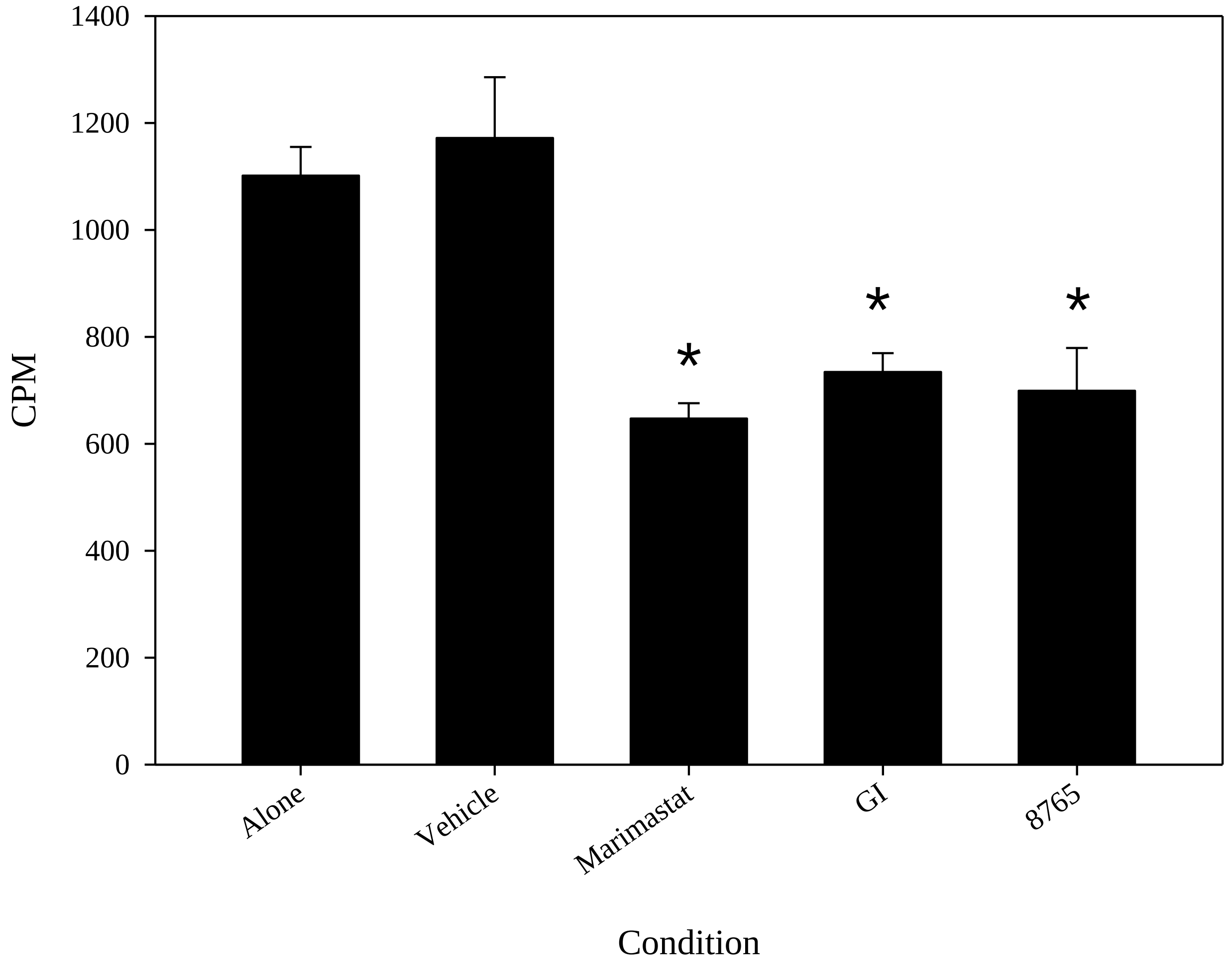
1400
1200
1000
800
600
400
200
0
CPM
Alone
Vehicle
Marimastat
GI
8765
*
*
*
Condition

Figure 48. ADAM10 Inhibition leads to apoptosis induction.

8866 were cultured in CRPMI-10 at a concentration of 1x10^6 cells/mL in the presence of vehicle control (DMSO), 10 µM marimastat, or 10 µM INCB008765. 24 hours later, cells were harvested and analyzed for apoptosis induction via the Annexin V FITC apoptosis kit (BD Pharmingen) per manufacturer’s protocol. Shown is one representative experiment of two of similar design.

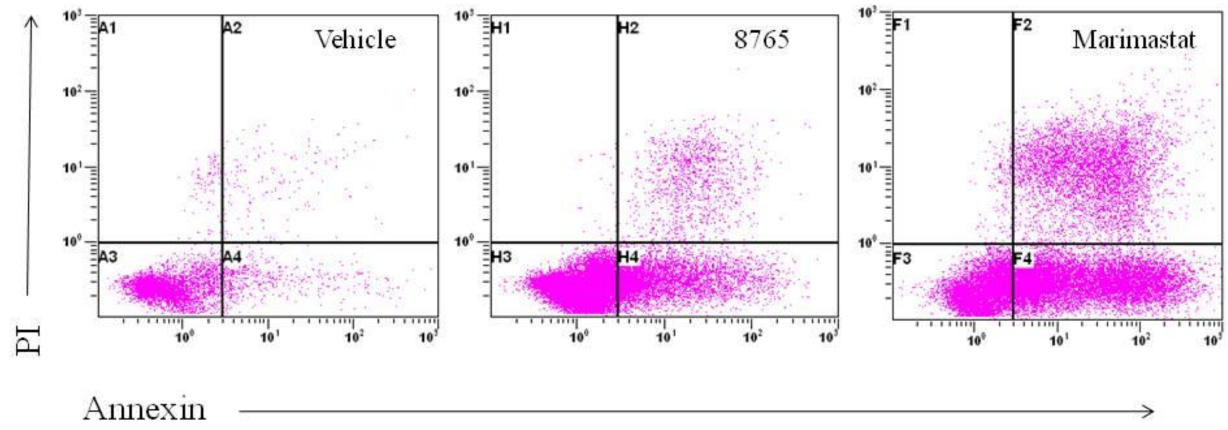
Vehicle
8765
Marimastat
A1
A2
A3
A4
H1
H2
H3
H4
F1
F2
F3
F4
PI
Annexin
10⁰
10¹
10²
10³

DISCUSSION

CD23 has long been appreciated to be a natural, negative regulator of IgE synthesis. This understanding is due in part to animal models in which CD23 deficient or CD23 transgenic animals display exacerbated or reduced IgE levels respectively. (For a comparison of mouse and human CD23 please see Figure 49) Interestingly, CD23 is susceptible to proteolytic cleavage from the cell surface. When this occurs, CD23 loses its regulatory capability. The soluble CD23 is important in itself because it can bind CD21 and further enhance B cell activation and IgE synthesis (112,113) as well as lead to pro-inflammatory events through its cytokinergic activity on macrophages (114). Thus, targeting this specific cleavage would be beneficial to the control of allergic and inflammatory disease by stabilizing CD23 at the cell surface. Our results from *in vitro* shedding assays, mice lacking candidate a disintegrin and metalloprotease (ADAM) genes, and ADAM10 inhibitors provide the first experimental evidence for a role of ADAM10 in CD23 cleavage in both the human and mouse systems. Our findings were corroborated by another group shortly after our initial report (115). This pivotal discovery allows for the further examination of the role of ADAM10 in allergic disease and importantly CD23 biology. Furthermore, developing strategies that would target ADAM10 could have an effect on sCD23 release and IgE production.

In view of the recent demonstration that ADAM10 is the primary CD23 sheddase, we searched for agents that would modify ADAM10 activity. The overall purpose was to test the hypothesis that ADAM10 modulation would, by virtue being the CD23 sheddase, result in IgE

Figure 49. Structures of human and mouse CD23.

CD23 contains an amino terminal cytoplasmic tail and an extracellular carboxyl terminal lectin domain. The cysteine residues (shown in pink) within the lectin domain help maintain the structure in the correct conformation. The inverted RGD sequence, present in human CD23 only, is thought to mediate adhesion to other molecules and is shown in red. The stalk region of CD23 contains a heptad repeat pattern with a hydrophobic amino acid at approximately every seventh position (shown in blue). The stalk is also the region of CD23 that is susceptible to proteolytic breakdown. The metalloprotease cleavage sites are denoted by the scissors. N-linked glycosylation sites, also present in the stalk, are shown in green. Two isoforms of CD23 (CD23a and CD23b), differing only in the first 6 amino acids, have been discovered and are indicated in the human cytoplasmic tail. (Taken from 116.)

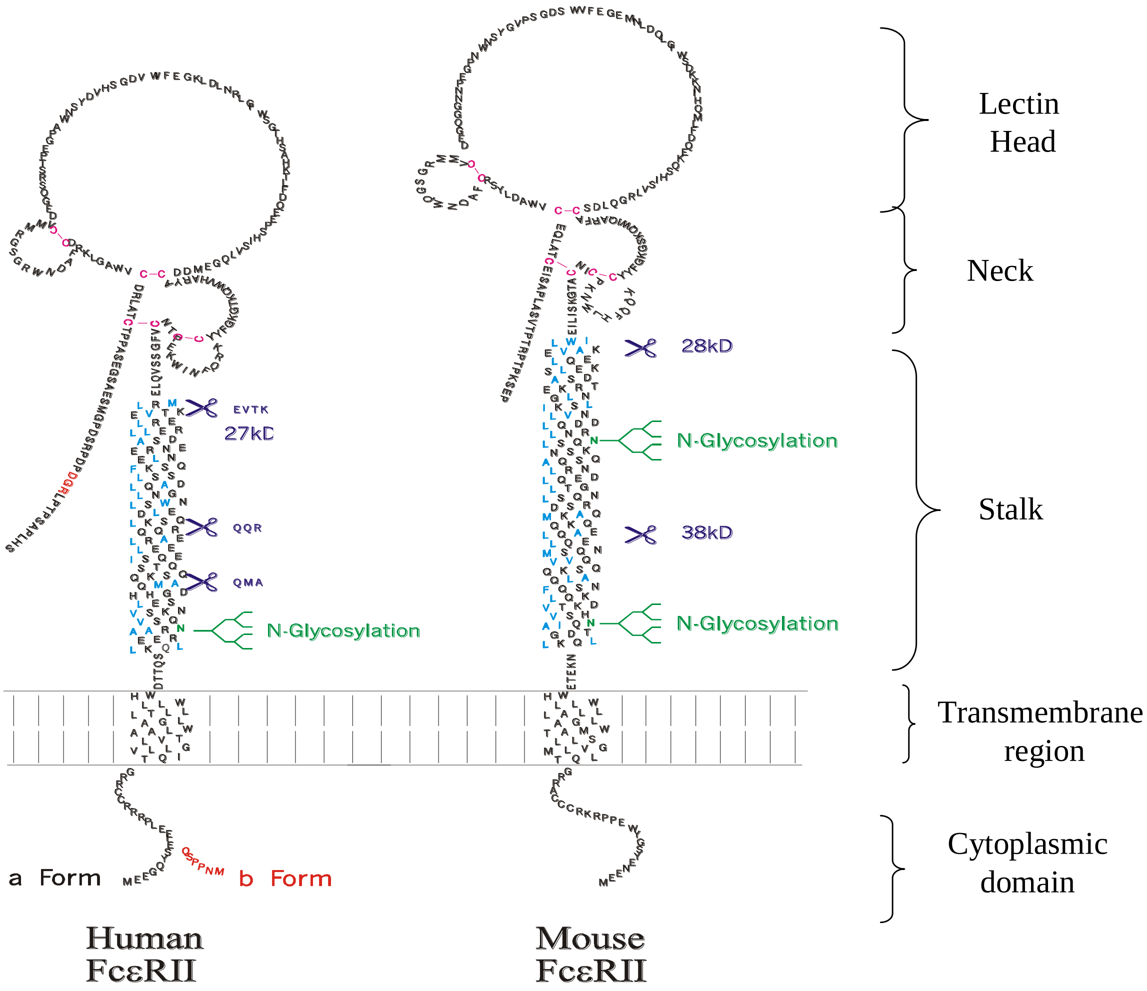
Lectin Head
Neck
Stalk
Transmembrane region
Cytoplasmic domain
EVTK
27kD
QQR
QMA
N-Glycosylation
a Form
b Form
28kD
N-Glycosylation
38kD
N-Glycosylation
Human FcεRII
Mouse FcεRII

modulation. It has been shown that specific ligation of the kainate receptor leads to an increase in ADAM10 mRNA in the CNS. Based upon the work by Ortiz *et al.* we wanted to determine if this kainate receptor existed in the immune system and activation of this receptor would lead to an increased expression of ADAM10 in a similar fashion in the immune system (88). This finding would allow for manipulation of ADAM10 as a direct means to influence B cell biology in the human system.

Interestingly, the receptor described by Ortiz was a glutamate receptor whose expression has primarily been reported to be CNS specific. Glutamate, the major excitatory neurotransmitter in the central nervous system (CNS) has recently been implicated in a variety of diseases. For example, it has been shown that patients with certain cancers (117), HIV (118), epilepsy (119), autism (120), and certain autoimmune illnesses such as rheumatoid arthritis (RA) (121), and systemic lupus erythematosus (SLE) (122) all have elevated levels of glutamate in the periphery. Interestingly, autoimmune disease treatments which include corticosteroid use can also increase peripheral glutamate levels (117,123,124).

This study is one of the first to show that a functional glutamate receptor of the kainate subtype exists in the human immune system. While there are studies to date which report that receptors of this family exist on human T cells (125) and macrophages (126), their presence has not been demonstrated on B cells. While those studies are important in illustrating that glutamate receptors do exist in the immune system, our study is pivotal in that receptors of the kainate subtype to our knowledge have never been reported to exist in lymphocytes. The only other KAR demonstration in the hematopoietic system was the very recent finding that KARs were on platelets, and stimulation thereof promoted cyclooxygenase activation (127).

Aside from the presence of the receptors themselves functional relevance was also shown. An increase in B cell ADAM10 mRNA was seen and this is in agreement with the report by Ortiz *et al*. showing an increase in ADAM10 mRNA in the CNS in response to KAR signaling. We focused on ADAM10 as our laboratory has recently identified this protease to be responsible for the cleavage of CD23 from the cell surface (128). While the Ortiz paper also illustrates that ADAMs 9 and 15 are also up-regulated in the presence of KA, no involvement of these two ADAMs in CD23 ectodomain shedding events was found, thus, up-regulation of ADAM10 is responsible for the changes in the CD23 observed.

KAR activation also leads to a significant increase in cell proliferation. As evidenced by our group as well as others, cellular proliferation is a key element in generating strong class switch recombination as multiple rounds of cell divisions are needed for this to occur (107). In the human system, it is known that at least eight cell divisions are needed in order to produce IgE (129). Thus, the increase in proliferation may help explain the increased class switching observed as indicated by elevated levels of total IgG and IgE. Note that class switching occurs both in the presence and absence of KAR stimulation and that what is seen is a dramatic increase in the synthesis of class switched Ig. There is precedent for KAR activation to cause increasing cell proliferation as it has been shown in the literature that elevated glutamate levels promote growth of human histiocytic lymphoma cells (130), yet the mechanism for this increase was not examined. Increased CD23 cleavage also correlates with elevated IgE production and this may also relate to the results shown here as past studies have highlighted CD23's important role as a negative regulator of IgE synthesis. Given the relatively modest influence on cell divisions, enhancement in proliferation is not likely to be the complete explanation for the Ig production enhancement. The increased ADAM10 activity results in increased sCD23. This has been shown to correlate with increased IgE production in the mouse system (62) as well as the human (63). High membrane CD23 levels, caused by transgene over-expression (131) resulted in decreased IgE and IgG1 expression, at least in the mouse system. Thus, CD23 alteration may at least provide a partial explanation for the results shown in this study, but the mechanism will require additional studies which will examine intracellular events post KAR activation.

It has been shown that patients with HIV, epilepsy, and certain autoimmune illnesses such as SLE and RA all have elevated levels of glutamate in the periphery. It is interesting to note that many of these diseases also have an accompanying increase in immunoglobulin production. For example, elevated serum immunoglobulin E (IgE) and increased prevalence of atopy is reported in patients infected with human immunodeficiency virus (HIV) (132). Frediani *et al.*. (133) performed a cohort study with 72 pediatric patients with epilepsy compared to 202 healthy age matched controls. This study showed a significantly increased incidence of allergies in the epileptic population as opposed to the control. One hallmark of B cell mediated autoimmunity is that patients have an accumulation of auto-reactive B cells which are hyper proliferative and produce pathogenic immunoglobulin, typically of the IgG isotype. In the case of SLE, other documented, but perhaps lesser known attributes of the disease include elevated levels of IgE (134) and elevated levels of soluble CD23 (135). Elevated levels of sCD23 have also been reported in rheumatoid arthritis and Sjogren’s syndrome (135,136). The aforementioned phenomena all clinically correlate to the phenomena we observe *in vitro* in the presence in KAR activation, suggesting that glutamate enhancement of IgG and IgE production may play a role in the disease progression

There continues to be mounting evidence indicating interplay between the immune and nervous systems such as the fact that cholinergic compounds are immunosuppressive (137) and the fact that norepinephrine can stimulate the immune system (138). Despite evidence for these and other neurotransmitters, little is known about the effects of glutamate on the immune system and what is known focuses primarily on T cells and macrophages. With more and more evidence pointing to a "neuro-immuno dichotomy", it is important to not only look at the immune system's effects on the nervous system but vice versa as well. Taken together, these findings serve to help elucidate the effects that a neurotransmitter signaling may exert on the immune system and may serve as a useful tool for developing new therapies for immune disease.

Especially intriguing is the strong inhibition of Ig production seen with the KAR antagonist, NS-102. NS102 is an antagonist to the GluK2 containing KARs thus confirming specificity of the KAR subtype observed in the human immune system. As KAR knockouts showed minimal CNS effects (67), NS-102 may represent a new tool to control Ig synthesis. Alternatively, it may be possible to produce related KAR antagonists that are engineered to not cross the blood brain barrier. These antagonists would potentially have no CNS issues and would thus have the potential to strongly reduce peripheral Ig production and control the IgG and IgE mediated diseases.

Aside from its role in atopic disease, ADAM10 was examined in a non-allergic disease state. When one thinks of CD23 outside the traditional T_H2 disease states, B cell chronic lymphocytic leukemia (BCLL) serves an ideal disease in order to better understand CD23 biology. BCLL is characterized by a large accumulation of circulating CD23+ B cells and high levels of soluble CD23 in the sera. In fact sCD23 is often a negative prognostic indicator used for the determination of clinical outcomes. Thus, we wanted to examine the relationship if any CD23 and ADAM10 had in the context of hematological malignancies. After further analysis, we show that ADAM10 is indeed over-expressed in BCLL and could account for the high levels of soluble CD23 seen in this patient population. While this finding is not necessarily novel as high levels of ADAM10 have been implicated in solid tumor malignancies, this is the first evidence to link ADAM10 to a leukemic state. Furthermore, specifically targeting ADAM10 resulted in reduced soluble CD23 release, reduced proliferation, and enhanced apoptosis induction thus based on our preliminary data, we note that marimastat holds promise as a novel chemotherapeutic agent for the treatment of BCLL. Taken together the novel finding that ADAM10 is involved in CD23 shedding allows for targeted therapeutic intervention of both atopic and non-atopic disease states. Additionally elevated glutamate levels have been reported in malignant states (as described above) thus the over-expression of ADAM10 in BCLL could be a result of chronic KAR stimulation. This avenue has yet to be explored but if this is the case, then perhaps agents which could block the KAR receptor, NS102, and agents that would inhibit ADAM10, marimastat, could be used in conjunction for novel, specific therapies.

A lot of the work that has been done in the immunology field has utilized mouse models of human disease. Murine models are useful in that *in vivo* work and efficacy of targeted genes or therapeutics can be determined without harmful effects in humans. Importantly much of the knowledge surrounding CD23 biology comes from the use of animals. CD23's regulatory role on IgE is best illustrated by this fact. However, as subsets of human disease have yet to be identified with CD23 deletion or over-expression of membrane CD23 alone, other means of CD23 regulation need to be explored to better understand *in vivo* relevance of CD23 in the human and for the creation and usefulness of CD23 targeted therapies. Eloquent work by our laboratory has illustrated the fact that stability of the CD23 molecule could be a potential goal. Through the use of mab targeted against the stalk of CD23, Ford *et al.* has shown that not only is the absolute presence of CD23 required, but that CD23 needs to be in a stable trimeric structure in order to retain its regulatory properties (62). Furthermore a de-stabilized molecule is more susceptible to proteolytic cleavage. Thus engineering antibodies that would stabilize CD23 could be an attractive target. A clinical trial that used an anti-CD23 mab (Lumiliximab) directed against the lectin part of the molecule resulted in about two-thirds reduction in serum IgE levels, but this was not sufficient to significantly influence disease symptomology (139). However use of this antibody in conjunction with ether an ADAM10 inhibitor or the monoclonal antibody used to block IgE binding (Xolair) remains to be tested.

This CD23 stability is also exemplified in the finding that certain mouse strains exhibiting hyper IgE phenotypes have a mutated CD23. 129/SvJ and NZB mice were found to have mutations within their CD23 protein. These mutations resulted in reduced B cell CD23 surface expression. In agreement with this finding, Kaminski and Stavnezer recently reported reduced CD23 expression in the spleens of 129/SvJ mice as compared to C57BL/6 mice (140). Since CD23 message levels are not reduced and the amount of sCD23 detected is lower, the mutant CD23 is most likely being degraded internally or the mutations are likely interfering with the stability of the protein, thus accounting for the reduced surface levels observed.

The CD23 mutations in the 129/SvJ and NZB mice are associated with a hyper IgE phenotype *in vivo*. Consistent with our data in the 129/SvJ strain, NZB mice produce significantly more total IgE after immunization with KLH-alum than NZW mice (141). In addition, several randomly sampled unimmunized NZB mice were also found to have hyper IgE levels (142). High levels of total IgE are associated with protection during parasitic infections thus, we observed that 129/SvJ mice produce significantly increased levels of total IgE after *Nb* infection and display increased clearance of *Nb* larvae from the intestine.

The *in vivo* IgE findings with the 129/SvJ mice are similar to those observed in individuals suffering from Hyper IgE Syndrome (HIES). HIES is an extremely rare primary immunodeficiency characterized by high levels of serum IgE and increased blood eosinophilia. The disease affects multiple organ systems, including the immune system and the skeletal system, and frequently manifests as recurring staphylococcal infections (143). In addition, PBMCs isolated from the blood of patients with HIES respond similarly to B cells isolated from the spleens of 129/SvJ mice when cultured *in vitro* (144). At this time, we can only correlate the increased IgE levels observed in the 129/SvJ and the NZB mice with the mutations in CD23. However, the finding that two unrelated strains (129 versus NZB) of mice contain exactly the same CD23 mutations as well as hyper IgE levels suggests that the mutations are important with respect to the IgE aberrations found. This supports previous studies that CD23 expression and stability are inversely correlated with IgE production.

The useful of mouse models is also highlighted in the GluK2 KO mice work presented. Although the studies using human cells are important in highlighting a novel pathway of IgE production, the argument that this system is an "*in vitro*" artifact remains. The GluK2 KO mice have been studied for mouse models of neurological disease, such as epilepsy, but their potential for immune system studies have yet to be tapped. We report that GluK2 KO mice fail to respond to glutamate *in vitro.* This data supports the use of NS102 as a targeted therapeutic in that the sole glutamate receptor responsible on the murine B cell is the GluK2 contains KAR subtype. The fact that these mice produce less IgE post antigen challenge also shows promise for the design of new treatments. Furthermore, the usefulness of the GluK2 KO mouse could potentially provide information regarding the pathway of the glutamate mediated affects on B cell biology.

In closing, we have identified the enzyme responsible for the cleavage of CD23. Upon the course of this discovery, we have been able to identify novel mutations in CD23, novel pathways leading to Ig production in both man and mouse, and novel therapeutic targets for the control of malignant disease.

Reference List

1. Gell, P., and R. Coombs. 1963. Clinical Aspects of Immunology. K. Blackwell, ed. Oxford, England.
2. Hurwitz, S. H. 1929. THE LURE OF MEDICAL HISTORY: JOHN BOSTOCK (1773-1846): Author of the First Clinical Description of Hay Fever. *Cal. West Med.* 31:137.
3. Tan, S. Y., and J. Yamanuha. 2010. Charles Robert Richet (1850-1935): discoverer of anaphylaxis. *Singapore Med. J.* 51:184.
4. Ramirez, M. 1919. Horse Asthma following blood transfusion: report on a case. *J. Am. Med. Assoc.* 73:984.
5. Prausnitz, D., and H. Kustner. 1921. Studien uber die Ueberempfindlichkeit. *Zentrabl. Bakteriol [A]* 86:160.
6. Coca, A., and R. Cooke. 1923. ON THE CLASSIFICATION OF THE PHENOMENA OF HYPERSENSITIVENESS. *J Immunol* 8:163.
7. Johansson, S. G. 2006. The discovery of immunoglobulin E. *Allergy Asthma Proc.* 27:S3-S6.
8. Stanworth, D. R., J. H. Humphrey, H. Bennich, and S. G. O. Johansson. 1968. Inhibition of Prausnitz-Kustner reaction by proteolytic-cleavage fragments of a human myeloma protein of immunoglobulin class E. *Lancet* 2:17.
9. Ishizaka, K., T. Ishizaka, and E. M. HATHORN. 1964. BLOCKING OF PRAUSNITZ-KUESTNER SENSITIZATION WITH REAGIN BY 'A CHAIN' OF HUMAN GAMMA1A-GLOBULIN. *Immunochemistry.* 1:197-207.:197.
10. Ishizaka, K., and T. Ishizaka. 1967. Identification of gamma-E-antibodies as a carrier of reaginic activity. *J. Immunol.* 99:1187.
11. Bennich, H. H., K. Ishizaka, S. G. Johansson, D. S. Rowe, D. R. Stanworth, and W. D. Terry. 1968. Immunoglobulin E: a new class of human immunoglobulin. *Immunology.* 15:323.
12. 2010. Nobel Prize.org.
13. Bennich, H., and S. G. O. Johansson. 1971. Structure and function of human immunoglobulin E. *Adv. Immunol.* 13:1.
14. Conrad, D. H. 1985. Structure and Synthesis of IgE. In *Allergy*. A. P. Kaplan, ed. Churchill Livingstone, New York, pp. 3.

15. Janeway, C. A., and P. Travers. 1996. *Immunobiology: The Immune System in Health and Disease*. Current Biology Ltd., New York.

16. Capron, M., and A. Capron. 1994. Immunoglobulin E and effector cells in schistosomiasis. *Science* 264:1876.

17. Conrad, D. H., S. B. Tinnell, and A. E. Kelly. 1998. Immunoglobulin E. In *Current Review of Allergic Disease*. M. A. Kaliner, ed. Blackwell Science, Philadelphia, pp. 39.

18. Spencer, L. A., P. Porte, C. Zetoff, and T. V. Rajan. 2003. Mice genetically deficient in immunoglobulin E are more permissive hosts than wild-type mice to a primary, but not secondary, infection with the filarial nematode Brugia malayi. *Infect. Immun.* 71:2462.

19. Gurish, M. F., P. J. Bryce, H. Tao, A. B. Kisselgof, E. M. Thornton, H. R. Miller, D. S. Friend, and H. C. Oettgen. 2004. IgE enhances parasite clearance and regulates mast cell responses in mice infected with Trichinella spiralis. *J. Immunol.* 172:1139.

20. Strachan DP. 1989. Hay fever, hygiene and household size. *Br. Med. J*1259.

21. Kinet, J. P. 1999. The high-affinity IgE receptor (Fc epsilon RI): From physiology to pathology. *Ann. Rev. Immunol.* 17:931.

22. Kraft, S., and J. P. Kinet. 2007. New developments in FcepsilonRI regulation, function and inhibition. *Nat. Rev. Immunol.* 7:365.

23. Turner, H., and J. P. Kinet. 1999. Signalling through the high-affinity IgE receptor Fc epsilonRI [In Process Citation]. *Nature* 402:B24-B30.

24. Schwarz, K., T. E. Hansen-Hagge, and C. R. Bartram. 1993. Recombinase deficiency in mouse and man. *Immunodeficiency.* 4:249.

25. Muramatsu, M., K. Kinoshita, S. Fagarasan, S. Yamada, Y. Shinkai, and T. Honjo. 2000. Class switch recombination and hypermutation require activation-induced cytidine deaminase (AID), a potential RNA editing enzyme. *C* 102:553.

26. Revy, P., T. Muto, Y. Levy, F. Geissmann, A. Plebani, O. Sanal, N. Catalan, M. Forveille, R. Dufourcq-Labelouse, A. Gennery, I. Tezcan, F. Ersoy, H. Kayserili, A. G. Ugazio, N. Brousse, M. Muramatsu, L. D. Notarangelo, K. Kinoshita, T. Honjo, A. Fischer, and A. Durandy. 2000. Activation-induced cytidine deaminase (AID) deficiency causes the autosomal recessive form of the Hyper-IgM syndrome (HIGM2) [see comments]. *C* 102:565.

27. De Vries, J. E., J. Punnonen, B. G. Cocks, R. De Waal Malefyt, and G. Aversa. 1993. Regulation of the human IgE response by IL4 and IL13. *Res. Immunol.* 144:597.

28. Shimoda, K., J. van Deursen, M. Y. Sangster, S. R. Sarawar, R. T. Carson, R. A. Tripp, C. Chu, F. W. Quelle, T. Nosaka, D. A. A. Vignali, P. C. Doherty, G. Grosveld, W. E.

Paul, and J. N. Ihle. 1996. Lack of IL-4-induced Th2 response and IgE class switching in mice with disrupted *Stat6* gene. *Nature* 380:630.

29. Durandy, A., C. Hivroz, F. Mazerolles, C. Schiff, F. Bernard, E. Jouanguy, P. Revy, J. P. DiSanto, J. F. Gauchat, J.-Y. Bonnefoy, J. L. Casanova, and A. Fischer. 1997. Abnormal CD40-mediated activation pathway in B lymphocytes from patients with hyper-IgM syndrome and normal CD40 ligand expression. *J. Immunol.* 158:2576.

30. Xu, J., T. M. Foy, J. D. Laman, E. A. Elliott, J. J. Dunn, T. J. Waldschmidt, J. Elsemore, R. J. Noelle, and R. A. Flavell. 1994. Mice deficient for the CD40 ligand. *Imm* 1:423.

31. Kawabe, T., T. Naka, K. Yoshida, T. Tanaka, H. Fujiwara, S. Suematsu, N. Yoshida, T. Kishimoto, and H. Kikutani. 1994. The immune responses in CD40-deficient mice: impaired immunoglobulin class switching and germinal center formation. *Immunity.* 1:167.

32. Sarfati, M., H. Luo, and G. Delespesse. 1989. IgE synthesis by chronic lymphocytic leukemia cells. *J. Exp. Med.* 170:1775.

33. Jabara, H. H., D. J. Ahern, D. Vercelli, and R. S. Geha. 1991. Hydrocortisone and IL-4 induce IgE isotype switching in human B cells. *J. Immunol.* 147:1557.

34. Beato, M., P. Herrlich, and G. Schutz. 1995. Steroid hormone receptors: many actors in search of a plot. *Cell.* 83:851.

35. Litinskiy, M. B., B. Nardelli, D. M. Hilbert, B. He, A. Schaffer, P. Casali, and A. Cerutti. 2002. DCs induce CD40-independent immunoglobulin class switching through BLyS and APRIL. *Nat. Immunol.* 3:822.

36. Stein, J. V., M. Lopez-Fraga, F. A. Elustondo, C. E. Carvalho-Pinto, D. Rodriguez, R. Gomez-Caro, J. J. De, A. Martinez, J. P. Medema, and M. Hahne. 2002. APRIL modulates B and T cell immunity. *J Clin. Invest.* 109:1587.

37. Uchida, J., T. Yasui, Y. Takaoka-Shichijo, M. Muraoka, W. Kulwichit, N. Raab-Traub, and H. Kikutani. 1999. Mimicry of CD40 signals by Epstein-Barr virus LMP1 in B lymphocyte responses. *Science.* 286:300.

38. O'Byrne, P. M. 2006. Cytokines or their antagonists for the treatment of asthma. *Chest.* 130:244.

39. Xu, L., and P. Rothman. 1994. IFN-gamma represses epsilon germline transcription and subsequently down-regulates switch recombination to epsilon. *Int. Immunol.* 6:515.

40. Hattori, K., M. Nishikawa, K. Watcharanurak, A. Ikoma, K. Kabashima, H. Toyota, Y. Takahashi, R. Takahashi, Y. Watanabe, and Y. Takakura. 2010. Sustained exogenous expression of therapeutic levels of IFN-gamma ameliorates atopic dermatitis in NC/Nga mice via Th1 polarization. *J Immunol.* 184:2729.

41. Nakagome, K., K. Okunishi, M. Imamura, H. Harada, T. Matsumoto, R. Tanaka, J. Miyazaki, K. Yamamoto, and M. Dohi. 2009. IFN-gamma attenuates antigen-induced overall immune response in the airway as a Th1-type immune regulatory cytokine. *J Immunol.* 183:209.

42. Wurzburg, B. A., S. C. Garman, and T. S. Jardetzky. 2000. Structure of the human IgE-Fc C epsilon 3-C epsilon 4 reveals conformational flexibility in the antibody effector domains. *Immunity.* 13:375.

43. Prenner, B. M. 2008. Asthma 2008: targeting immunoglobulin E to achieve disease control. *J. Asthma.* 45:429.

44. Plosker, G. L., and S. J. Keam. 2008. Omalizumab: a review of its use in the treatment of allergic asthma. *BioDrugs.* 22:189.

45. McCloskey, N., J. Hunt, R. L. Beavil, M. R. Jutton, G. J. Grundy, E. Girardi, S. M. Fabiane, D. J. Fear, D. H. Conrad, B. J. Sutton, and H. J. Gould. 2007. Soluble CD23 monomers inhibit and oligomers stimulate IGE synthesis in human B cells. *J Biol. Chem.* 282:24083.

46. Hibbert, R. G., P. Teriete, G. J. Grundy, R. L. Beavil, R. Reljic, V. M. Holers, J. P. Hannan, B. J. Sutton, H. J. Gould, and J. M. McDonnell. 2005. The structure of human CD23 and its interactions with IgE and CD21. *J. Exp. Med.* 202:751.

47. Gould, H. J., and B. J. Sutton. 2008. IgE in allergy and asthma today. *Nat. Rev. Immunol.* 8:205.

48. Conrad, D. H. 1990. Fc epsilon RII/CD23: the low affinity receptor for IgE. *Annu Rev Immunol* 8:623.

49. Lawrence, D. A., W. O. Weigle, and H. L. Spiegelberg. 1975. Immunoglobulins cytophilic for human lymphocytes, monocytes, and neutrophils. *J Clin Invest* 55:368.

50. Kintner, C., and B. Sugden. 1981. Identification of antigenic determinants unique to the surfaces of cells transformed by Epstein-Barr virus. *Nature* 294:458.

51. Sugden, B., and S. Metzenberg. 1983. Characterization of an antigen whose cell surface expression is induced by infection with Epstein-Barr virus. *J Virol.* 46:800.

52. Thorley-Lawson, D. A., L. M. Nadler, A. K. Bhan, and R. T. Schooley. 1985. BLAST-2 [EBVCS], an early cell surface marker of human B cell activation, is superinduced by Epstein Barr virus. *J. Immunol.* 134:3007.

53. Yukawa, K., H. Kikutani, H. Owaki, K. Yamasaki, A. Yokota, H. Nakamura, E. L. Barsumian, R. R. Hardy, M. Suemura, and T. Kishimoto. 1987. A B cell-specific differentiation antigen CD23, is a receptor for IgE (FcεR) on lymphocytes. *J. Immunol.* 138:2576.

54. Bonnefoy, J.-Y., J.-P. Aubry, C. Peronne, J. Wijdenes, and J. Banchereau. 1987. Production and characterization of a monoclonal antibody specific for the human lymphocyte low affinity receptor for IgE: CD23 is a low affinity receptor for IgE. *J. Immunol.* 138:2970.

55. Sherr, E., E. Macy, H. Kimata, M. Gilly, and A. Saxon. 1989. Binding the low affinity FcεR on B cells suppresses ongoing human IgE synthesis. *J. Immunol.* 142:481.

56. Yu, P., M. Kosco-Vilbois, M. Richards, G. Köhler, M. C. Lamers, and G. Kohler. 1994. Negative feedback regulation of IgE synthesis by murine CD23. *Nature* 369:753.

57. Texido, G., H. Eibel, G. Le Gros, and H. Van der Putten. 1994. Transgene CD23 expression on lymphoid cells modulates IgE and IgG1 responses. *J. Immunol.* 153:3028.

58. Payet, M. E., E. C. Woodward, and D. H. Conrad. 1999. Humoral response suppression observed with CD23 transgenics. *J. Immunol.* 163:217.

59. Cernadas, M., G. T. De Sanctis, S. J. Krinzman, D. A. Mark, C. E. Donovan, J. A. Listman, L. Kobzik, H. Kikutani, D. C. Christiani, D. L. Perkins, and P. W. Finn. 1999. CD23 and allergic pulmonary inflammation: potential role as an inhibitor. *Am. J. Respir. Cell Mol. Biol.* 20:1.

60. Haczku, A., K. Takeda, E. Hamelmann, A. Oshiba, J. Loader, A. Joetham, C. Irvin, H. Kikutani, and E. W. Gelfand. 1997. CD23 deficient mice develop allergic airway hyperresponsiveness following sensitization with ovalbumin. *Am. J. Respir. Crit Care Med.* 156:1945.

61. Lewis, G., E. Rapsomaniki, T. Bouriez, T. Crockford, H. Ferry, R. Rigby, T. Vyse, T. Lambe, and R. Cornall. 2004. Hyper IgE in New Zealand black mice due to a dominant-negative CD23 mutation. *Immunogenetics* 56:564.

62. Ford, J. W., M. A. Kilmon, K. M. Haas, A. E. Shelburne, Y. Chan-Li, and D. H. Conrad. 2006. In vivo murine CD23 destabilization enhances CD23 shedding and IgE synthesis. *Cell Immunol.* 243:107.

63. Saxon, A., Z. Ke, L. Bahati, and R. H. Stevens. 1990. Soluble CD23 containing B cell supernatants induce IgE from peripheral blood B-lymphocytes and costimulate with interleukin- 4 in induction of IgE. *J. Allergy Clin. Immunol.* 86:333.

64. Marolewski, A. E., D. R. Buckle, G. Christie, D. L. Earnshaw, P. L. Flamberg, L. A. Marshall, D. G. Smith, and R. J. Mayer. 1998. CD23 (FcεRII) release from cell membranes is mediated by a membrane-bound metalloprotease. *Biochem. J.* 333:573.

65. Christie, G., A. Barton, B. Bolognese, D. R. Buckle, R. M. Cook, M. J. Hansbury, G. P. Harper, L. A. Marshall, M. E. McCord, K. Moulder, P. R. Murdock, S. M. Seal, V. M. Spackman, B. J. Weston, and R. J. Mayer. 1997. IgE secretion is attenuated by an inhibitor of proteolytic processing of CD23 (FcεRII). *Eur. J. Immunol.* 27:3228.

66. Lecoanet-Henchoz, S., J. F. Gauchat, J. P. Aubry, P. Graber, P. Life, N. Paul-Eugene, B. Ferrua, A. L. Corbi, B. Dugas, C. Plater-Zyberk, and . 1995. CD23 regulates monocyte activation through a novel interaction with the adhesion molecules CD11b-CD18 and CD11c-CD18. *Immunity.* 3:119.

67. Mulle, C., A. Sailer, I. Perez-Otano, H. ckinson-Anson, P. E. Castillo, I. Bureau, C. Maron, F. H. Gage, J. R. Mann, B. Bettler, and S. F. Heinemann. 1998. Altered synaptic physiology and reduced susceptibility to kainate-induced seizures in GluR6-deficient mice. *Nature.* 392:601.

68. Kelly, A. E., B.-H. Chen, E. C. Woodward, and D. H. Conrad. 1998. Production of a chimeric form of CD23 that is oligomeric and blocks IgE binding to the Fc epsilonRI. *J Immunol* 161:6696.

69. Chen, B. H., C. Ma, T. H. Caven, Y. Chan-Li, A. Beavil, R. Beavil, H. Gould, and D. H. Conrad. 2002. Necessity of the stalk region for immunoglobulin E interaction with CD23. *Immunology* 107:373.

70. Keegan, A. D., C. Fratazzi, B. Shopes, B. Baird, and D. H. Conrad. 1991. Characterization of new rat anti-mouse IgE monoclonals and their use along with chimeric IgE to further define the site that interacts with Fc$_{\varepsilon}$RII and Fc$_{\varepsilon}$RI. *Mol. Immunol.* 28:1149.

71. Caven, T. H., A. Shelburne, J. Sato, Y. Chan-Li, S. Becker, and D. H. Conrad. 2005. IL-21 dependent IgE production in human and mouse in vitro culture systems is cell density and cell division dependent and is augmented by IL-10. *Cell Immunol.* 238:123.

72. Schwartz, W., J. Jiao, J. Ford, D. Conrad, J. F. Hamel, P. Santanbien, L. Bradbury, and T. Robin. 2004. Application of Chemically-Stable Immunoglobulin-Selective Sorbents: Harvest and Purification of Antibodies with Resolution of Aggregate. *BioProcessing Journal* 3:53.

73. Campbell, K. A., E. J. Studer, M. A. Kilmon, A. Lees, F. D. Finkelman, and D. H. Conrad. 1997. Induction of B cell apoptosis by co-crosslinking CD23 and sIg involves aberrant regulation of c-*myc* and is inhibited by *bcl*-2. *Int. Immunol.* 9:1131.

74. Rabah, D., and D. H. Conrad. 2002. Effect of Cell Density on *in vitro* mouse IgE production.

75. Caven, T. H., A. Shelburne, and D. Conrad. 2004. rHuIL-21 enhances IgE production in human PBMC and purified tonsilar B cells stimulated with IL-4 and anti-CD40 in a cell number, IL-21 concentration and proliferation dependent manner.

76. Oie, H. K., E. K. Russell, D. N. Carney, and A. F. Gazdar. 1996. Cell culture methods for the establishment of the NCI series of lung cancer cell lines. *J. Cell Biochem. Suppl.* 24:24-31.:24.

77. Ludwig, A., C. Hundhausen, M. H. Lambert, N. Broadway, R. C. Andrews, D. M. Bickett, M. A. Leesnitzer, and J. D. Becherer. 2005. Metalloproteinase inhibitors for the disintegrin-like metalloproteinases ADAM10 and ADAM17 that differentially block constitutive and phorbol ester-inducible shedding of cell surface molecules. *Comb. Chem. High Throughput. Screen.* 8:161.

78. Fridman, J. S., E. Caulder, M. Hansbury, X. Liu, G. Yang, Q. Wang, Y. Lo, B. B. Zhou, M. Pan, S. M. Thomas, J. R. Grandis, J. Zhuo, W. Yao, R. C. Newton, S. M. Friedman, P. A. Scherle, and K. Vaddi. 2007. Selective inhibition of ADAM metalloproteases as a novel approach for modulating ErbB pathways in cancer. *Clin. Cancer Res.* 13:1892.

79. Urban, J. 2006. Maintenance and propagation of Nippostrongylus brasiliensis.

80. Marolewski, A. E., D. R. Buckle, G. Christie, D. L. Earnshaw, P. L. Flamberg, L. A. Marshall, D. G. Smith, and R. J. Mayer. 1998. CD23 (FcepsilonRII) release from cell membranes is mediated by a membrane-bound metalloprotease. *Biochem J* 333:573.

81. Fourie, A. M., F. Coles, V. Moreno, and L. Karlsson. 2003. Catalytic activity of ADAM8, ADAM15, and MDC-L (ADAM28) on synthetic peptide substrates and in ectodomain cleavage of CD23. *J. Biol. Chem.* 278:30469.

82. Hartmann, D., S. B. de, L. Serneels, K. Craessaerts, A. Herreman, W. Annaert, L. Umans, T. Lubke, I. A. Lena, F. K. von, and P. Saftig. 2002. The disintegrin/metalloprotease ADAM 10 is essential for Notch signalling but not for alpha-secretase activity in fibroblasts. *Hum. Mol. Genet.* 11:2615.

83. Simpson, E. M., C. C. Linder, E. E. Sargent, M. T. Davisson, L. E. Mobraaten, and J. J. Sharp. 1997. Genetic variation among 129 substrains and its importance for targeted mutagenesis in mice. *Nat. Genet.* 16:19.

84. Seong, E., T. L. Saunders, C. L. Stewart, and M. Burmeister. 2004. To knockout in 129 or in C57BL/6: that is the question. *Trends Genet.* 20:59.

85. Lewis G., Rapsomaniki E., Bouriez T., Crockford T., Ferry H., Rigby R., Vyse T., Lambe T., and Cornall R. 2004. Hyper IgE in New Zealand black mice due to a dominant-negative CD23 mutation. *Immunogenetics* 56:564.

86. Ford, J. W., J. L. Sturgill, and D. H. Conrad. 2008. 129/SvJ mice have mutated CD23 and hyper IgE. *Cell. Immunol.* 10.1016/j.cellimm.2008.08.003.

87. Lewis G., Rapsomaniki E., Bouriez T., Crockford T., Ferry H., Rigby R., Vyse T., Lambe T., and Cornall R. 2004. Hyper IgE in New Zealand black mice due to a dominant-negative CD23 mutation. *Immunogenetics* 56:564.

88. Ortiz, R. M., I. Karkkainen, A. P. Huovila, and J. Honkaniemi. 2005. ADAM9, ADAM10, and ADAM15 mRNA levels in the rat brain after kainic acid-induced status epilepticus. *Brain Res. Mol. Brain Res.* 137:272.

89. Chittajallu, R., S. P. Braithwaite, V. R. Clarke, and J. M. Henley. 1999. Kainate receptors: subunits, synaptic localization and function. *Trends Pharmacol. Sci.* 20:26.

90. Lerma, J. 2006. Kainate receptor physiology. *Curr. Opin. Pharmacol.* 6:89.

91. Oprica, M., S. D. Spulber, A. F. Aronsson, C. Post, B. Winblad, and M. Schultzberg. 2006. The influence of kainic acid on core temperature and cytokine levels in the brain. *Cytokine.* 35:77.

92. Engel, T., B. M. Murphy, S. Hatazaki, E. M. Jimenez-Mateos, C. G. Concannon, I. Woods, J. H. Prehn, and D. C. Henshall. 2009. Reduced hippocampal damage and epileptic seizures after status epilepticus in mice lacking proapoptotic Puma. *FASEB J.*

93. Ramsdell, J. S., and C. E. Stafstrom. 2009. Rat kainic Acid model provides unexpected insight into an emerging epilepsy syndrome in sea lions. *Epilepsy Curr.* 9:142.

94. Gupta, Y. K., S. Briyal, and M. Sharma. 2009. Protective effect of curcumin against kainic acid induced seizures and oxidative stress in rats. *Indian J. Physiol Pharmacol.* 53:39.

95. Zemlyak, I., N. Manley, I. Vulih-Shultzman, A. B. Cutler, K. Graber, R. M. Sapolsky, and I. Gozes. 2009. The microtubule interacting drug candidate NAP protects against kainic acid toxicity in a rat model of epilepsy. *J. Neurochem.* 111:1252.

96. Collingridge, G. L., R. W. Olsen, J. Peters, and M. Spedding. 2009. A nomenclature for ligand-gated ion channels. *Neuropharmacology.* 56:2.

97. Lerma, J., A. V. Paternain, A. Rodriguez-Moreno, and J. C. Lopez-Garcia. 2001. Molecular physiology of kainate receptors. *Physiol Rev.* 81:971.

98. Ganor, Y., M. Besser, N. Ben-Zakay, T. Unger, and M. Levite. 2003. Human T cells express a functional ionotropic glutamate receptor GluR3, and glutamate by itself triggers integrin-mediated adhesion to laminin and fibronectin and chemotactic migration. *J. Immunol.* 170:4362.

99. Boldyrev, A. A., D. O. Carpenter, and P. Johnson. 2005. Emerging evidence for a similar role of glutamate receptors in the nervous and immune systems. *J. Neurochem.* 95:913.

100. Du, Y., C. Li, W. W. Hu, Y. J. Song, and G. Y. Zhang. 2009. Neuroprotection of preconditioning against ischemic brain injury in rat hippocampus through inhibition of the assembly of GluR6-PSD95-mixed lineage kinase 3 signaling module via nuclear and non-nuclear pathways. *Neuroscience.* 161:370.

101. Verdoorn, T. A., T. H. Johansen, J. Drejer, and E. O. Nielsen. 1994. Selective block of recombinant glur6 receptors by NS-102, a novel non-NMDA receptor antagonist. *Eur. J. Pharmacol.* 269:43.

102. Hou, Y. Y., Y. Liu, S. Kang, C. Yu, Z. Q. Chi, and J. G. Liu. 2009. Glutamate receptors in the dorsal hippocampus mediate the acquisition, but not the expression, of conditioned place aversion induced by acute morphine withdrawal in rats. *Acta Pharmacol. Sin.* 30:1385.

103. Rawls, S. M., T. Thomas, M. Adeola, T. Patil, N. Raymondi, A. Poles, M. Loo, and R. B. Raffa. 2009. Topiramate antagonizes NMDA- and AMPA-induced seizure-like activity in planarians. *Pharmacol. Biochem. Behav.* 93:363.

104. Szklarczyk, A., J. Lapinska, M. Rylski, R. D. McKay, and L. Kaczmarek. 2002. Matrix metalloproteinase-9 undergoes expression and activation during dendritic remodeling in adult hippocampus. *J Neurosci.* 22:920.

105. Flood, S., R. Parri, A. Williams, V. Duance, and D. Mason. 2007. Modulation of interleukin-6 and matrix metalloproteinase 2 expression in human fibroblast-like synoviocytes by functional ionotropic glutamate receptors. *Arthritis Rheum.* 56:2523.

106. Caven, T. H., J. L. Sturgill, and D. H. Conrad. 2007. BCR ligation antagonizes the IL-21 enhancement of anti-CD40/IL-4 plasma cell differentiation and IgE production found in low density human B cell cultures. *Cell Immunol.* 247:49.

107. Hasbold, J., A. B. Lyons, M. R. Kehry, and P. D. Hodgkin. 1998. Cell division number regulates IgG1 and IgE switching of B cells following stimulation by CD40 ligand and IL-4. *Eur. J. Immunol.* 28:1040.

108. Sarfati, M., S. Chevret, C. Chastang, G. Biron, P. Stryckmans, G. Delespesse, J. L. Binet, H. Merle-Beral, and D. Bron. 1996. Prognostic importance of serum soluble CD23 level in chronic lymphocytic leukemia. *Blood.* 88:4259.

109. Moss, M. L., A. Stoeck, W. Yan, and P. J. Dempsey. 2008. ADAM10 as a target for anti-cancer therapy. *Curr. Pharm. Biotechnol.* 9:2.

110. Millar, A. W., P. D. Brown, J. Moore, W. A. Galloway, A. G. Cornish, T. J. Lenehan, and K. P. Lynch. 1998. Results of single and repeat dose studies of the oral matrix metalloproteinase inhibitor marimastat in healthy male volunteers. *Br. J. Clin. Pharmacol.* 45:21.

111. Rai, K. R., B. L. Peterson, F. R. Appelbaum, J. Kolitz, L. Elias, L. Shepherd, J. Hines, G. A. Threatte, R. A. Larson, B. D. Cheson, and C. A. Schiffer. 2000. Fludarabine compared with chlorambucil as primary therapy for chronic lymphocytic leukemia. *N. Engl. J Med.* 343:1750.

112. Aubry, J. P., S. Pochon, P. Graber, K. U. Jansen, and J.-Y. Bonnefoy. 1992. CD21 is a ligand for CD23 and regulates IgE production. *Nature* 358:505.

113. Bonnefoy, J.-Y., J.-F. Gauchat, P. Life, P. Graber, J.-P. Aubry, and S. Lecoanet-Henchoz. 1995. Regulation of IgE synthesis by CD23/CD21 interaction. *Int. Arch. Allergy Immunol.* 107:40.

114. Lecoanet-Henchoz, S., J.-F. Gauchat, J.-P. Aubry, P. Graber, P. Life, N. Paul Eugene, B. Ferrua, A. L. Corbi, B. Dugas, C. Plater-Zyberk, and J.-Y. Bonnefoy. 1995. CD23 regulates monocyte activation through a novel interaction with the adhesion molecules CD11b-CD18 and CD11c-CD18. *Imm* 3:119.

115. Lemieux, G. A., F. Blumenkron, N. Yeung, P. Zhou, J. Williams, A. C. Grammer, R. Petrovich, P. E. Lipsky, M. L. Moss, and Z. Werb. 2007. The low affinity IgE receptor (CD23) is cleaved by the metalloproteinase ADAM10. *J Biol. Chem.* ..

116. Conrad, D. H. 1991. Murine CD23/Fc epsilon RII. Structure and function and comparison with the human counterpart. *Monogr Allergy* 29:9.

117. Eck, H. P., M. Betzler, P. Schlag, and W. Droge. 1990. Partial recovery of lymphocyte activity in patients with colorectal carcinoma after curative surgical treatment and return of plasma glutamate concentrations to normal levels. *J. Cancer Res. Clin. Oncol.* 116:648.

118. Eck, H. P., H. Frey, and W. Droge. 1989. Elevated plasma glutamate concentrations in HIV-1-infected patients may contribute to loss of macrophage and lymphocyte functions. *Int. Immunol.* 1:367.

119. Rainesalo, S., T. Keranen, J. Palmio, J. Peltola, S. S. Oja, and P. Saransaari. 2004. Plasma and cerebrospinal fluid amino acids in epileptic patients. *Neurochem. Res.* 29:319.

120. Aitken, K. J. 2008. Intersubjectivity, affective neuroscience, and the neurobiology of autistic spectrum disorders: a systematic review. *Keio J. Med.* 57:15.

121. McNearney, T., D. Speegle, N. Lawand, J. Lisse, and K. N. Westlund. 2000. Excitatory amino acid profiles of synovial fluid from patients with arthritis. *J. Rheumatol.* 27:739.

122. West, S. G. 2007. The Nervous System. In ***Dubois' lupus erythematosus***. D. J. Wallace, B. Hahn, and E. L. Dubois, eds. Lippincott Wiliams and Wilkins, Philadelphia, pp. 707.

123. Borsody, M. K., and M. L. Coco. 2001. A hypothesis accounting for the inconsistent benefit of glucocorticoid therapy in closed head trauma. *Med. Hypotheses.* 56:65.

124. Raber, J. 1998. Detrimental effects of chronic hypothalamic-pituitary-adrenal axis activation. From obesity to memory deficits. *Mol. Neurobiol.* 18:1.

125. Ganor, Y., M. Besser, N. Ben-Zakay, T. Unger, and M. Levite. 2003. Human T cells express a functional ionotropic glutamate receptor GluR3, and glutamate by itself triggers integrin-mediated adhesion to laminin and fibronectin and chemotactic migration. *J. Immunol.* 170:4362.

126. Boldyrev, A. A., V. I. Kazey, T. A. Leinsoo, A. P. Mashkina, O. V. Tyulina, P. Johnson, J. O. Tuneva, S. Chittur, and D. O. Carpenter. 2004. Rodent lymphocytes express functionally active glutamate receptors. *Biochem. Biophys. Res. Commun.* 324:133.

127. Sun, H., A. Swaim, J. E. Herrera, D. Becker, L. Becker, K. Srivastava, L. E. Thompson, M. R. Shero, A. Perez-Tamayo, B. Suktitipat, R. Mathias, A. Contractor, N. Faraday, and C. N. Morrell. 2009. Platelet kainate receptor signaling promotes thrombosis by stimulating cyclooxygenase activation. *Circ. Res.* 105:595.

128. Weskamp, G., J. W. Ford, J. Sturgill, S. Martin, A. J. Docherty, S. Swendeman, N. Broadway, D. Hartmann, P. Saftig, S. Umland, A. Sehara-Fujisawa, R. A. Black, A. Ludwig, J. D. Becherer, D. H. Conrad, and C. P. Blobel. 2006. ADAM10 is a principal 'sheddase' of the low-affinity immunoglobulin E receptor CD23. *Nat. Immunol.* 7:1293.

129. Caven, T. H., A. Shelburne, J. Sato, Y. Chan-Li, S. Becker, and D. H. Conrad. 2005. IL-21 dependent IgE production in human and mouse in vitro culture systems is cell density and cell division dependent and is augmented by IL-10. *Cell Immunol.* 238:123.

130. Haas, H. S., R. Pfragner, V. Siegl, E. Ingolic, E. Heintz, and K. Schauenstein. 2005. Glutamate receptor-mediated effects on growth and morphology of human histiocytic lymphoma cells. *Int. J. Oncol.* 27:867.

131. Payet-Jamroz, M., S. L. Helm, J. Wu, M. Kilmon, M. Fakher, A. Basalp, J. G. Tew, A. K. Szakal, N. Noben-Trauth, and D. H. Conrad. 2001. Suppression of IgE responses in CD23-transgenic animals is due to expression of CD23 on nonlymphoid cells. *J Immunol* 166:4863.

132. Bowser, C. S., J. Kaye, R. O. Joks, C. A. Charlot, and H. J. Moallem. 2007. IgE and atopy in perinatally HIV-infected children. *Pediatr. Allergy Immunol.* 18:298.

133. Frediani, T., S. Lucarelli, A. Pelliccia, B. Vagnucci, C. Cerminara, M. Barbato, and E. Cardi. 2001. Allergy and childhood epilepsy: a close relationship? *Acta Neurol. Scand.* 104:349.

134. Atta, A. M., C. P. Sousa, E. M. Carvalho, and M. L. Sousa-Atta. 2004. Immunoglobulin E and systemic lupus erythematosus. *Braz. J. Med. Biol. Res.* 37:1497.

135. Bansal, A., T. Roberts, E. M. Hay, R. Kay, R. S. Pumphrey, and P. B. Wilson. 1992. Soluble CD23 levels are elevated in the serum of patients with primary Sjogren's syndrome and systemic lupus erythematosus. *Clin. Exp. Immunol.* 89:452.

136. Bansal, A. S., A. J. MacGregor, R. S. Pumphrey, A. J. Silman, W. E. Ollier, and P. B. Wilson. 1994. Increased levels of sCD23 in rheumatoid arthritis are related to disease status. *Clin. Exp. Rheumatol.* 12:281.

137. Wrona, D. 2006. Neural-immune interactions: an integrative view of the bidirectional relationship between the brain and immune systems. *J. Neuroimmunol.* 172:38.

138. Nance, D. M., and V. M. Sanders. 2007. Autonomic innervation and regulation of the immune system (1987-2007). *Brain Behav. Immun.* 21:736.

139. Poole, J. A., J. Meng, M. Reff, M. C. Spellman, and L. J. Rosenwasser. 2005. Anti-CD23 monoclonal antibody, lumiliximab, inhibited allergen-induced responses in antigen-presenting cells and T cells from atopic subjects. *J Allergy Clin. Immunol.* 116:780.

140. Kaminski, D. A., and J. Stavnezer. 2007. Antibody class switching differs among SJL, C57BL/6 and 129 mice. *Int. Immunol.* 19:545.

141. Lewis G., Rapsomaniki E., Bouriez T., Crockford T., Ferry H., Rigby R., Vyse T., Lambe T., and Cornall R. 2004. Hyper IgE in New Zealand black mice due to a dominant-negative CD23 mutation. *Immunogenetics* 56:564.

142. Lewis G., Rapsomaniki E., Bouriez T., Crockford T., Ferry H., Rigby R., Vyse T., Lambe T., and Cornall R. 2004. Hyper IgE in New Zealand black mice due to a dominant-negative CD23 mutation. *Immunogenetics* 56:564.

143. Grimbacher, B., S. M. Holland, and J. M. Puck. 2005. Hyper-IgE syndromes. *Immunol. Rev.* 203:244-50.:244.

144. Claasen, J. J., A. D. Levine, S. E. Schiff, and R. H. Buckley. 1991. Mononuclear cells from patients with the hyper-IgE syndrome produce little IgE when they are stimulated with recombinant human interleukin-4. *J. Allergy Clin. Immunol.* 88:713.

VITA

Jamie Lynn Sturgill was born on November 20, 1979 at Central Baptist Hospital in Lexington, KY and is an American Citizen. She lived in Premium, KY until the age of 9 when her family relocated to Culloden, WV. She graduated from Cabell Midland High School, Ona, West Virginia in June of 1998 with very high honors. She received her Bachelor of Science degree in Biology from the University of Kentucky in Lexington, KY in May of 2002 where she graduated cum laude. Prior to continuing her education, she worked at the University of Kentucky for two years as a Research Assistant at the Markey Cancer Center in the laboratory of John Yannelli. She received a Basic Health Science Certificate in Microbiology and Immunology from Virginia Commonwealth University in May of 2005. She then enrolled in the Ph.D. program in Immunology at Virginia Commonwealth University in August of 2005